Cytokine-induced Extracellular Matrix Alterations in Diabetic Retinopathy Pathogenesis

By

Meredith J. Giblin

Dissertation
Submitted to the Faculty of the
Graduate School of Vanderbilt University
in partial fulfillment of the requirements
for the degree of

DOCTOR OF PHILOSOPHY
in

Cell and Developmental Biology
December 18, 2021
Nashville, Tennessee

Approved:

John S. Penn, Ph.D.

David M. Miller III, Ph.D.

Edward M. Levine, Ph.D.

William P. Tansey, Ph.D.

Jeffrey M. Davidson, Ph.D.

ACKNOWLEDGEMENTS

This work would not have been possible without the financial support of National Institutes of Health grants R01-EY07533, R01-EY023639, R01-EY023397, P30-EY008126 (Core Grant in Vision Research), and T32-EY021453 (Training Program in Ocular Genomics); an unrestricted grant from Research to Prevent Blindness, Inc.; the Phyllis G. and William B. Snyder Endowment; and the Carl Marshall Reeves & Mildred Almen Reeves Foundation, Inc.

First, I would like to thank the members of my committee for their expert guidance and support throughout this project. I would also like to thank the many wonderful people I had the pleasure of working with in the Penn lab, many of whom also became great friends: Cayla Ontko, Tyler Kilburn, Hannah Pendergrass, Angie Mudrick, Amy Stark, Dolly Ann Padovani-Claudio, Gary McCollum, and Rong Yang. I would like to especially thank Megan Capozzi who provided so much wonderful guidance and advice during my first years in the lab and who has continued to be an important mentor to me throughout graduate school. I am incredibly grateful to Taylor Smith for her years of support and friendship. Taylor was the best work, conference, food, concert, walking, and adventure buddy I could have asked for; I am so grateful to have had her as a co-worker and dear friend throughout my time in the lab. Finally, I am thankful for my mentor, John Penn, who has always been supportive, patient, and dedicated in shaping my scientific and professional development. John has always given me the freedom and encouragement to follow my scientific curiosity. I am a better scientist and a better person for having worked in his lab.

I am fortunate to have many wonderful people in my life who have been an indispensable support system during graduate school. First, I would like to thank Stephanie Singer and Laura Fritzsche; their incredible skill and compassion have made my life immeasurably better. I would like to thank my IGP friends, especially Nicole Fisher, Kelly Barnett, and Michael Dudley, who made graduate school fun with many relaxing beers and delicious meals. I am incredibly grateful for the community I found in the Nashville Rowing Club. NRC, and the wonderful people I met there, really made Nashville feel like my home and always cleared my head after a long day in lab. I am especially grateful to Liz, Katie, Michele, Emily, and Gracie for their love, support, and encouragement on and off the water. I am thankful for a lifetime of love and support from Weeze and Chuck, Lottie, and Jen. I would like to thank my brothers, Jack, for always being there to lend a sympathetic ear about the difficulties of graduate school or to chat science, and Peter, for his encouragement, support, and a never-ending stream of entertaining Tweets/memes/etc. I am eternally and forever grateful for my sister, Madelyn. She has been there for me through every high and every low, big or small, during this degree and has loved, supported, and believed in me every step of the way. Last and most of all, I would like to thank my parents, Thomas and Kelly, for being an endless well of unconditional love and support. I could not have done this without them. I am not sure how I got so lucky but I feel so fortunate to be their daughter.

TABLE OF CONTENTS

Page

LIST OF TABLES

Table Page

LIST OF FIGURES

CHAPTER I

INTRODUCTION

Diabetic retinopathy background

Diabetes mellitus (DM) is a chronic, systemic metabolic disease commonly characterized by elevated blood glucose, aberrant insulin signaling, and altered blood lipid levels. There are numerous subtypes of diabetes, but the two most common classifications are type 1 and type 2 DM. Type 1 DM is an auto-immune disease in which T-cells destroy pancreatic β-cells resulting in an inability to produce insulin. Type 2 DM, often referred to as adult-onset, is characterized by insulin resistance and a subsequent decline in insulin production.[1] Globally, the prevalence of diabetes is predicted to grow from 382 million people in 2013 to 592 million by 2035, with the prevalence of both Type 1 and Type 2 increasing.[2] Indeed, Type 2 diabetes is now considered a global epidemic.[3]

Diabetes has a number of associated complications, including three microvascular complications: diabetic nephropathy, diabetic neuropathy, and diabetic retinopathy. Diabetic retinopathy (DR) is the leading cause of new cases of blindness in working age Americans.[4] Among US adults with diabetes aged 40 and older, 28.5% have DR (4.2 million people). It is estimated that worldwide, this prevalence increases to 34.6% or 93 million people.[5-7] Therefore, DR represents a significant clinical burden in society, which will only increase as the diabetes epidemic worsens. DR can be broken into two clinically distinct stages: non-proliferative DR (NPDR) and proliferative DR

(PDR). NPDR is characterized by several retinal features, including basement membrane thickening, pericyte dropout, acellular capillaries, vascular hyperpermeability, and leukostasis, which give rise to the appearance of characteristic fundus abnormalities, including microaneurysms, hemorrhages, and lipid exudates. Collectively, these events are believed to cause local ischemia leading to focal hypoxia. A subsequent upregulation of vasoproliferative factors stimulates pre-retinal neovascularization in the affected retinal regions, the characteristic pathology of PDR. Diabetic macular edema (DME), swelling of the retinal region responsible for central vision, is the clinical feature most closely associated with patient vision loss and primarily results from leakage of retinal vessels.[8] DME can arise at any stage of DR progression; however, with treatment, it is a reversible form of vision loss in some patients, as discussed below.

One of the most effective ways to prevent or slow DR progression is tight glycemic control, as demonstrated by two large-scale clinical trials: the Diabetes Control and Complications Trial (DCCT), and its observational follow-up the Epidemiology of Diabetes Interventions and Complications (EDIC), for Type 1 diabetes[9] and the United Kingdom Prospective Diabetes Trial (UKPDS) for Type 2 diabetes.[10] Both studies demonstrated that intensive glycemic control reduces the incidence and progression of DR. For instance, in the DCCT, intensive glycemic control reduced the risk for the development of DR by 76% and slowed progression of DR by 54%.[11] However, intensive glycemic control can be difficult for patients to achieve, is associated with significantly higher levels of weight gain, and comes with a threefold increased risk of hypoglycemia.[9] Furthermore, although glycated-hemoglobin level is the strongest risk

factor identified thus far for DR development and progression, it only accounted for 11% of the risk of DR in the DCCT.[12] These data suggest that other, as yet unidentified, factors exist with critical contributions to the risk of DR development and progression.

Since tight glycemic control is difficult to achieve and DR continues to develop in some patients, development of additional therapeutic strategies was paramount. There are currently two standard therapeutic strategies for treatment of DR: laser photocoagulation and anti-vascular endothelial growth factor (VEGF). Laser photocoagulation involves the creation of thermal burns in the retinal periphery or in a focal/grid pattern in the central retina.[13] Laser photocoagulation proved to be efficacious in reducing severe vision loss in PDR[14] and moderate vision loss in DME.[15] However, this approach, by its very nature, is highly destructive; as such, side effects occur and include loss of both peripheral and night vision.

Due to the destructive nature and harmful side effects of laser photocoagulation, it was desirable to develop alternative therapeutic approaches. Anti-VEGF therapies were developed in the early 2000's and have since demonstrated superior efficacy for attenuating vision loss and improving visual gain in both DME and PDR in multiple phase 3 clinical trials.[16-22] Three anti-VEGF therapies are currently used in the clinic to treat DME or PDR: ranibizumab, an affinity-enhanced Fab fragment; bevacizumab, a humanized full length murine monoclonal antibody against VEGF; and aflibercept, a VEGF-trap created by fusing the VEGF-binding extracellular domains of VEGFR1 and VEGFR2 to the Fc portion of human IgG1.[23] Anti-VEGF therapy is administered intravitreally with the goal of reducing VEGF signaling in the retina. All three therapies target all VEGF isoforms, with aflibercept also binding placental growth factor. In

addition to superior efficacy, anti-VEGF therapies are also associated with less peripheral vision loss and decreased rates of DME onset and vitrectomies compared to laser photocoagulation.[13] Despite anti-VEGF representing a major advancement in DR treatment, this therapeutic approach still has significant drawbacks. First, anti-VEGF is not efficacious in all patients. Indeed, a recent meta-analysis comparing the efficacies of aflibercept, ranibizumab, and bevacizumab predicted that only 3-4 out of every 10 DME patients will experience improvement after one year of anti-VEGF therapy.[24] Second, since intraocular injections are a highly invasive and unpleasant procedure for patients and are required near-monthly over a significant time period, compliance issues often arise, decreasing therapeutic efficacy. Overall, both of the current therapeutic strategies focus on treating DR at an advanced stage, where irreparable damage to the retina has already occurred. Therefore, there is a great clinical need for therapeutic strategies against DR that are noninvasive, nondestructive, and, preferably, slow or halt disease progression before retinal damage has occurred.

Diabetic retinopathy pathology

The retina has a diverse range of cells, including neuronal, vascular, and glial subtypes, and evidence has demonstrated that each are affected by the diabetic environment (**Figure 1**). Pathogenic changes in retinal cells occur first on the cellular and molecular levels, eventually leading to the appearance of lesions on a fundus examination and diagnosable disease. The causes of pathogenic changes in retinal cells are highly interrelated, as each cell responds to the diabetic environment to further potentiate disease in both autocrine and paracrine mechanisms.

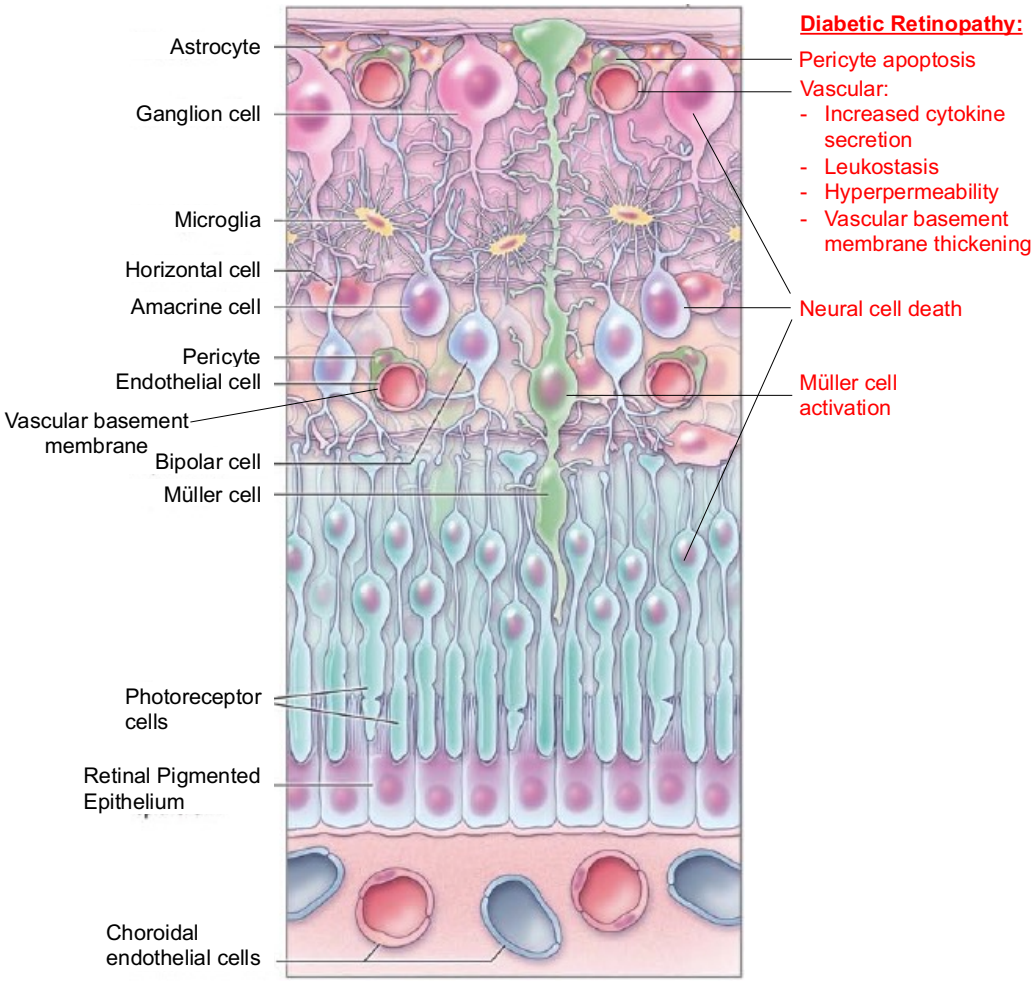

Figure 1: Overview of retinal cells and their pathogenic changes in diabetic retinopathy. Adapted from Antonetti et al. (2012).[8] This diagram demonstrates the laminar structure of the retina and the relative location of all retinal cells. For orientation, the vitreous and front of the eye are above the top of the image and sclera and back of the eye are below. Retinal cells and structures are labeled in black on the left. On the right, in red, are the pathogenic alterations observed in these cells during diabetic retinopathy and discussed in the introduction. Reproduced with permission from Antonetti et al. (2012),[8] Copyright Massachusetts Medical Society.

There are numerous neuronal cell types in the retina, including photoreceptors, bipolar cells, horizontal cells, amacrine cells, and retinal ganglion cells. Although DR is typically thought of as a vasodegenerative disease, increasing evidence demonstrates a significant neurodegenerative component that likely develops before observable

microvascular changes.[25,26] Apoptosis has been observed in a variety of retinal neurons, including retinal ganglion cells, amacrine cells, and photoreceptors, in animal models of diabetes and diabetic eyes.[27-29] Additionally, studies have demonstrated that neurons likely secrete growth factors, cytokines, and other inflammatory molecules which promote other events in DR progression, including retinal inflammation and blood retina barrier dysfunction.[30,31] These pathogenic changes in retinal neurons also drive measurable functional changes, including alterations in color vision and contrast sensitivity, reduced electroretinogram (ERG) responses, and retinal thinning.[32-44]

Another component of diabetes-induced retinal neurodegeneration is glial cell activation and dysfunction. The retina contains multiple glial cell types, specifically astrocytes, microglia, and macroglia. Alterations have been observed in all glial cell types; however, as Müller glia are an important component of two chapters in this dissertation, only their diabetes-induced changes are summarized here. Müller cells are retina-specific macroglia cell that span the length of the retina, providing structural support and playing a central role in regulating retinal metabolism and homeostasis. Müller cell activation has been identified in both patients and animals models and is associated with both increased glial fibrillary acidic protein (GFAP) levels, demonstrating a retinal gliotic state, and increased pro-inflammatory cytokine secretion.[45-48] Although gliosis is beneficial in an acute manner, as it facilitates the phagocytosis of apoptotic cells and debris, chronic gliosis is damaging to the retina. Activated glia lose functionality in regulating blood flow and maintaining the blood retina barrier and secrete inflammatory mediators thereby propagating retinal inflammation, vascular dysfunction, and neurodegeneration.[5,49] Increasingly, Müller cells are thought

to serve as a primary source of the retinal VEGF and inflammatory mediators driving DR pathology.[5,50-53] Importantly, Müller-cell specific knockout of VEGF in diabetic mice attenuated virtually all known pathogenic events in NPDR, demonstrating that Müller cell inflammation is a major driver of retinal inflammation and an important target for DR therapeutics.[54]

As vasodegeneration is the clinically defining pathology of NPDR, it is not surprising that significant damage and dysfunction occurs in retinal vascular cells on the molecular level. Both retinal vascular cell types, pericytes and endothelial cells, demonstrate pathogenic changes in DR. It is well-established that pericyte loss, via apoptosis, is one of the earliest pathogenic changes in a diabetic retina; it has been observed in both animal models of diabetes and human diabetic retinas.[55,56] Pericyte loss has a number of downstream consequences, including weakening of the vessel wall which contributes to both microaneurysm and hemorrhage development. Additionally, as pericytes are an essential microvascular support cell, pericyte loss is also associated with decreased trophic support for vascular endothelial cells leading to endothelial cell apoptosis and further potentiating weakened vessel walls. Indeed, pericyte loss, induced by genetic deletion of platelet-derived growth factor, was seen to recapitulate in mice the microvascular damage observed in human diabetic retinas, suggesting that pericyte dropout is a key event in driving DR pathology.[57]

Retinal microvascular endothelial cell dysfunction underlies the development of all pathogenic DR lesions. Retinal endothelial cells demonstrate numerous pathogenic behaviors in both humans and animal models including: increased apoptosis, leading to the development of acellular capillaries;[58] vascular hyperpermeability, leading to retinal

edema, hemorrhages and lipid exudates;[5,8,59] and increased leukocyte adhesion or leukostasis, leading to further propagation of local apoptotic and inflammatory factors as well as vessel occlusion.[60-67] Additionally, endothelial cells, similar to glial cells, become activated by the diabetic environment and show increased secretion of inflammatory cytokines.[68] Vascular hyperpermeability is a particularly important component of endothelial dysfunction as it leads to DME, the most common cause of vision loss in DR patients.[5,8] Highly organized junctional complexes form the barrier of the retinal endothelium. Various elements of the diabetic environment, including hyperglycemia, growth factors, and inflammatory mediators, cause junctional complex disorganization and a subsequent deficit of barrier function leading to retinal hyperpermeability.[5,8,59]

Ultimately, as retinal capillaries become non-patent due to vascular cell dysfunction, areas of focal ischemia develop throughout the retina. It is hypothesized that these ischemic areas drive retinal hypoxia, which in turn increases retinal cell production of VEGF. Increased levels of VEGF then signal to retinal endothelial cells to initiate angiogenesis. The development of visible retinal neovascular tufts clinically defines the transition to PDR. Despite significant hypoxia and proangiogenic growth signals, these new blood vessels are aberrantly formed and often not patent. Neovascular tufts can grow into the preretinal space, causing vitreous hemorrhage or tractional retinal detachment and associated severe vision loss.

Due to the highly complex and interdependent changes at the hemodynamic, metabolic, and cytokine levels, the mechanisms by which the diabetic milieu cause the development of DR remain to be fully understood.[69] After tight glycemic control was shown to slow DR progression, hyperglycemia has remained the primary focus of DR

mechanistic studies.[10,70] However, recent evidence has shifted focus to the significant contributions made by diabetic dyslipidemia and chronic retinal inflammation. Diabetic dyslipidemia involves the elevation of serum triglycerides and/or cholesterol and a variety of evidence suggests that dyslipidemia is an important DR risk factor. For instance, studies have shown increased levels of circulating free fatty acids in diabetics, as well as correlations between DR severity and serum lipid levels in type 1 diabetics.[71-75] Furthermore, in the Fenofibrate Intervention and Event Lowering in Diabetes (FIELD) and the Action to Control Cardiovascular Risk in Diabetes (ACCORD) studies, DR progression was delayed and need for laser treatment was reduced in patients treated with the lipid-lowering agents, fenofibrate and simvastatin.[71,76-79] Of particular note, these lipid-lowering drugs were able to slow DR progression independent of glycemic control. Hyperglycemia and dyslipidemia also contribute to the development of chronic, progressive inflammation in the retina. Increasing evidence suggests that chronic retinal inflammation is a major driver of DR pathogenesis.[5]

Inflammation in diabetic retinopathy

Inflammation is the body's response to stress, injury, or pathogens; it is a critical response to tissue damage and essential to healing. It involves a variety of mediators, including inflammatory cytokines and chemokines, and a diverse range of cells, including leukocytes, monocytes, and the endothelium. During an inflammatory event, pro-inflammatory cytokines lead to the activation of the endothelium and subsequent attraction, via chemo-attractants such as CCL2, and binding, via endothelial and leukocyte adhesion proteins, of circulating immune cells such as leukocytes. These

immune cells can then extravasate through the tissue and work to resolve local damage. Inflammation is typically resolved over a short time frame utilizing anti-inflammatory cytokines and other coordinate proteins. When activated and resolved acutely, inflammation is highly beneficial, as in the case of wound healing or infection. However, increasing evidence demonstrates that many diseases involve and are potentiated by a state of sustained inflammation leading to tissue damage.

Chronic low-grade inflammation is a component of early NPDR and, in recent years, its potential as a therapeutic target has received considerable attention (**Figure 2**). Elevated retinal or vitreous levels of cytokines, including IL-1β, TNFα, IL-8, IL-6, CCL2, and CCL5, have been observed early in DR in both animal models [80-84] and patients.[5,80,81,85-92] Increased levels of IL-1β are observed in the serum and vitreous of diabetics and, unlike VEGF, correlate closely with DR severity and progression.[93-95]

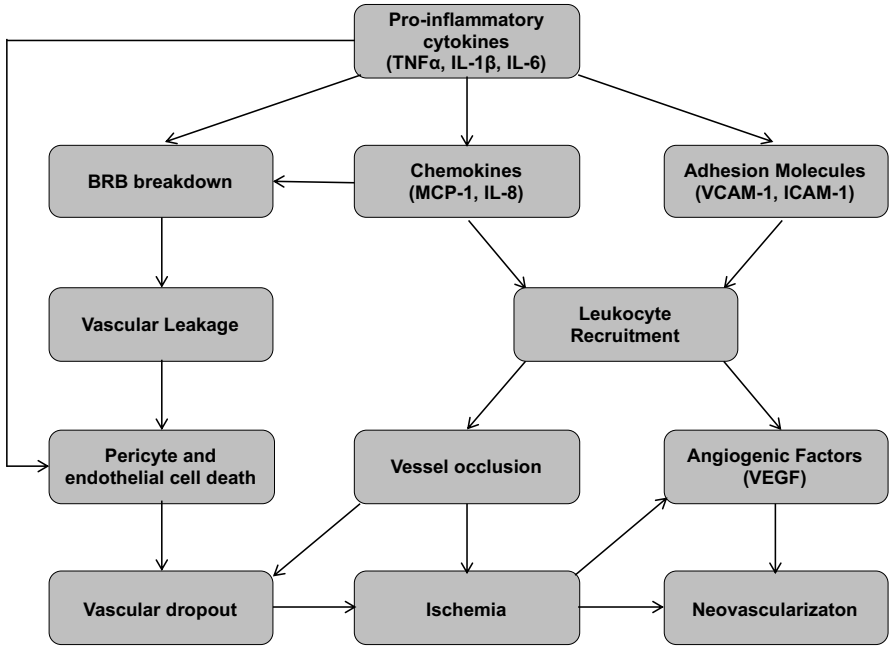

Figure 2: The role of inflammation in diabetic retinopathy pathogenesis. Adapted from Zhang et al. 2011.[81] This model depicts the hypothesized propagation of retinal inflammation and its downstream consequences in the development of vision-threatening pathology in late stage DR.

Meanwhile, Doganay and colleagues demonstrated a correlation between the stage of DR and serum IL-8 and TNFα levels.[96]

In numerous cell culture and animal models, cytokine treatment has been shown to drive every type of pathogenic NPDR event, including glial activation,[97-102] cell death,[103] vascular permeability,[98,104] leukocyte adhesion,[98,99,105-108] and vasoregression.[103] Of particular importance to this dissertation, inflammation is a key driver of the increased leukocyte adhesion, or leukostasis, seen early in DR in both animal models[60-63] and patients.[64-67] Leukostasis is a result of increased endothelial levels of the leukocyte adhesion proteins VCAM-1, ICAM-1, and E-selectin (**Figure 3**). Adherent leukocytes can occlude capillaries leading to downstream ischemia as well as further amplify local inflammation and release of pro-apoptotic factors.[5,60-62,64,94]

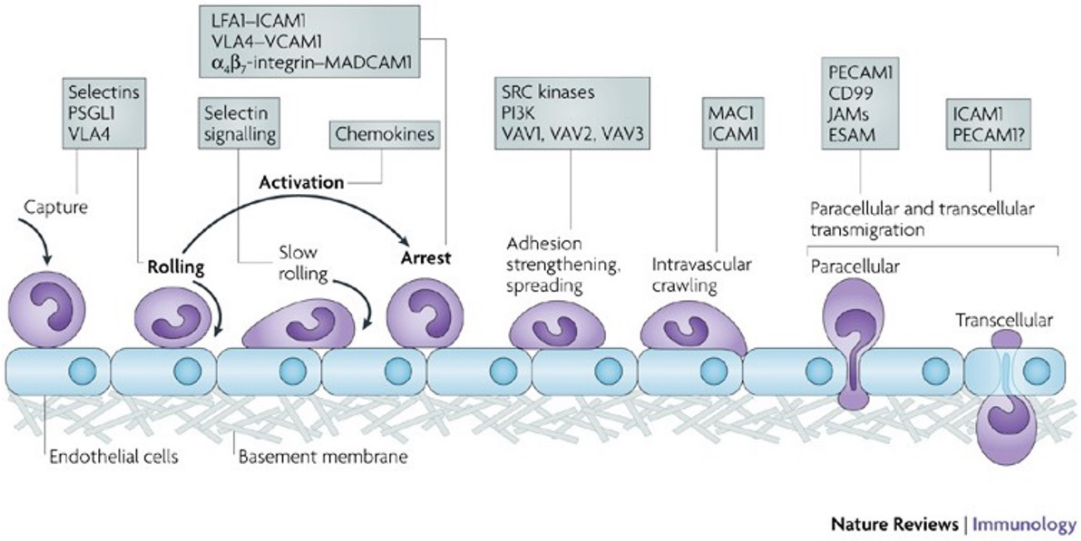

Figure 3: Leukocyte adhesion cascade. Leukocytes flowing through capillaries become adhered through the following cascade. First, endothelial selectins capture the leukocyte, causing it to begin to roll along the capillary wall. As the leukocyte rolls, it becomes further activated by local chemokines, causing the upregulation of adhesion molecules responsible for the arrest and firm adhesion of the leukocyte. Finally, leukocytes seek preferred sites of transmigration and then migrate into the inflamed tissue. Adapted from Ley et al, 2007.[236]

As a result of the increased scrutiny of the role of inflammation in driving DR pathogenesis, a number of anti-inflammatory reagents are under development, are being tested in pre-clinical and clinical trials, and/or have demonstrated efficacy. In one clinical trial, treatment with anti-inflammatory drugs lowered incidence of DR.[109] A small clinical trial using the anti-inflammatory reagent minocycline demonstrated efficacy in improving visual function and reducing macular edema and vascular leakage.[110] COX-2 inhibition has demonstrated efficacy in both rodent and dog models for attenuating leukocyte adhesion and vessel degeneration,[111-114] although aspirin has not demonstrated substantial benefit for patients in the clinic.[115-117] Anti-inflammatory steroids, such as dexamethasone, have demonstrated efficacy in reducing ICAM-1 levels, leukocyte adhesion, and vascular leakage in DR.[115,118] However, long-term steroid treatment comes with increased risk of both glaucoma and cataracts.[119] Finally, a number of combination therapies, in which anti-inflammatory reagents are combined with anti-VEGF therapy, are currently in development.[120,121]

Of the numerous inflammatory cytokines that have been identified in the diabetic retina, evidence suggests that TNFα and IL-1β are particularly important contributors to the initiation and propagation of retinal inflammation. TNFα inhibitors have been shown to prevent a wide range of NPDR events in diabetic animals,[111,122-124] while genetic depletion of TNFα signaling similarly attenuated NPDR pathogenic events in multiple animal models of diabetes.[122,125] Inhibition of the IL-1β-activating enzyme caspase 1 reduced retinal IL-1β levels and retinal capillary regression in both STZ and galactose-fed mice. Furthermore, deletion of the IL-1β receptor IL-1R1 also protected against

capillary loss in both models.[126] These data suggest that among inflammatory cytokines, TNFα and IL-1β are important drivers and regulators of retinal inflammation.

Vascular basement membrane

Vascular basement membrane (BM) is a thin, electron dense sheet of extracellular matrix (ECM) proteins that surrounds the endothelium (**Figure 4A**). The vascular BM structure and composition varies with the type of vasculature enveloped as well as with the tissue type. The BM functions as a structural support, a substratum for cell attachment and communication, and a selective permeability barrier.[127] BM plays essential roles in both development and mature tissue function, with mutations in key BM constituents causing a large variety of human diseases.[128,129] Depending on the tissue and vasculature type, a variety of cells are in direct contact with the vascular BM and have been identified as contributors to its initial development and sustained homeostasis. In the capillary BM, pericytes and endothelial cells are thought to be the primary ECM depositing cells in direct contact with the BM (**Figure 4A**).

Regardless of the tissue or organism, basement membranes are comprised of a common set of proteins: laminin, collagen IV, nidogen, and heparan sulfate

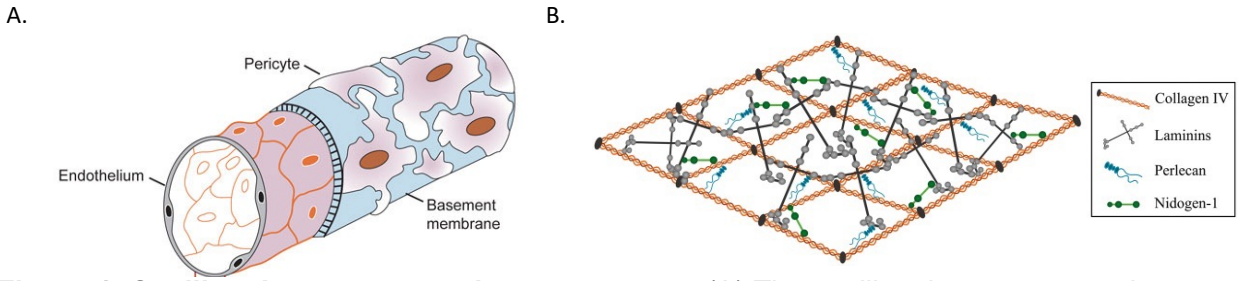

Figure 4: Capillary basement membrane structure. (A) The capillary basement membrane surrounds the endothelium, with pericytes embedded within the matrix. (B) The common set of basement membrane proteins, laminin, collagen IV, nidogen, and heparan sulfate proteoglycans (perlecan, here), form extensive covalent and non-covalent bonds to create a mature vascular basement membrane. (A) Adapted from Bilous, Donnelly, 2010.[320] (B) Adapted from Thomsen et al. 2017.[131]

proteoglycans (HSPG) (**Figure 4B**).[130] In addition to this core network, a diverse range of other minor constituents, such as fibronectin, tenascin-C, and thrombospondin, are present depending on the development stage, physiological state, or tissue type of the vascular BM.[131] Numerous ECM proteins form key elements of a vascular BM, however five specific ECM proteins were the focus of this dissertation and thus only their background is summarized here.

Collagen IV is a network-forming collagen found exclusively in BM. It is composed of three α-helix chains rich in hydroxyproline and hydroxylysine. In humans, six unique chains have been identified (α1-6) with only three unique heterotrimeric isoforms: $\alpha1\alpha1\alpha2$, $\alpha3\alpha4\alpha5$, and $\alpha5\alpha5\alpha6$. Levels of each heterotrimer vary based on tissue and developmental stage; $\alpha1\alpha1\alpha2$ is the primary heterotrimer found in retinal vascular BM. The collagen IV network is covalently linked through numerous interactions, including disulfide and sulfilimine bonds, which form dimers of the carboxy NC1 domain, tetramers of the amino terminal 7S domain, and lateral associations along the length of the molecule.[128,131] This extensive linkage between collagen IV heterotrimers provides tensile strength to the network. Collagen IV's primary function is to provide the scaffold on which the vascular BM is built, providing important tensile strength to the interconnected networks. Indeed, collagen IV forms one of two essential networks that serves as the backbone of the vascular BM; the other primary BM network is formed by laminin. Finally, evidence also suggests that collagen IV can regulate cellular behavior, including proliferation, migration, and polarity.[128]

Laminin is a cross-shaped heterotrimeric protein formed by an α, β, and γ chain. Five α chains, four β chains, and three γ chains are found in humans, with 16

heterotrimer combinations having been identified to date. Laminin 411 and 511 are considered the typical vascular BM laminins, however this can vary with tissue type, developmental stage, and disease.[132] The laminin network interacts with both cell surface integrins and dystroglycan receptors through laminin globular-like domains in the α chain, serving as an important platform for cell binding and adhesion.[128,132] Through these receptors, laminin is also involved in activating and regulating cell polarity, survival, migration, and differentiation.[128] The independent laminin and collagen networks are intricately bound together via network-bridging BM constituents; particularly important among these connections, the dumbbell-shaped glycoprotein nidogen (two isoforms: nidogen 1 and nidogen 2) facilitates noncovalent connection of the laminin and collagen IV networks.

Heparan sulfate proteoglycans (HSPG) are glycoproteins composed of a core protein with one or more covalently attached heparan sulfate chains. There are three subfamilies of HSPG: membrane, secretory vesicle, and secreted ECM HSPG. The two most prominent members of the secreted ECM HSPG subfamily found in vascular BM are agrin and perlecan (also referred to as HSPG2).[129] HSPG serve a number of key functions in vascular BM, including providing significant structural contributions to BM integrity. Importantly, HSPG also serve as depots of regulatory factors such as cytokines and growth factors, thereby facilitating and regulating the formation of chemokine gradients for leukocyte recruitment and homing in tissues.[130,133] By binding chemokines, HSPG create local chemokine gradients in the vascular BM, which spatially restricts the activation of vascular endothelial cells and therefore the site of leukocyte recruitment. Additionally, once leukocytes have transmigrated through the

endothelial cell layer, these HSPG-created chemokine gradients control the direction of leukocyte movement within a tissue.[134,135]

Fibronectin is a multidomain glycoprotein composed of multiple repeated modular domains, which give the molecule functional flexibility depending on the splicing and modular domains present. Fibronectin has a diverse array of splice variants and isoforms, with at least 20 distinct isoforms identified in humans, which are differentially expressed based on developmental stage, tissue type, and disease state.[136,137] It is typically found as a dimer connected by two disulfide bonds at the C termini. There are two types of fibronectin; plasma fibronectin is the soluble and compact form which is an important component in fibrin clot formation. Meanwhile, cellular fibronectin is secreted into the ECM where it is involved in cellular adhesion, tissue organization, scaffolding, and facilitation of specific binding between other BM constituents.[136,137]

Basement membrane homeostasis and turnover are regulated through a complex interplay of proteases and protease inhibitors, including plasminogen activators (uPA and tPA), plasminogen activator inhibitors (PAI-1 and -2), matrix metalloproteinases (MMP), tissue inhibitor of metalloproteinases (TIMP), and adamalysins (includes ADAM and ADAMTS). PA and PAI balance the selective cleaving of MMP pro-forms by plasmin, thus regulating MMP activation.[138,139] MMP are the primary proteases in ECM, with the ability to digest all ECM components with a wide range of substrate specificity.[140] As their name suggests, TIMP are important mediators of MMP activity. TIMP can inhibit MMP, ADAM, and ADAMTS, with each of the four members (TIMP1-4) demonstrating preferential specificity for different ECM proteases.[140] ADAM cleave the ectodomains of transmembrane proteins, allowing for

the release of cytokines, growth factors, and signaling molecules. Finally, ADAMTS are involved in the control of the structure and function of vascular ECM, including cleavage of pro-collagen molecules, von Willebrand factor, and proteoglycans.[141] Within a healthy BM, degradation enzymes and their inhibitors exist in a delicate balance, working to ensure BM turnover and homeostasis as well as contributing to controlled tissue responses through the cleavage and/or release of cytokines, growth factors, and signaling molecules. Dysregulation of this balance can significantly alter the structure and function of a vascular BM and, as such, has been identified as a contributor to numerous diseases.[140,142]

Aberrant remodeling of tissue ECM or BM, through irregular ECM deposition, dysregulation of degradation, or both, has been observed and linked to disease progression across a wide range of injury and disease types, including diabetes complications, cancer, atherosclerosis, and osteoarthritis.[140,143,144] Vascular BM thickening has been identified in all diabetic microangiopathies, including retinopathy, nephropathy, and neuropathy.[144-146] Its role in diabetic nephropathy has been extensively studied due to the important contributions of the glomerular BM to glomerular filtration. Glomerular BM thickening is one of the earliest detectable features of diabetic nephropathy, developing before any albuminuria is clinically evident.[147] Glomerular BM thickening is thought to arise from a combination of increased ECM deposition and dysregulation of ECM degradation by podocytes.[147] Additionally, mesangial matrix expansion and tubular basement membrane thickening are also observed.[147,148] Although glomerular BM thickening is considered an important

component of diabetic nephropathy, in the diabetic retina, BM thickening was long neglected as an active contributor to disease progression.

Vascular basement membrane thickening in diabetic retinopathy

Retinal vascular BM thickening is one of the earliest structural abnormalities in DR pathogenesis (**Figure 5**).[149] These structural abnormalities in the retinal vascular BM were first noted by Norman Ashton in 1949.[150] Studies have since shown that diabetic exposure causes morphological, biomechanical, and compositional changes in ocular BM,[151,152,153] and vascular BM thickening has become accepted as a classic pathogenic change in NPDR.[63,145]

As discussed above, numerous events occur on the molecular and cellular levels that give rise to the characteristic lesions in NPDR. The roles of many of these events,

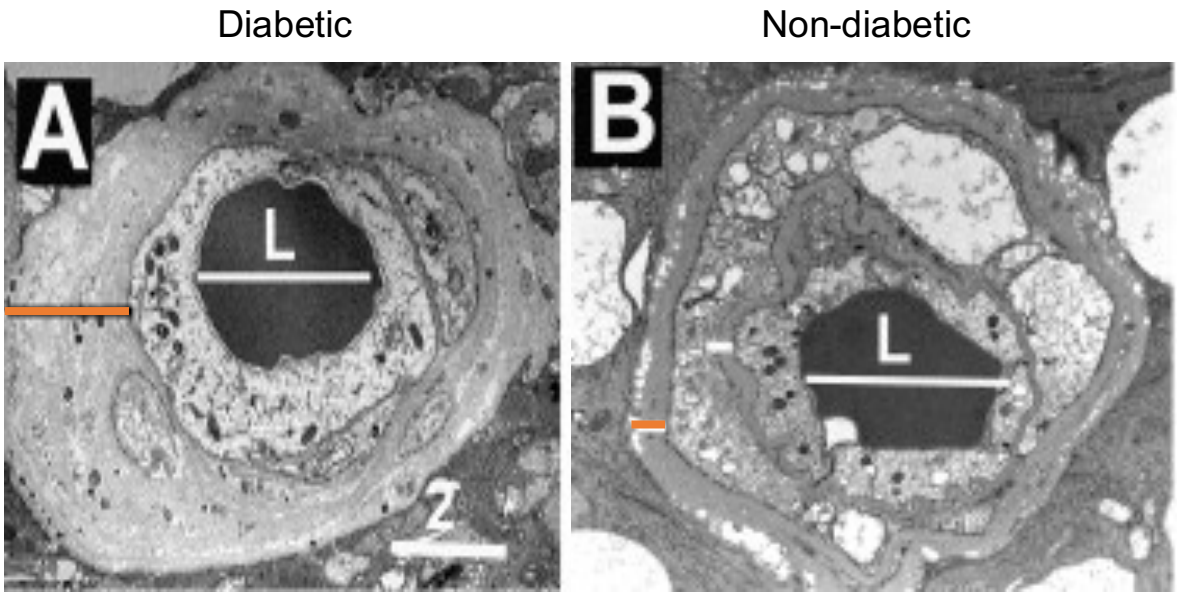

Figure 5: Vascular basement membrane thickening in DR. Representative electron micrographs of retinal capillaries from a 62-year-old diabetic (A) and a 74-year-old non-diabetic patient (B). The diameters of the blood vessel lumens (L) are similar, while the vascular BM is significantly thicker in the diabetic eye (A; orange bar) than in the non-diabetic eye (B; orange bar). This figure is adapted from To et al. 2013.[152]

including pericyte apoptosis, increased vascular permeability, leukostasis, and capillary dropout, in driving the pathogenic cascade have been extensively studied.[5,8,13,94] Conversely, although capillary BM thickening has long been considered a characteristic event in NPDR,[154] relatively little is known about its contributions to DR pathogenesis.[145] Indeed, for decades after its discovery, BM thickening was believed to be a consequence, not a cause, of retinal pathology in DR. However, the therapeutic promise of targeting BM thickening was demonstrated when intravitreal injections of antisense oligonucleotides targeting collagen IV, fibronectin, and laminin in diabetic rats prevented not only retinal vascular BM thickening but also led to a decrease in acellular capillaries, pericyte loss, and retinal vascular leakage.[155,156]

Current understanding of how retinal BM constituency is altered in DR is primarily based on immunohistochemistry or mRNA studies of whole retina.[152,157-161] These studies have demonstrated increased expression of key BM components including collagen IV, fibronectin, laminin, and tenascin C in both diabetic animal models and human diabetic retinal tissue.[145,149,152,157-160,162,163] Additionally, *in vitro* studies have demonstrated that conditions mimicking the diabetic environment, particularly high glucose, caused altered expression or deposition of ECM constituents by retinal endothelial cells.[145,149,163-169] However, these studies have a number of drawbacks including their qualitative nature and contamination from other retinal ECM such as the inner limiting and outer limiting membranes. Recent advances in proteomic techniques and ECM isolation methods have made studies of whole ECM proteomes increasingly feasible, including two studies that established the proteome of the retinal vascular BM and subsequently compared the constituency of the retinal vascular BM in non-diabetics

and diabetics with DR.[153,170] These two studies provided the first comprehensive insight into the unique constituency of the retinal vascular BM and how it might be altered in DR.

The specific mechanisms by which a thicker BM might contribute to DR pathology remains to be fully understood**.** However, in other tissues, alterations in ECM constituency are known to contribute to a range of pathogenic cell behaviors with similarities to NPDR pathology, including impaired EC-pericyte communication, changes in microvascular permeability, inappropriate cell-matrix adhesions, and alterations in leukocyte extravasation.[143,145,149,171-179] Recently, studies have begun to elucidate the ways in which cell-matrix interactions might drive pathogenic behaviors in the retina. For instance, evidence suggests that high glucose-induced changes in ECM composition can affect the integrity of endothelial junctional complexes, providing one hypothesis for how thicker BM could drive vascular hyperpermeability.[166] ECM grown under high glucose conditions has also been shown to promote apoptosis.[145] Additionally, alterations in the ratio and constituency of the BM could alter its architecture and therefore its functionality; two studies using retinal endothelial cells have demonstrated that high glucose-induced changes in ECM stiffness cause increased monocyte adhesion.[178,179] Despite these advances in understanding retinal cell-matrix dynamics, much remains to be understood about how diabetes affects retinal cells to cause BM thickening and how these events contribute to DR progression.

In the following chapters, I sought to expand our understanding of retinal inflammation and its role in driving pathogenic events in NPDR, including BM thickening. In **Chapter III**, I provided further support for the role of IL-1β in driving a

range of DR pathologies, including Müller cell auto-amplification of IL-1β, and identified a small molecule inhibitor with significant efficacy in attenuating multiple IL-1β-induced pathogenic behaviors in both Müller cells and endothelial cells. In **Chapter IV**, I identified a novel role for inflammatory cytokines and retinal pericytes in driving alterations in ECM expression and established a connection between cytokine-induced ECM changes and retinal leukostasis. Finally, in **Chapter V**, I utilized quantitative mass spectrometry to identify the endothelial cell-specific constituency of retinal ECM and interrogate how TNFα and IL-1β change this constituency. Overall, in this dissertation, I worked to build an experimental platform that lends itself to the discovery of the molecular mechanisms that underlie BM thickening, thereby enabling the rapid, facile assessment of the roles of retinal cells, elements of the diabetic environment, and/or the relevant transcription factors and signaling molecules controlling these processes.

CHAPTER II

METHODS

Human retinal cell culture

Human Müller cell (hMC) isolation, culture, and treatment

Primary hMC were isolated from human donor tissue (NDRI) within 24 hours post-mortem, using an adapted protocol from previously developed methods.[180] Briefly, the retina was dissected from the eye cup and dissociated in Dulbecco's Modified Eagle Medium (DMEM; Gibco; Carlsbad, CA) supplemented with trypsin and collagenase. After incubation in dissociation medium, hMC were cultured in DMEM supplemented with 10% FBS (R&D Systems; Minneapolis, MN) and 1x antibiotic/antimycotic solution (Gibco). Passages 4-6 were used for all experiments. Cultures were incubated at 37 °C, 5% CO_2, and 20.9% O_2 and 95% relative humidity.

For experiments in **Chapter III**, hMC were cultured in 6-well plates until 70% confluence, then cultured in serum-reduced conditions (DMEM supplemented with 2% FBS and 1x antibiotic/antimycotic solution) for 12 hours before treatment. hMC were treated in serum-reduced media containing 50pg/mL IL-1β (Sino Biological; Wayne, PA) with or without 1 or 2.5μM INCA-6 (Tocris; Minneapolis, MN) for 8 hours. After treatment, cultures were collected for mRNA expression analysis.

For experiments in **Chapter IV,** at 70% confluency, hMC were treated in serum-reduced conditions for 24 hours with diabetes-relevant stimuli (DRS): inflammatory cytokines (10 ng/mL TNFα, IL-1β, or 0.1% BSA in H_2O vehicle) or high glucose conditions

(5 mM or 25 mM D-glucose, with L-glucose used as an osmotic control). After treatment, cultures were collected for mRNA expression analysis.

Human retinal microvascular endothelial cell (hRMEC) culture and treatment

Primary hRMEC (Cell Systems; Kirkland, WA) were cultured in phenol red-free endothelial basal medium (EBM; Cell Systems) supplemented with 10% FBS (R&D Systems) and SingleQuots (Lonza, Inc.; Allendale, NJ) and grown on attachment factor- (Cell Systems) coated culture dishes. Passages 5-8 were used for all experiments.

For experiments in **Chapter III**, hRMEC were plated in 6-well plates and grown in 10% EBM to 75-85% confluency before treatment. Cells were treated for 2 hours with 1ng/mL IL-1β in the presence or absence of 1, 2.5, or 5μM INCA-6 in serum-reduced media (EBM supplemented with 2% FBS and 1x antibiotic/antimycotic solution). After treatment, cultures were collected for mRNA expression analysis.

For experiments in **Chapter IV**, hRMEC were allowed to grow for 24-36 hours in EBM supplemented with 10% FBS and SingleQuots until a confluent monolayer was reached. The media was then switched to serum-reduced media for 48 hours to allow sufficient time for cells to deposit ECM. In 2% FBS EBM, hRMEC were then treated with a variety of DRS for 48 hours. Included were inflammatory cytokines (10 ng/mL TNFα, IL-1β, IL-6, IL-8, or 0.1% BSA in H_2O vehicle), free fatty acids (250 μM palmitic acid, 100 μM oleic acid, 60 μM linoleic acid, or fatty acid-free BSA as vehicle), and high glucose conditions (5 mM or 25 mM D-glucose, with L-glucose used as an osmotic control). Free fatty acid concentrations were chosen for their physiological relevance. Total circulating levels of free fatty acids can be as high as 600 μM in diabetics; [181-183] more specifically, plasma palmitic acid levels were determined to be 234.9 +/-

58.1 μmol/l in obese diabetic individuals fasted overnight.[184] Furthermore, these concentrations fall within ranges used in studies of retinal cell behaviors[185] and *in vitro* studies of diabetes.[186,187] Likewise, my chosen cytokine concentrations fall within the range of concentrations tested in a variety of *in vitro* models of DR.[100,102,167,188,189] After treatment, cultures were collected for mRNA expression analysis.

For experiments in **Chapter V**, 150mm plates were coated with 2% (w/v) gelatin from porcine skin (G1890 Sigma; St. Louis, MO) for 2 hours at room temperature. hRMEC were allowed to grow for 72 hours in endothelial basal medium (EBM; Cell Systems) supplemented with 10% FBS and SingleQuots until a confluent monolayer was reached. Media was then changed to EBM supplemented with 5% FBS and SingleQuots for 24 hours before 48 hour treatment with 10ng/mL IL-1β, TNFα (Sigma), or respective vehicles in 5% EBM. After treatment, cultures were collected for quantitative mass spectrometry analysis.

Human retinal pericyte (hRP) culture and treatment

Primary human retinal pericytes (hRP) were purchased from Cell Systems and maintained in normal glucose (5.5mM) DMEM supplemented with 10% FBS and SingleQuots on attachment factor-coated plates. Passages 6-8 were used for all experiments. In **Chapter IV**, at 75% confluency, hRP were treated with DRS at the same concentrations as hRMEC (see above) in serum-reduced media (2% FBS DMEM with 1x antibiotic/antimycotic solution) for 24 hours. After treatment, cultures were collected for mRNA expression analysis.

Conditioned media (CM) experiments

hMC were cultured in 6-well plates until 70% confluency, then cultured in serum-reduced conditions for 12 hours before treatment. hMC were treated with TNFα (5 ng/mL or 10 ng/mL), IL-1β (1, 5, or 10 ng/mL), or corresponding vehicles for 2 hours in serum-reduced media. Stimuli were removed and fresh 2% EBM media was placed onto hMC; CM was allowed to generate for 6 hours before collection for treatment of hRMEC. Once cultures reached confluence, hRMEC media was changed to 5% FBS EBM (plus SingleQuots) for 24 hours prior to treatment with hMC CM. hRMEC were treated with hMC CM for 48 hours prior to collection for mRNA expression analysis.

Quantitative real time RT-PCR

Total RNA was collected using an RNeasy Mini kit (Qiagen; Valencia, CA), according to the manufacturer's protocol. The High-Capacity cDNA Archive Kit (Applied Biosystems; Waltham, MA) was used to reverse transcribe the total RNA. Quantitative RT-PCR was performed using gene-specific TaqMan Gene Expression Assays (**Table 1**; Applied Biosystems). Using technical duplicates, the co-amplification of the gene of interest was compared with *TBP (TATA-binding protein*) (endogenous normalization control). Data were analyzed using the comparative Ct method. Experiments were performed using a minimum of 3 biologically independent samples as well as technical replicates for each sample.

Target	Primer	Species	Chapter
TBP	Hs00427620_m1	Human	3, 4, 5
IL1B	Hs01555410_m1	Human	3
TNFA	Hs00174128_m1	Human	3
VEGF	Hs00900055_m1	Human	3
CCL2	Hs00234140_m1	Human	3
CCL5	Hs00982282_m1	Human	3
IL8	Hs00174103_m1	Human	3
IL6	Hs00174131_m1	Human	3
VCAM1	Hs1003372_m1	Human	3, 4
ICAM1	Hs00164932_m1	Human	3, 4, 5
SELE	Hs00174057_m1	Human	3, 4, 5
COL4A1	Hs00266237_m1	Human	3, 4, 5
FN1	Hs00365052_m1	Human	4
LAMB1	Hs01055967_m1	Human	4
AGRN	Hs00394748_m1	Human	4
HSPG2	Hs01078536_m1	Human	4
MMP2	Hs01548727_m1	Human	Appendix
MMP9	Hs00957562_m1	Human	Appendix

Table 1: Gene expression assays used in studies

Parallel plate flow chamber assay (PPFC)

Slides were used to assemble the PPFC (GlycoTech; Gaithersburg, MD) and leukocyte adhesion was assayed as previously described.[108] Briefly, human peripheral blood mononuclear cells (PBMC; Precision for Medicine; Fredrick, MD) were resuspended at a concentration of 5×10^5 cells/mL in Hank's Buffered Salt Solution (HBSS; Gibco). PBMC were flowed at a shear stress of 1 dyn/cm^2 over treated monolayers for 7 minutes. Non-adherent cells were then washed away by flowing HBSS over the monolayers at 2 dyn/cm^2 for 2 minutes. Eight fields per slide were randomly selected prior to PBMC flow and images were captured before and after flow. A masked

observer compared the two sets of images to count adherent leukocytes in the after images. Each data point represents the average number of adherent leukocytes across the eight captured fields per slide divided by the count area (mm^2).

In **Chapter III**, hRMEC were plated onto attachment factor-coated glass slides (Thermo Fisher; Waltham, MA). Once cells formed a complete monolayer, slides were treated with 1ng/mL IL-1β with or without 5μM INCA-6 in serum-reduced media for 4 hours.

In **Chapter IV**, hRMEC were plated onto attachment factor-coated glass slides. A pap pen was used to create standard growth area borders on each slide, to ensure that naïve hRMEC only plated where conditioned ECM had been deposited. Once cells formed a complete monolayer (~24 hours), media was changed to 5% FBS EBM for 24 hours before 48 hour treatment with 10ng/mL TNFα or IL-1β. To decellularize, slides were washed once with PBS and then submerged in decellularization buffer (20 mM NH_4OH and 0.5% Triton-X (vol/vol) in PBS (with Ca and Mg)) at 37°C. Slides were then submerged three times in fresh PBS. Naïve hRMEC were plated onto the slides with the decellularized ECM and allowed to settle for 16 hours. In these experiments, PBMC were stained with NucBlue (Thermo Fisher) for 20 minutes at 37°C at the manufacturer's suggested concentration before being spun down and resuspended for use in the PPFC.

Retinal leukostasis

All experiments were approved by the Vanderbilt University Institutional Animal Care and Use Committee and were performed in accordance with the ARVO Statement for the Use of Animals in Ophthalmic and Vision Research. Six- to eight-week-old

C57BL/6J mice (Charles River; Wilmington, MA) received intravitreal injections of vehicle, IL-1β (50pg), INCA-6 (150ng), or IL-1β (50pg) + INCA-6 (150ng). Retinal leukostasis was performed as described previously.[107,108] Briefly, 12 hours after treatment mice were anesthetized with ketamine/xylazine and then perfused with 0.9% saline for 2.5 minutes followed by FITC-conjugated concanavalin-A (40μg/mL in 5.0mL PBS; Vector Laboratories; Burlingame, CA). Saline was then perfused for 2.5 minutes to remove any non-adherent leukocytes. Retinas were immediately dissected into 4% paraformaldehyde, flat-mounted, and images were captured with a Zeiss LSM710 Confocal Microscope (Zeiss; Pleasanton, CA) at 20x magnification. Using ImageJ (NIH; Bethesda, MD), a masked observer selected 4 regions per retina and adherent leukocytes in the superficial plexus of the retinal vasculature were counted. Each data point represents the average number of adherent leukocytes across the 4 regions divided by the count area (mm^2). This method was used in **Chapter III**.

Transendothelial electrical resistance (TEER) measurements

hRMEC were plated at a density of 40,000 cells/well in 96W10idf plates (Applied Biophysics; Troy, NY) in 10% FBS EBM. Per the manufacturer's instructions, hRMEC were allowed to settle onto plates for 15 minutes at room temperature before insertion into the Electric Cell-substrate Impedance Sensing (ECIS) Z-Theta instrument (Applied Biophysics). After resistance plateaued between 24 and 48 hours, monolayers were treated with 1ng/mL IL-1β with or without 5μM INCA-6. Resistance was monitored for 24 hours after treatment and normalized resistance was calculated using Applied Biophysics

software.[190,191] Each well was normalized to its resistance 1 hour prior to treatment. This method was used in **Chapter III**.

Quantitative fluorescein angiography (qFA)

Six- to eight-week-old C57BL/6J mice (Charles River) received intravitreal injections of vehicle, IL-1β (50pg), INCA-6 (150ng), or IL-1β (50pg) + INCA-6 (150ng). Eight hours after treatment, vascular permeability was assessed using qFA. Mice were anesthetized with an intraperitoneal injection of ketamine/xylazine and their pupils were dilated with tropicamide and phenylephrine before receiving an intraperitoneal injection of sodium fluorescein (NDC 17478-250-20; Akorn; Lake Forest, IL) at 10μL/g body weight. At 2 and 4 minutes after injection, fluorescent fundus images were captured with the Micron IV retinal imaging system (Phoenix Research Labs; Pleasanton, CA). A masked observer checked all images for quality, ensuring proper visualization of the vasculature was achieved in each. ImageJ software was then used to quantify the fluorescence intensity of the images using the integrated density function, an algorithm that measures the mean gray value in a selected area of the image and then multiplies it by the selected area. The integrated density was measured for both the 2 minute and 4 minute images. The integrated density at 2 minutes (baseline) was then subtracted from the integrated density at 4 minutes, with the difference in integrated density between 2 and 4 minutes employed as a readout of vascular leakage. This method was used in **Chapter III**.

Decellularization experiments

For experiments with hRMEC-derived matrices, media was changed to EBM supplemented with 5% FBS and SingleQuots for 24 hours once cultures reached 100% confluency. hRMEC were then treated for 48 hours with 10 ng/mL TNFα or IL-1β in 5% EBM. For experiments with hRP-derived matrices, hRP were treated at 75% confluency with 10 ng/mL TNFα or IL-1β for 48 hours in serum-reduced media. Subsequently, hRMEC or hRP cultures were decellularized using methods adapted from published protocols.[192-194] Briefly, cultures were washed once with PBS before treatment with decellularization buffer (20 mM NH_4OH and 0.5% Triton-X (vol/vol) in PBS (with Ca and Mg)) at 37°C; cultures were monitored visually for complete decellularization (5-10 minutes). Decellularized ECM was washed three times by adding PBS in equal volume

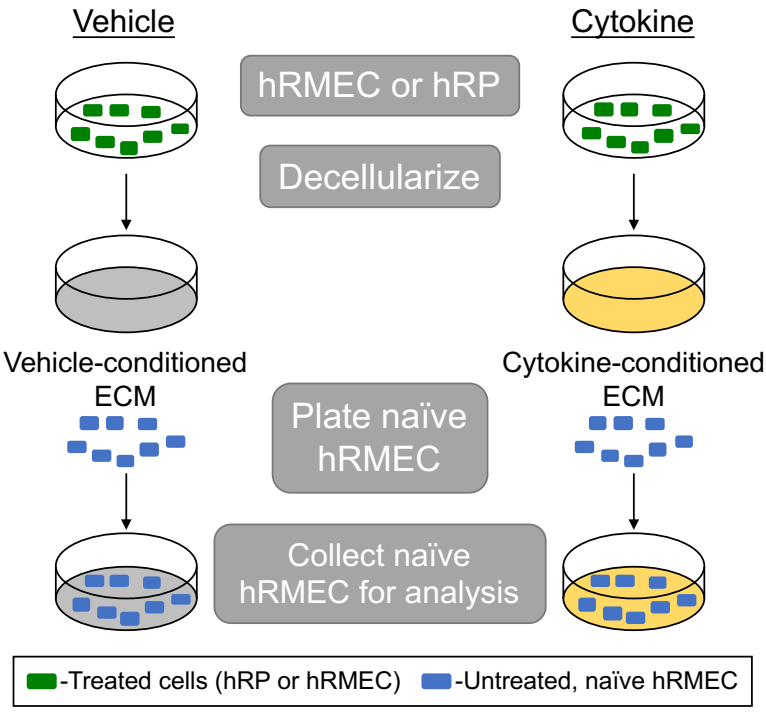

Figure 6: Experimental design of decellularization experiments. hRMEC or hRP were treated with cytokines, either TNFα or IL-1β, and allowed to deposit ECM before cultures were decellularized. Naïve hRMEC were then plated onto the cytokine-conditioned ECM and subsequently collected for qRT-PCR analysis or utilized in static adhesion assays or PPFC.

to the dish to dilute cellular debris and then removing half of the volume.[194] Naïve hRMEC were plated to settle at a density of 85% confluency onto the hRMEC- or hRP-derived matrices and allowed to settle onto the decellularized ECM for 16 hours before collection for qRT-PCR analysis (**Figure 6**). This method was used in **Chapter IV**.

Immunocytochemistry

Complete decellularization of cultures was confirmed by immunocytochemistry, using methods adapted from published protocols (**Figure 7**).[195] Cultures were decellularized and washed as described above. Decellularized ECM was then fixed in 4% PFA (Electron Microscopy Sciences; Hatfield, PA) for 30 minutes at 37°C. Slides were blocked in 1.5% BSA in PBST for 1 hour at room temperature and then incubated with the following primary antibodies for 1 hour at room temperature: anti-collagen IV (Abcam; Waltham, MA) and anti-fibronectin (Santa Cruz Biotechnology; Dallas, TX). Slides were then incubated with Alexa Fluor-labeled secondary antibodies (Invitrogen; Waltham, MA) for 1 hour at room temperature. F-actin and nuclei were subsequently

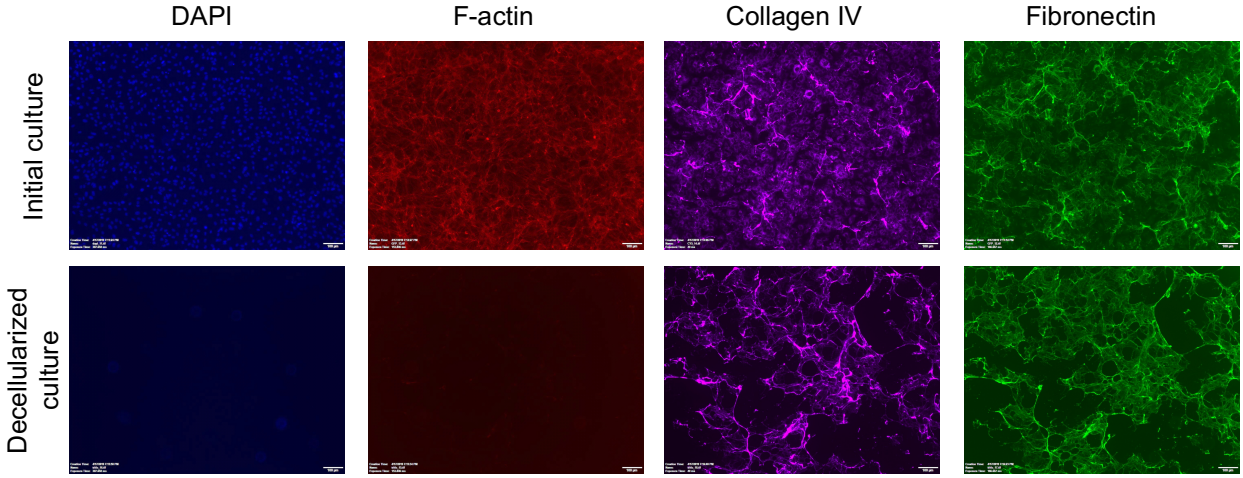

Figure 7: Representative images of successful decellularization of hRMEC culture. hRMEC were stained for DAPI, F-actin, collagen IV, and fibronectin. The top row is a normal hRMEC culture and the bottom row demonstrates the ECM left after the complete removal of cells using decellularization buffer.

labeled, following the manufacturer's instructions, using 555 Fluorescent Phalloidin (Cytoskeleton, Inc; Denver, CO) and DAPI (Tocris), respectively.

Static adhesion assay (SAA)

hRMEC or hRP were plated onto attachment factor-coated 24-well plates and allowed to settle at room temperature for 15 minutes (to ensure proper monolayer formation). Cells were treated as indicated above for decellularization experiments. After treatment, cultures were decellularized, decellularized ECM was washed three times as above, and naïve hRMEC were plated to settle as a confluent monolayer and allowed to settle for 8 hours before SAA was performed. The SAA protocol was adapted from published protocols;[178,179] briefly, human PBMC were stained with NucBlue for 20 minutes at 37°C at the manufacturer's suggested concentration and then spun down and resuspended. PBMC were added to each well at a concentration of 125,000 cells/cm^2 and allowed to settle onto monolayers for 30 minutes at 37°C. Subsequently, PBMC were removed and cultures were gently washed three times with warm PBS to remove non-adherent cells. Cultures were then fixed in 1% PFA for 10 minutes at 37°C. Cultures were washed once with warm PBS. Three fields were randomly selected per well and adherent PBMC were counted. Each data point represents the average number of adherent leukocytes for the three captured fields per well and is reported as adherent cells per mm^2. This method was used in **Chapter IV**.

Decellularization and sample solubilization for mass spectrometry

After treatment (see "hRMEC culture and treatment"), cultures were decellularized and ECM was solubilized using methods adapted from published protocols.[192-194] Cultures were washed once with PBS and treated with decellularization buffer (20 mM NH_4OH and 0.5% Triton-X (vol/vol) in PBS (with calcium and magnesium)) for 5 minutes at 37°C. To wash decellularized ECM, PBS was added in equal volume to the dish to dilute cellular debris and then half of the volume was removed.[194] This washing was repeated three times. Decellularized ECM was then treated with 10μg/mL DNase I (Roche; Basel, Switzerland) for 30 minutes at 37°C. Decellularized ECM was washed twice with PBS. Warm solubilization buffer (62.5mM TrisHCl, pH 6.8 25% glycerol, 5% βME, 5% SDS, and 0.01% bromophenol blue) was added and decellularized ECM was physically removed using cell scrapers. Samples were then heat denatured for 20 minutes at 70°C and subsequently spun down at 14,000 rpm for 5 min at 4°C. Protein concentration was measured using the Pierce 660nm Protein Assay (Thermo Fisher), according to the manufacturer's instructions including use of the ionic detergent compatibility reagent to account for the high SDS concentration. This method was used in **Chapter V**.

Mass spectrometry (MS), quantification, and analysis

S-Trap micro spin column digestion was performed on ECM extracts according to the manufacturer's recommendations. Briefly, protein samples (10μg) in solubilization buffer (see above) were reduced with 20 mM DTT and alkylated with iodoacetamide at a final concentration of 40 mM. Aqueous phosphoric acid was added to the sample to

obtain a final concentration of 1.2% phosphoric acid. A volume of 600 μL of S-Trap binding buffer was added to each sample. The mixture was placed on S-Trap micro columns and centrifuged (4000 x *g*) until all the volume was passed through the column. Columns were washed five times with 150 μl of S-Trap binding buffer, and proteins were digested with 20 μL of 50ng/μL trypsin (Promega; Madison, WI) in 50mM ammonium bicarbonate for 1 hours at 47C. Peptides were then eluted with 40 μl of 50 mM ammonium bicarbonate followed by 40 μl of 0.2% aqueous formic acid and 35 μl of 0.2% formic acid in 50% acetonitrile. Peptides were dried by speed vac centrifugation.

Peptides were then analyzed by LC-coupled tandem mass spectrometry (LC-MS/MS). First, an analytical column was packed with 20cm of C18 reverse phase material (Jupiter, 3 μm beads, 300Å, Phenomenox) directly into a laser-pulled emitter tip. Peptides were loaded on the capillary reverse phase analytical column (360 μm O.D. x 100 μm I.D.) using a Dionex Ultimate 3000 nanoLC and autosampler. The mobile phase solvents consisted of 0.1% formic acid, 99.9% water (solvent A) and 0.1% formic acid, 99.9% acetonitrile (solvent B). Peptides were gradient-eluted at a flow rate of 350 nL/min, using a 90-minute gradient. The gradient consisted of the following: 1-73 min, 2-50% B; 73-78 min, 50-95% B; 78-79 min, 95% B; 79-80 min, 95-2% B; 80-90 min (column re-equilibration), 2% B. Upon gradient elution, peptides were analyzed using a data-dependent method on a Q Exactive Plus mass spectrometer (Thermo Scientific), equipped with a nanoelectrospray ionization source. The instrument method consisted of MS1 using an MS AGC target value of 3e6, followed by up to 15 MS/MS scans of the most abundant ions detected in the preceding MS scan. The MS2 AGC target was set

to 5e4, dynamic exclusion was set to 10s, HCD collision energy was set to 28 nce, and peptide match and isotope exclusion were enabled.

To determine the matrisome proteins identified in each sample, each protein list was annotated using the Matrisome Project's Matrisome Annotator tool.[196] MS/MS of peptide fragmentation were searched within the Skyline program (https://skyline.ms/project/home/software/Skyline) using the MSAmanda search engine (http://pubs.acs.org/articlesonrequest/AOR-6DyVQ3j4YTcGXyaskJvi), collated to protein level and filtered to require a minimum of two unique peptides. Peak selection and integration were performed within Skyline requiring the peak to be selected within 5 minutes of an identified MS/MS spectrum. Data were normalized using the "equalize medians" with the summary method of "Tukey's median polish" implemented from the MSStats package (Bioconductor - MSstats) directly in Skyline. This method was used in **Chapter V**.

Statistical analysis

All data were analyzed with Prism software (GraphPad; La Jolla, CA); values of $p < 0.05$ were considered statistically significant.

For **Chapter III**, analysis of variance (ANOVA) with Tukey's multiple comparisons post hoc analysis was used. Grubbs' test was utilized to identify outliers. For ECIS, two-way ANOVA with Tukey's multiple comparisons post hoc analysis was used.

For **Chapter IV**, student's *t*-test and ANOVA with Tukey's multiple comparisons post hoc analysis was used. The ROUT method was utilized to identify outliers.

CHAPTER III

Nuclear factor of activated T-cells (NFAT) regulation of IL-1β-induced retinal vascular inflammation

From: Giblin, M.J., Smith, T.E., Winkler, G., Pendergrass, H., Kim, M.J., Capozzi, M.E., McCollum, G.W., Yang, R., Penn, J.S. Nuclear factor of activated T-cells (NFAT) regulation of IL-1β-induced retinal vascular inflammation. *Biochim Biophys Acta Mol Basis Dis.* 2021 Dec 1;1867(12):166238. Epub 2021 Jul 31. PMC8565496.

Overview

Chronic low-grade retinal inflammation is an essential contributor to the pathogenesis of DR. It is characterized by increased retinal cell expression and secretion of a variety of inflammatory cytokines; among these, IL-1β has the reputation of being a major driver of cytokine-induced inflammation. Cytokines not only initiate retinal vascular damage but also activate autocrine and paracrine signaling cascades that promote chronic retinal inflammation, all of which contributes to the development of vision-threatening pathology.[5,94] Numerous studies have identified IL-1β as a primary driver of inflammation in a wide-range of pathological conditions, including neuro-inflammatory diseases, diabetes, and DR.[94,102,197-200] Abundant data suggest that IL-1β plays a causative role in several hallmark DR pathologies, including glial activation,[97] cell death,[103] vascular permeability,[104] leukocyte adhesion,[105,106] and vasoregression.[103] I became particularly interested in IL-1β as a driver of retinal inflammation after RNA sequencing experiments from our lab comparing human Müller cell (hMC) responses to

treatment with IL-1β, TNFα, IL-8, and IL-6 demonstrated that IL-1β caused the greatest and longest lasting inflammatory response in hMC. Interestingly, these data also identified IL-1β itself as one of the most highly upregulated genes in IL-1β-treated hMC, supporting existing evidence that increased IL-1β levels via auto-amplification may exacerbate and sustain retinal inflammation in DR.[102] In aggregate, this evidence suggests that IL-1β acts as a "master regulator" of inflammation in the pathological cascade of DR, and that preventing its downstream effects in retinal cells may therefore significantly slow inflammation-induced damage.[102,197,201]

IL-1β mediates downstream inflammatory signaling via the activation of several transcription factors, including nuclear factor of activated T-cells (NFAT).[202,203] The NFAT family consists of five proteins, four of which (c1-c4) are regulated by the calcium-dependent phosphatase calcineurin (CN).[204-206] In quiescent cells, NFAT exists in the cytosol in a hyperphosphorylated state. Upon challenge with an inflammatory stimulus, CN dephosphorylates NFAT, causing it to shuttle to the nucleus where it increases the transcription of inflammatory genes.[207-209] The small molecule inhibitor, Inhibitor of NFAT-Calcineurin Association-6 (INCA-6), blocks CN-NFAT association, thereby preventing the dephosphorylation/activation of the four CN-dependent NFAT isoforms.[210,211] NFAT is known to play a role in the regulation of inflammatory mediators, extracellular matrix proteins, vascular permeability, and adhesion molecules,[108,204,207,212-222] and as such may control multiple pathogenic steps early in DR. Additionally, published evidence demonstrates that NFAT inhibition is a successful strategy in preventing pathogenic retinal cell behaviors downstream of both hyperglycemia and TNFα.[108,218] Combined, these data demonstrate that NFAT mediates a variety of characteristic pathogenic

changes that arise in response to multiple components of the diabetic environment; therefore, I hypothesized that NFAT may likewise influence the response of retinal cells to elevated IL-1β in the diabetic milieu.

The diabetic retina is a complex environment of multiple cell types, including endothelial cells, pericytes, astrocytes, and Müller cells.[50] Pathogenic behaviors by each of these cell types do not exist in isolation, rather they can produce both autocrine and paracrine factors that potentiate disease progression in surrounding cells. For instance, VEGF, a major target of DR therapeutics, is secreted predominantly by Müller cells and subsequently causes downstream pathogenic responses in endothelial cells.[8,52,54] Since multiple retinal cell types are involved in the DR cascade and cell-specific targeting is difficult *in vivo*, it would be ideal to identify a therapeutic target with the capacity to inhibit pathological responses in more than one retinal cell type. Therefore, in this study, I sought to investigate the role of NFAT in regulating key cell-specific responses to IL-1β, specifically Müller cell auto-amplification of IL-1β and endothelial cell inflammation, leukocyte adhesion, and permeability. I found that inhibition of NFAT not only attenuates Müller cell amplification of inflammation but also inhibits the downstream pathologic response of human retinal microvascular endothelial cells (hRMEC) to IL-1β challenge. These results suggest that targeting NFAT has significant therapeutic potential for slowing early inflammation and subsequent endothelial cell dysfunction in DR.

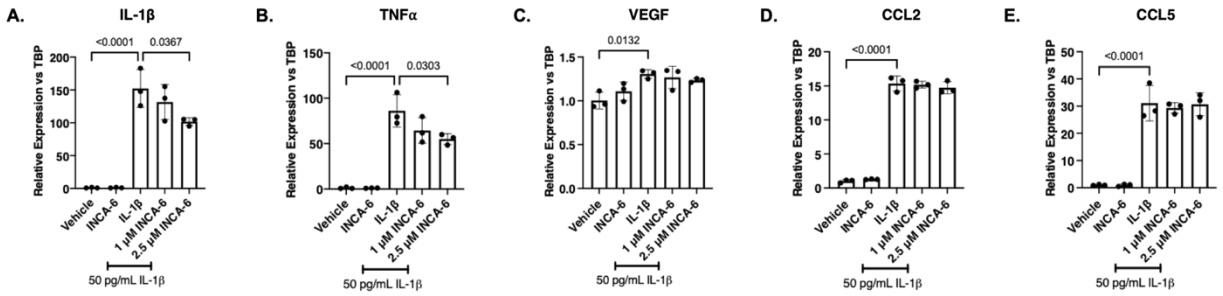

Figure 8: NFAT inhibition attenuates cytokine expression in hMC. hMC were treated for 8hrs with 50pg/mL IL-1β with or without INCA-6. Cells were collected and assayed for expression of (A) IL-1β, (B) TNFα, (C) VEGF, (D) CCL2, or (E) CCL5. Expression data are reported as fold induction over vehicle with bars representing mean +/- SD (n=3).

Results

INCA-6 decreases IL-1β-induced inflammatory cytokine expression in hMC

Based on Müller cells' known role as major propagators of retinal inflammation,[50,52,53,223] I first sought to determine if NFAT is involved in the regulation of hMC inflammatory responses in an autocrine and paracrine manner. IL-1β increased the expression of IL-1β (152-fold, $p<0.0001$), TNFα (86-fold, $p<0.0001$), VEGF (1.3-fold, $p=0.0132$), CCL2 (15-fold, $p<0.0001$), and CCL5 (31-fold, $p<0.0001$) in hMC. IL-1β and TNFα expression levels were decreased 34% ($p=0.0367$) and 36% ($p=0.0303$), respectively, in hMC co-treated with IL-1β and 2.5 μM INCA-6, compared to IL-1β alone (**Figure 8A-B**). INCA-6 had no effect on the IL-1β-induced expression of VEGF, CCL2, or CCL5 at either of the concentrations tested (**Figure 8C-E**).

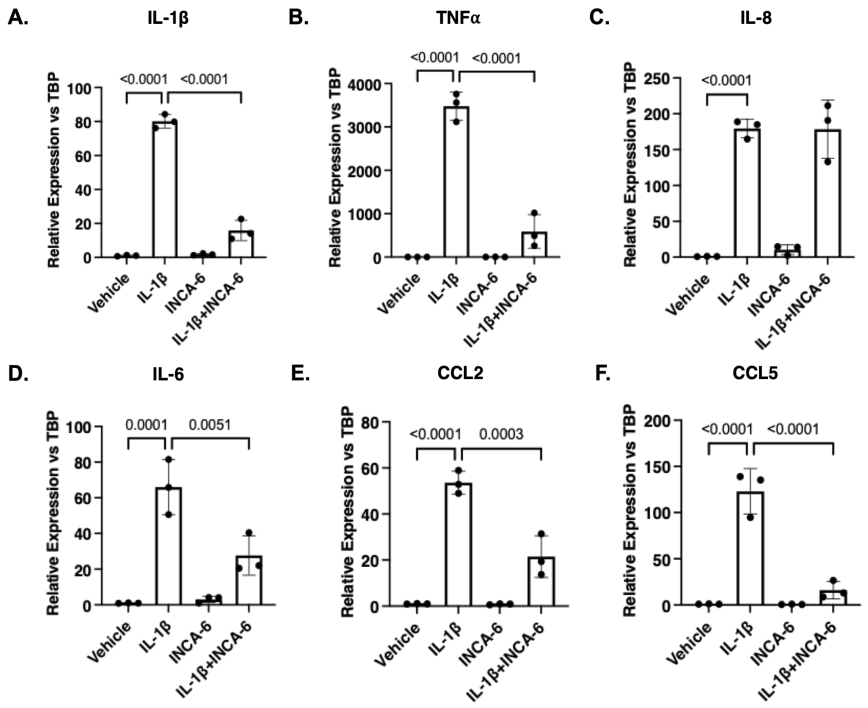

Figure 9: INCA-6 inhibits IL-1β induced cytokine expression in hRMEC. hRMEC were treated for 2hrs with 1ng/mL IL-1β with or without 5μM INCA-6. Cells were collected and assayed for expression of (A) IL-1β, (B) TNFα, (C) IL-8, (D) IL-6, (E) CCL2, or (F) CCL5. Expression data are reported as fold induction over vehicle with bars representing mean +/- SD (n=3).

INCA-6 decreases IL-1β-induced inflammatory cytokine expression in hRMEC

Similar to hMC, hRMEC respond to cytokine treatment by increasing expression and secretion of inflammatory cytokines, thereby propagating and sustaining local inflammation.[5,102] Therefore, I examined the NFAT-dependency of the hRMEC inflammatory response to IL-1β. IL-1β increased the expression of IL-1β (80-fold, $p<0.0001$), TNFα (3479-fold, $p<0.0001$), IL-8 (179-fold, $p<0.0001$), and IL-6 (66-fold, $p=0.0001$) in hRMEC. IL-1β, TNFα, and IL-6 expression decreased 81% ($p<0.0001$), 83% ($p<0.0001$), and 59% ($p=0.0051$), respectively, in hRMEC co-treated with IL-1β and 5μM INCA-6 compared to IL-1β alone. However, INCA-6 had no significant effect on IL-1β-induced IL-8 expression (**Figure 9A-D**). Additionally, I examined the chemokines, CCL2

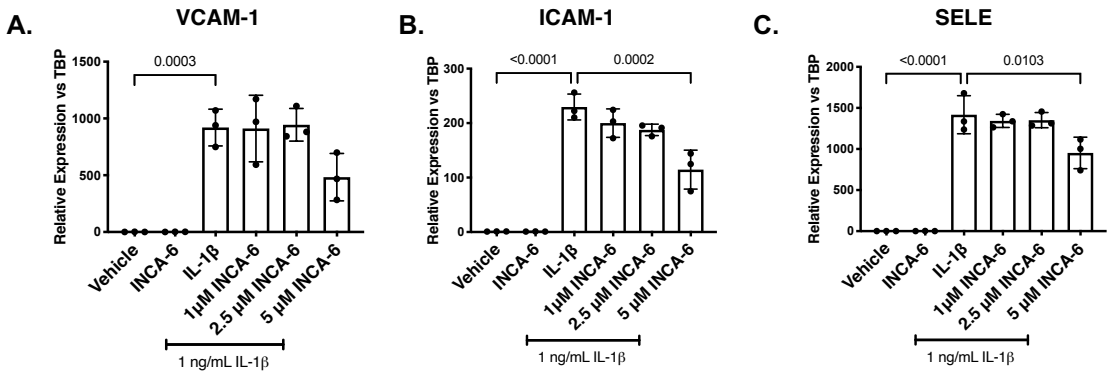

Figure 10: INCA-6 inhibits IL-1β-induced expression of leukocyte adhesion molecules in hRMEC. hRMEC were treated for 2hr with 1ng/mL IL-1β with or without INCA-6. Cells were collected and assayed for expression of (A) VCAM-1, (B) ICAM-1, or (C) E-selectin (gene name: SELE). Expression data are reported as fold induction over vehicle with bars representing mean +/- SD (n=3).

and CCL5. IL-1β increased the expression of CCL2 (53-fold, p<0.0001) and CCL5 (122-fold, p<0.0001) in hRMEC. CCL2 and CCL5 expression decreased 60% (p=0.0003) and 87% (p<0.0001), respectively, in hRMEC co-treated with IL-1β and 5μM INCA-6, compared to IL-1β alone (**Figure 9E-F**).

INCA-6 mitigates IL-1β-induced leukocyte adhesion to hRMEC

I sought to investigate the efficacy of INCA-6 in preventing inflammation-induced leukocyte-endothelial cell adhesion, a characteristic pathogenic event in NPDR.[5] For these experiments, I selected the optimal treatment times based previous data wherein I performed a time course of hRMEC adhesion molecule expression in response to IL-1β and TNFα treatment (**Appendix A**). I performed a brief dose response experiment to determine the optimal concentration of INCA-6 to mitigate IL-1β-induced adhesion molecule expression in hRMEC. IL-1β increased VCAM-1, ICAM-1, and E-selectin expression 920-(p=0.0003), 229-(p<0.0001), and 1417-fold (p<0.0001), respectively, in hRMEC. Statistically significant decreases in ICAM-1 (51%; p=0.0002) and E-selectin

(32%, p=0.0103) expression were achieved in hRMEC co-treated with IL-1β and 5μM INCA-6 (highest dose) compared to IL-1β alone (**Figure 10A-C**).

Next, I sought to determine if these changes in adhesion molecule expression translated into similar trends in PBMC adhesion to hRMEC monolayers using the parallel plate flow chamber (PPFC)

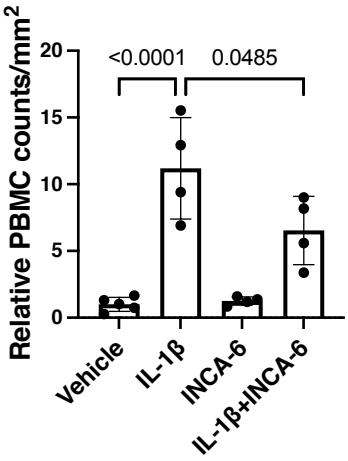

Figure 12: INCA-6 prevents IL-1β-induced PBMC adhesion to hRMEC. hRMEC were grown on slides until a confluent monolayer formed and then treated for 4hr with 1ng/mL IL-1β with or without 5μM INCA-6. Slides were placed in a PPFC, PBMC were flowed over the monolayers, and non-adherent cells were washed away. Adherent PBMC were counted in 8 fields per slide and averaged. Average counts were then divided by field area. Data are reported as fold induction over vehicle with bars representing mean +/- SD (vehicle: n=5; IL-1β: n=4; INCA-6: n=4; IL-1β+INCA-6: n=4).

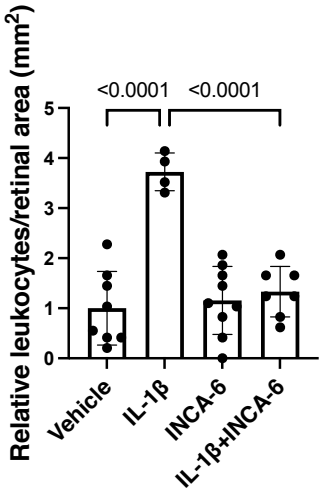

Figure 11: INCA-6 prevents IL-1β-induced retinal leukostasis in an acute model of retinal inflammation. Mice received intravitreal injections of IL-1β +/- INCA-6. 12hr-post injection, leukostasis analysis was performed. Adherent leukocytes were counted in 4 fields per retina and averaged. Average counts were then divided by field area. Data are reported as fold induction over vehicle with bars representing mean +/- SD (vehicle: n=8; IL-1β: n=4; INCA-6: n=9; IL-1β+INCA-6: n=7).

assay. IL-1β caused an 11-fold (p<0.0001) increase in PBMC adhesion to hRMEC monolayers. When monolayers were co-treated with IL-1β and 5μM INCA-6, the optimal

dose identified in Figure 10, PBMC adhesion to hRMEC monolayers decreased 41% (p=0.0485) compared to monolayers treated with IL-1β alone (**Figure 11**).

INCA-6 attenuates IL-1β-induced leukostasis in mice

Next, I investigated whether the efficacy of INCA-6 for inhibiting leukocyte adhesion *in vitro* could be translated *in vivo.* I used a mouse model of acute cytokine-induced retinal inflammation to test the efficacy of INCA-6 against retinal leukostasis. Retinal leukostasis increased 3.72-fold (p<0.0001) in C57BL/6J mice receiving intravitreal injections of IL-1β compared to vehicle. When mice received intravitreal injections of an IL-1β/INCA-6 cocktail, retinal leukostasis decreased to near vehicle levels (p<0.0001) (**Figure 12**).

INCA-6 rescues IL-1β-induced permeability

Finally, I was interested in determining whether INCA-6 was similarly efficacious in attenuating inflammation-induced vascular hyperpermeability, another characteristic pathology of NPDR.[5] Transendothelial electrical resistance (TEER) measurements were

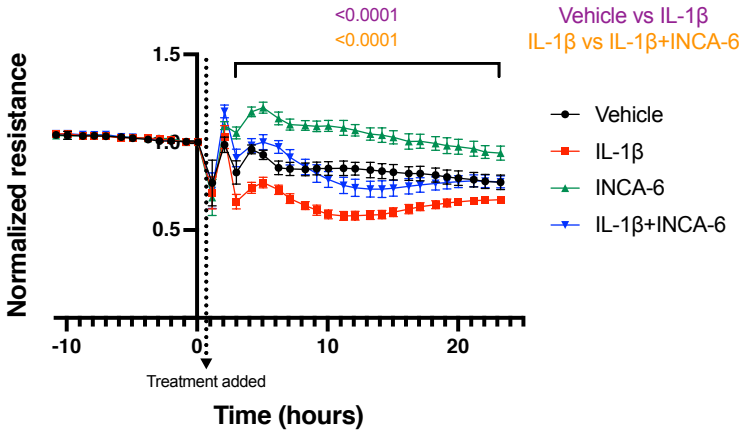

Figure 13: NFAT inhibition prevents IL-1β-induced hRMEC monolayer hyperpermeability. hRMEC were allowed to settle and form a monolayer on 96-well ECIS plates. Once resistance plateaued, monolayers were treated with 1ng/mL IL-1β with or without 5μM INCA-6 and changes in resistance were monitored over 24hr. Resistance was normalized to plateaued resistance directly prior to treatment (timepoint 0). Data represent mean +/- SD (vehicle, IL-1β, and IL-1β+INCA-6: n=12; INCA-6: n=6).

performed to assess whether INCA-6 has the capacity to correct IL-1β-induced defects in hRMEC barrier function. IL-1β decreased the normalized resistance of hRMEC monolayers 40% (t=2-23 hours, p<0.0001) compared to vehicle. This decreased barrier function was essentially reversed in hRMEC monolayers co-treated with IL-1β and INCA-6 (t=2-23 hours, p<0.0001) (**Figure 13**). This is clearly demonstrated during the last 6 hours of monitoring, during which there were no significant differences between the normalized resistance measures of hRMEC monolayers treated with vehicle compared to those co-treated with IL-1β and INCA-6; control phenotype was completely restored. Interestingly, INCA-6 alone caused an increase in resistance over vehicle (t=2-23 hours, p<0.0001).

I also tested the capacity of INCA-6 to rescue retinal vascular hyperpermeability *in vivo*, assessed by fluorescein angiography, in our acute model of retinal inflammation. The fluorescein intensity in retinal fundus images nearly doubled (p=0.0296) in mice receiving intravitreal injections of IL-1β, indicating pronounced leakage from retinal

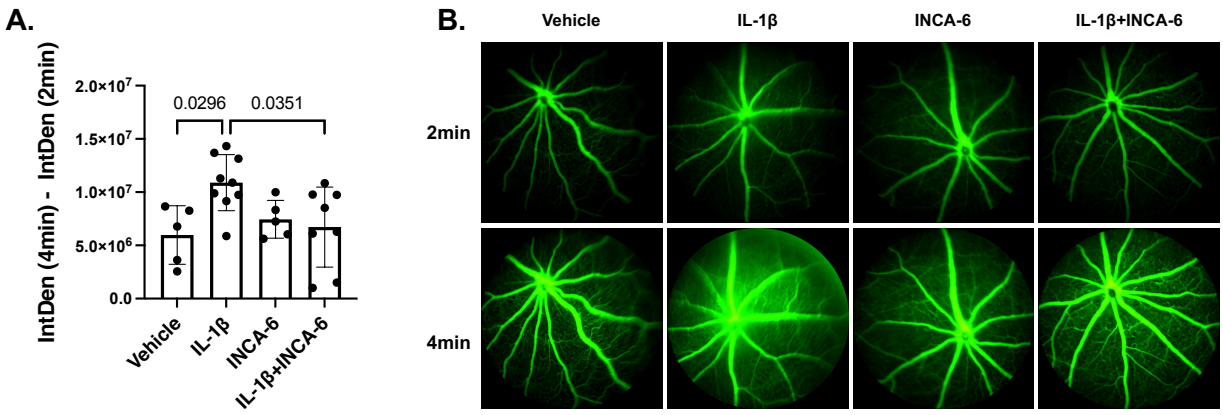

Figure 14: INCA-6 prevents IL-1β-induced vascular hyperpermeability in an acute model of retinal inflammation. Mice received intravitreal injections of IL-1β +/- INCA-6. 8hr post-injection, fluorescein was injected and fluorescent fundus images were captured at 2 and 4min post-fluorescein injection. (A) The difference in integrated density between images was calculated and recorded as a readout of vascular leakage. Bars represent mean +/- SD (vehicle: n=5; IL-1β: n=9; INCA-6: n=5; IL-1β+INCA-6: n=8). (B) Representative images of fluorescent fundus images obtained 2min (top row) and 4min (bottom row) after fluorescein injection.

capillaries. The fluorescein intensity decreased 84% (p=0.0351) in mice receiving intravitreal injections of an IL-1β/INCA-6 cocktail (**Figure 14A-B**).

Conclusions

My findings demonstrate for the first time that NFAT controls multiple IL-1β-induced inflammatory responses in both Müller cells and retinal microvascular endothelial cells. We had previously demonstrated that NFAT inhibition prevents TNFα-induced retinal leukostasis.[108] However, since the diabetic retinal environment contains a complex mix of inflammatory cytokines, it is desirable to identify a therapeutic target that can universally slow pathogenic responses to multiple stimuli. Additionally, mounting evidence indicates that IL-1β acts as a master regulator of the retinal inflammation consequent to diabetes. Therefore, I tested the potential of INCA-6 to inhibit IL-1β-induced Müller cell and endothelial cell inflammation, leukocyte-endothelial cell adhesion, and vascular hyperpermeability in order to investigate the importance of CN/NFAT signaling in multiple pathogenic events of relevance to DR.

The current clinical approach to targeting the CN/NFAT signaling axis utilizes drugs (cyclosporin A and Tacrolimus) that block CN's ability to phosphorylate any substrate.[208,209,211] Therefore, they indiscriminately prevent downstream signaling, including important signaling hubs like MAP-K, contributing to severe side effects. Recent efforts have focused on identifying small molecule inhibitors that can specifically inhibit NFAT activation with minimal effects on CN's other substrates.[209] INCA-6 prevents the protein-protein interaction between CN and NFAT at the NFAT docking site and was identified based on its ability to compete out the high affinity VIVIT peptide. INCA-6 not

only inhibited NFAT activation – as measured by phospho-NFAT Western blot, NFAT nuclear translocation staining, and expression levels of known NFAT target mRNA – but also showed no inhibition of CN phosphatase activity, no changes in MAP-K activation, and no changes in non-NFAT controlled mRNA expression.[211] Based on this favorable specificity profile, I chose to utilize INCA-6 for my studies, selecting dose ranges in the lowest concentrations conventionally used *in vitro*.[108,224-228]

Müller cells are retina-specific macroglia that act as sensors of the local environment, and it is well established that Müller cells become activated in the diabetic milieu.[53,229] We have previously demonstrated that, among non-neuronal retinal cells, Müller cells have the most potent inflammatory response to a variety of diabetes-relevant stimuli.[52] Furthermore, we have also observed that IL-1β potently induces its own expression in hMC, supporting published findings that suggest IL-1β auto-amplification propagates and sustains retinal inflammation.[102] Although NFAT has been previously implicated in the control of inflammatory responses in other glial cell types,[221,230-232] a potential role in Müller cell inflammation has not been established. To determine whether NFAT inhibition could attenuate Müller cell inflammatory responses, I examined hMC expression of key representative inflammatory mediators: IL-1β, TNFα, VEGF, CCL2 (also MCP-1), and CCL5 (also RANTES). Analogous to findings in other investigations of glial cell responses,[221,230-232] my data demonstrated that INCA-6 effectively inhibits the potent IL-1β-induced expression of IL-1β and TNFα in hMC. Recent evidence, in microglia, has indicated that NFAT can signal not only via calcium-dependent nuclear translocation but also via a calcium-independent mechanism involving mitochondrial translocation.[233] However, since INCA-6 acts by blocking the binding of CN and NFAT, I

believe that, here, NFAT is acting in hMC via its canonical calcium-dependent mechanism, not this novel calcium-independent mechanism. INCA-6 was not efficacious in preventing the modest IL-1β-induced increases in VEGF, CCL2, or CCL5 expression in hMC. I believe it is likely an advantage that this therapeutic approach acts independently of VEGF regulation. Despite diabetic macular edema (DME) being the leading cause of vision loss in DR patients, a recent meta-analysis comparing the efficacies of aflibercept, ranibizumab, and bevacizumab predicted that only 3-4 out of every 10 DME patients will experience improvement after one year of anti-VEGF therapy.[24] Consequently, numerous combination therapies in which anti-VEGF therapy is combined with an additional target are currently in development with the goal of achieving greater efficacy in a wider patient population than anti-VEGF alone.[120,121] Therefore, my data suggest that NFAT inhibition may be a potent and effective complement to anti-VEGF, though further study is certainly needed. Overall, these data suggest that NFAT inhibition can block the effects of both autocrine and paracrine sources of inflammation in hMC and represent the first report of the role of NFAT in regulating Müller cell expression of inflammatory genes.

Retinal microvascular endothelial cells demonstrate a wide range of molecular responses to the diabetic environment that contribute to the development of characteristic DR lesions.[68] Therefore, the identification of therapeutic targets whose inhibition could halt these endothelial responses would be highly beneficial in slowing DR pathogenesis. Although endothelial cell inflammatory responses to primary metabolic stimuli are lower in magnitude compared to those seen in Müller cells,[52] endothelial cells still become activated in response to cytokines and contribute to autocrine and paracrine inflammatory

signaling.[68] Indeed, it is likely that the potent response of Müller cells to primary metabolic stimuli in the diabetic environment contributes heavily to the initiation and subsequent propagation of inflammation by endothelial cells. NFAT inhibition has been shown to mitigate vascular inflammation in a variety of disease contexts.[215,217,219] Importantly, previous findings demonstrated that NFAT inhibition attenuated TNFα-induced chemokine expression in hRMEC[108,212] and prevented diabetes-induced IL-10 reduction in STZ mice.[218] Therefore, I investigated whether INCA-6 could inhibit hRMEC expression of an array of inflammatory cytokines and chemokines, in a manner similar to the results I saw in hMC. When hRMEC were treated with IL-1β in the presence of INCA-6, NFAT inhibition caused a significant decrease in the expression of IL-1β, TNFα, IL-6, CCL2, and CCL5. Interestingly, NFAT showed differential regulation of inflammatory genes in hRMEC compared to hMC. Given the capacity of each of these cytokines to induce downstream pathological behaviors in endothelial cells, including leukostasis and vascular hyperpermeability,[5,84,92,126,234] I find it highly encouraging that INCA-6 attenuates cytokine expression across a range of genes in hRMEC. Particularly in the case of CCL2 and CCL5, whose primary function is chemotaxis of leukocytes, inhibition in hRMEC is significant owing to the immediate proximity of the endothelium to the circulation. Overall, these results demonstrate that NFAT regulates IL-1β-dependent inflammatory responses in both Müller cells and microvascular endothelial cells, suggesting that targeting NFAT might significantly inhibit retinal inflammation at multiple points along the pathogenic cascade of DR.

Increased leukocyte adhesion, or leukostasis, is considered a landmark event of NPDR and has been observed in both diabetic animals[60-63] and patients.[64-67] Adherent

leukocytes contribute to DR pathogenesis in multiple ways, including eliciting and propagating local inflammation as well as occluding capillaries, leading to focal retinal ischemia.[5,8] The diabetic milieu induces the expression of several endothelial cell adhesion proteins leading to increased leukocyte adherence. Specifically, E-selectin is responsible for the initial tethering and rolling of leukocytes on the endothelium, while VCAM-1 and ICAM-1 are responsible for the arrest and firm anchoring of leukocytes.[235,236] Our previous studies demonstrated that targeting NFAT using INCA-6 or NFAT isoform-specific siRNA inhibited TNFα-induced expression and presentation of adhesion proteins in hRMEC and decreased leukocyte adherence to both hRMEC monolayers *in vitro* and blood vessel walls *in vivo*.[108] Consistent with these data, NFAT inhibition has also proven efficacious in preventing inflammation-induced increases in adhesion molecule levels in a variety of disease contexts.[214,215,219] Therefore, I advanced the hypothesis that INCA-6 would mitigate IL-1β-induced leukocyte adherence owing to decreased NFAT-dependent leukocyte adhesion molecule expression; my results suggest that this is indeed the case. Furthermore, I confirmed that these changes had beneficial functional outcomes by demonstrating the efficacy of INCA-6 against leukocyte adhesion *in vitro* using the PPFC. Finally, I chose to utilize an acute inflammation model to confirm the therapeutic potential of my NFAT inhibitory strategy *in vivo.* Using intraocular injections of IL-1β and an intraocular dose of INCA-6 that had proven efficacious in our hands,[108,228] I modeled the increased leukostasis characteristic of early DR in a high throughput approach with a short experimental timeline and demonstrated that INCA-6 significantly attenuates this IL-1β-induced increase in retinal leukostasis. It is important to note that all my *in vitro* data are exclusively focused on endothelial cells' role in endothelial cell-leukocyte adhesion.

However, NFAT was initially characterized in T-lymphocytes and extensive evidence exists supporting its role in leukocyte biology.[237-239] Therefore, it is possible that in the *in vivo* setting INCA-6 is acting not only on endothelial cells, as characterized by my PPFC experiments, but also on circulating immune cells. Further characterization of these effects will be sought in future studies.

The barrier function of the retinal endothelium depends on highly-organized junctional complexes that occlude the paracellular cleft between adjacent endothelial cells.[59] Metabolic dysfunction and increased retinal levels of inflammatory cytokines occurring in DR activate molecular signals that lead to junctional complex disorganization and the associated deficit of barrier function. The changes result in vascular hyperpermeability leading to the development of characteristic fundus lesions of NPDR and/or DME, the most common cause of vision loss in DR patients.[5,8] It is well established that IL-1β promotes retinal vascular hyperpermeability,[5,104,240] and evidence in other disease models suggests that NFAT is involved in control of vascular permeability. For instance, NFAT inhibition attenuated lung vascular permeability in an animal model of sepsis[216] and completely abrogated the retinal vascular hyperpermeability observed in Akita mice.[218] Therefore, I utilized ECIS to measure TEER across hRMEC monolayers and demonstrated that INCA-6 had significant efficacy in attenuating the decreased resistance seen in IL-1β-treated monolayers. I further supported these findings by using qFA to demonstrate that INCA-6 similarly rescued IL-1β-induced hyperpermeability in our model of acute retinal inflammation. Interestingly, in my ECIS experiments, treatment with INCA-6 alone caused an increase in resistance over vehicle, suggesting that INCA-6 can

improve barrier function of even healthy hRMEC monolayers. Taken together, my findings demonstrate that NFAT inhibition mitigates multiple inflammatory responses in hRMEC.

Our studies utilized an acute model of retinal inflammation to allow for the rapid assessment of efficacy of my NFAT inhibitory strategy, and it will be important to expand investigations of NFAT inhibition to diabetic animals with retinopathy. Furthermore, because a number of characteristic NPDR events, such as pericyte dropout or acellular capillaries, are not recapitulated by our acute inflammation model, I did not directly investigate the role of NFAT in their regulation. However, since chronic retinal inflammation is ultimately responsible for driving all types of NPDR lesions, I believe that by attenuating the propagation of early inflammation in DR, NFAT inhibition will likewise attenuate downstream events. For instance, in **Chapters IV** and **V**, I demonstrate a novel role for TNFα and IL-1β in driving the increased retinal expression of ECM constituents that underlies retinal capillary BM thickening. Thus, if INCA-6 can slow Müller and endothelial cell-derived inflammation, it would also have the indirect, downstream benefit of slowing cytokine-induced BM thickening development. Moreover, though my primary focus here was prevention of damage early in DR pathology, significant evidence from our lab and others suggests that NFAT inhibition could also be efficacious against the angiogenesis and neovascularization characteristic of late stage DR.[215,228,241-246] Of particular relevance, our previous work demonstrated that INCA-6 inhibits VEGF-induced hRMEC proliferation and tube formation and that both INCA-6 and the CN inhibitor, FK-506, significantly reduced pathologic neovascularization in a rat model of oxygen-induced retinopathy.[228] These findings further support the therapeutic potential of NFAT inhibition to slow or prevent DR progression at any stage.

There is an urgent need for therapies targeting early DR that prevent disease progression to the irreparable damage caused by PDR. Since early DR pathology involves a variety of altered behaviors in several retinal cells, identifying a therapy that can target multiple pathogenic events in multiple cell types is ideal. To this end, I have demonstrated that NFAT inhibition can attenuate multiple IL-1β-induced pathogenic cell behaviors in both hMC and hRMEC. Combined with our previous findings that NFAT inhibition can similarly prevent TNFα-induced retinal leukostasis,[108] I have significant evidence that NFAT is a target with substantial therapeutic potential for slowing retinal inflammation under DR-relevant conditions. Furthermore, previous studies have demonstrated that NFAT inhibition is similarly efficacious against hyperglycemia-induced retinal changes.[218] When considered in combination with our previous TNFα and my current IL-1β findings, it appears that NFAT inhibition can block retinal pathogenic responses elicited by a range of diabetes-relevant stimuli, suggesting NFAT is an excellent target to globally slow the downstream inflammatory effects of the complex diabetic milieu. Overall, I have identified a multi-faceted therapeutic target to inhibit not only Müller cell amplification of diabetic inflammation but also endothelial pathogenic responses, including increased inflammation, leukocyte adhesion, and vascular hyperpermeability.

CHAPTER IV

Effect of cytokine-induced alterations in extracellular matrix composition on diabetic retinopathy-relevant endothelial cell behaviors

From: Giblin, M.J., Penn, J.S. Effect of cytokine-induced alterations in extracellular matrix composition on diabetic retinopathy-relevant endothelial cell behaviors. *Scientific Reports* (Under review)

Overview

Compared to the other molecular events known to give rise to NPDR lesions, including pericyte apoptosis, increased vascular permeability, leukostasis, and capillary dropout, BM thickening has been vastly understudied for its potential to contribute to DR pathology. However, a few pivotal studies have since demonstrated that BM thickening plays a role in driving other events in NPDR, including pericyte loss, acellular capillaries, and vascular hyperpermeability.[155,156] Additionally, a number of studies have expanded our understanding of how BM thickening progresses, demonstrating in *in vitro* and *in vivo* models that increased expression and deposition of key ECM constituents, such as collagen IV, fibronectin, and laminin, are likely to advance the development of a thicker BM. [145,149,152,157-160,162-169] However, much remains to be understood about both the development of BM thickening and how BM thickening may contribute to the DR pathological cascade.

Among the limited studies of BM thickening in DR, the focus has been almost exclusively on the role of high glucose in stimulating changes in ECM expression and protein secretion by endothelial cells (EC). Although an important aspect of BM thickening, this approach ignores the potential contributions of other elements of the diabetic environment as well as other retinal cell types. First, while hyperglycemia is an important element, the diabetic environment is a complex mix of metabolic and inflammatory signals.[5,247] In recent years, the roles of dyslipidemia and chronic inflammation in DR pathogenesis have come under increased scrutiny.[5,51,52,62,98,99,107,108,247,248] However, few studies have explored the potential roles of lipid metabolites[249] or inflammatory cytokines[167,250] in promoting retinal BM thickening. Second, pericytes, Müller glia, and astrocytes are also key components of the neurovascular unit in addition to EC, and therefore could be involved in dysregulation of BM deposition.[251-255] In particular, both pericytes and EC are considered important sources of microvascular BM constituents, and pericyte ECM deposition is known to be altered in other disease states.[174,177,254,256-259] The retina has the highest pericyte coverage of any vascular bed in the body, with pericytes present in a 1:1 ratio with EC, suggesting that pericytes could contribute significantly to retinal BM thickening.

Since cell-matrix interactions in the vascular unit represent complex mechanical and trophic signals, diabetes-induced changes in retinal BM could significantly alter the behavior of surrounding cells.[145] In other tissues, alterations in ECM constituency are known to contribute to impaired EC-pericyte communication, changes in microvascular permeability, inappropriate cell-matrix adhesions, and alterations in leukocyte

extravasation.[143,145,149,171-179] Yet, despite this significant evidence from other tissues and disease states that cell-matrix interactions contribute to pathogenic cell behaviors, little is known about how changes in retinal BM might accelerate characteristic NPDR events. For instance, it is well established that cell-matrix interactions and alterations in ECM constituency affect the leukocyte adhesion cascade.[171,174,176,260] Evidence has shown that both EC- and pericyte-derived ECM alterations can promote changes in expression of adhesion molecules and subsequent leukocyte behavior.[174,178,179] Overall, substantial evidence exists that changes in both EC- and pericyte-derived ECM can directly affect EC-leukocyte adherence, suggesting that diabetes-induced BM alterations might contribute to leukostasis in NPDR.

Therefore, in this chapter, I sought to better understand how BM thickening might develop in response to the diabetic environment, and the potential of diabetes-related BM changes to promote the increased leukocyte adherence characteristic of NPDR. First, I undertook a systematic analysis to determine how multiple retinal cell types change their expression patterns of ECM constituents under a variety of diabetes-relevant conditions. In this initial assessment, I chose to examine five ECM constituents: collagen IV, fibronectin, laminin β1, and the core proteins of the heparan sulfate proteoglycans agrin and perlecan. These proteins were selected based on their upregulation in diabetic animal models and human tissue and/or their central roles in BM function.[130,133,152,153,155-161,261] I utilized diabetes-relevant stimuli (DRS) which modeled the three major insults of the diabetic environment: hyperglycemia, dyslipidemia, and chronic retinal inflammation.[5,8,247] After surveying changes in the expression of key ECM constituents by hRMEC and human retinal pericytes (hRP) in

response to DRS, I identified the inflammatory cytokines TNFα and IL-1β as having the most consistent and potent effects on ECM expression in retinal cells. Both TNFα and IL-1β are known to be elevated in the ocular fluids and retinal tissues of humans with DR and diabetic animals.[5,81-83,85,88,89,93,262-264] Furthermore, inhibition of TNFα or IL-1β signaling has been shown to attenuate retinal vascular pathologies in diabetic rodents,[111,122,124-126] and the nonsteroidal anti-inflammatory drug, Sulindac, prevented retinal capillary BM thickening in diabetic dogs.[250] I then utilized decellularized matrices derived from hRMEC or hRP under inflammatory conditions to investigate how changes in ECM might contribute to pathogenic behaviors in hRMEC. I demonstrated that inflammation-induced changes in ECM alone are sufficient to drive increased leukocyte adhesion molecule expression in, as well as increased leukocyte adherence to, naïve hRMEC.

Results

Inflammatory cytokines TNFα and IL-1β cause significant changes in expression of key ECM constituents in hRMEC

The limited focus of previous studies on high glucose in driving BM thickening ignores the potential contributions that chronic inflammation or diabetic dyslipidemia may also make. Therefore, I utilized a number of DRS to model different elements of the diabetic environment, specifically: TNFα, IL-1β, IL-6, and IL-8 to model chronic retinal inflammation;[5,80-83,85-89,93,262-266] palmitic, oleic, and linoleic acid to model diabetic dyslipidemia;[73,181-184,247,267] and high glucose to model diabetic hyperglycemia.[11] Using these DRS, I undertook a systematic assessment using qRT-PCR to determine how

	Collagen IV		Fibronectin		Laminin β1		Agrin		Perlecan	
Diabetes-relevant stimulus	Fold change	P-value	Fold change	P-value	Fold change	P-value	Fold change	P-value	Fold change	P-value
High glucose	1.04	ns	0.86	ns	0.88	ns	1.07	ns	**1.20**	**.0203**
Palmitic acid	0.94	ns	**0.74**	**0.0101**	0.82	ns	0.97	ns	0.99	ns
Oleic acid	1.08	ns	**0.55**	**0.0045**	0.76	ns	0.67	ns	0.81	ns
Linoleic acid	0.99	ns	**0.69**	**0.003**	1.01	ns	0.99	ns	**1.17**	**0.0348**
TNFα	**2.13**	**0.0002**	**0.68**	**0.0032**	0.97	ns	**2.31**	**<0.0001**	**0.56**	**0.0075**
IL-1β	**2.03**	**<0.0001**	1.07	ns	1.08	ns	**1.44**	**0.0036**	0.83	ns
IL-6	**0.80**	**0.0354**	1.01	ns	0.99	ns	1.16	ns	0.89	ns
IL-8	**0.89**	**0.0244**	0.86	ns	**0.86**	**0.0148**	0.90	ns	0.85	ns

Table 2: Diabetes-relevant stimuli cause significant effects in ECM expression by hRMEC. ECM gene expression was measured using qRT-PCR. All statistical comparisons used t-tests between the DRS-treated group and its respective vehicle, except for the case where normal glucose, L-glucose (osmotic control), and high glucose were compared. In that case ANOVA with Tukey post-hoc was used. For simplicity, only L-glucose vs high glucose is reported here. Expression data are reported as fold induction over vehicle. Red cells highlight statistically significant decreases in expression; green cells highlight statistically significant increases in expression.

different elements of the diabetic environment alter hRMEC expression of key ECM constituents: collagen IV, fibronectin, laminin β1, and the core proteins of the heparan sulfate proteoglycans agrin and perlecan. Under my experimental conditions, I did not observe any significant changes in the expression of four of the five ECM constituents under high glucose conditions (**Table 2**); high glucose only caused a modest significant increase in perlecan expression (1.20-fold, p=0.0203). All three free fatty acids caused significant decreases in fibronectin, while linoleic acid caused a small but significant increase in perlecan expression. No other significant changes were observed with free fatty acid treatment. Interestingly, I found that the cytokines TNFα and IL-1β were most consistent in causing alterations in ECM expression across multiple genes. TNFα caused 2.13- (p=.0002), 0.68- (p=0.0032), 2.31- (p<0.0001), and 0.56-fold (p=.0075) changes in the expression of collagen IV, fibronectin, agrin, and perlecan, respectively. Similarly, IL-1β caused 2.03- (p<0.0001) and 1.44-fold (p=.0036) changes in the expression of collagen IV and agrin, respectively.

	Collagen IV		Fibronectin		Laminin β1		Agrin		Perlecan	
Diabetes-relevant stimulus	Fold change	P-value	Fold change	P-value	Fold change	P-value	Fold change	P-value	Fold change	P-value
High glucose	0.88	ns	1.05	ns	1.01	ns	1.10	ns	1.06	ns
Palmitic acid	**0.71**	**0.0151**	**0.84**	**0.0078**	**0.58**	**0.0016**	**0.58**	**0.0037**	**0.50**	**0.0041**
Oleic acid	0.92	ns	**0.75**	**0.0215**	**0.77**	**0.0189**	0.86	ns	**0.77**	**0.001**
Linoleic acid	0.83	ns	0.80	ns	**0.76**	**0.029**	0.86	ns	0.88	ns
TNFα	**2.76**	**<0.0001**	0.97	ns	**0.65**	**0.0027**	**3.27**	**<0.0001**	**1.32**	**0.0012**
IL-1β	**1.83**	**0.002**	**0.81**	**0.0311**	**0.59**	**0.0025**	**1.18**	**0.0166**	**1.18**	**0.0099**
IL-6	1.45	ns	1.16	ns	1.24	ns	0.93	ns	0.95	ns
IL-8	1.06	ns	1.07	ns	1.08	ns	1.00	ns	1.06	ns

Table 3: Diabetes-relevant stimuli cause significant effects in ECM expression by hRP. ECM gene expression was measured using qRT-PCR. All statistical comparisons used t-tests between the DRS-treated group and its respective vehicle, except for the case where normal glucose, L-glucose (osmotic control), and high glucose were compared. In that case ANOVA with Tukey post-hoc was used. For simplicity, only L-glucose vs high glucose is reported here. Expression data are reported as fold induction over vehicle. Red cells highlight statistically significant decreases in expression; green cells highlight statistically significant increases in expression.

Inflammatory cytokines are also the most potent inducers of changes in ECM expression in hRP

Pericytes are known contributors to both normal and pathogenic deposition of vascular BM, and yet their role in BM thickening in DR has been previously ignored.[174,177,256-259] Therefore, I also completed a systematic assessment, using qRT-PCR, of how hRP alter expression of key ECM constituents under DRS treatment. Interestingly, similar trends were observed in the types of DRS that caused significant alterations in expression of ECM constituents by hRP. Specifically, high glucose, IL-6, and IL-8 did not cause any significant changes, while TNFα and IL-1β caused potent alterations in hRP expression of most ECM constituents (**Table 3**). TNFα caused 2.76- ($p<0.0001$), 0.65- ($p=0.0027$), 3.27- ($p<0.0001$), and 1.32-fold ($p=0.0012$) changes in the expression of collagen IV, laminin β1, agrin, and perlecan, respectively. Similarly, IL-1β caused alterations in the expression of all five constituents under study, specifically: 1.83- ($p=0.002$), 0.81- ($p=0.0311$), 0.59- ($p=0.0025$), 1.18- ($p=0.0166$), and 1.18-fold ($p=0.0099$) changes in the expression of collagen IV, fibronectin, laminin β1, agrin, and perlecan, respectively. Interestingly, palmitic acid caused significant decreases in the

expression of all five constituents. Oleic acid caused significant decreases in both fibronectin and laminin β1, while linoleic acid only caused a significant decrease in laminin β1 expression. I noted many interesting findings in this survey, which will provide the basis for future studies. However, based on the increasing importance of inflammation in DR and the lack of investigations into its role in BM thickening, I chose to narrow my focus to TNFα and IL-1β in subsequent experiments.

hMC cause only minor alterations in ECM expression but hMC-derived inflammation can influence hRMEC ECM expression

I performed a small pilot study utilizing key DRS (high glucose, TNFα, and IL-1β) to investigate if hMC similarly altered their expression of ECM constituents under DRS. No significant changes in collagen IV expression were observed and only TNFα caused a significant decrease in fibronectin expression (**Figure 15A**). All three DRS caused changes in laminin β1 expression with high glucose causing a slight increase (1.23-fold, p=0.0056) and both TNFα and IL-1β causing a 0.71-fold decrease (p=0.0014 and p=0.0139, respectively) (**Figure 15A**). Overall, the expression changes observed were smaller compared to changes observed in hRMEC and hRP and thus I did not pursue hMC in subsequent decellularization experiments. However, evidence suggests that Müller cells are a primary driver of retinal inflammation.[50,52,53,99,223,268,269] Conditioned media (CM) from TNFα-treated hMC caused no significant changes in collagen IV or agrin expression in hRMEC (**Figure 15B-C**). Conversely, when hRMEC were treated with CM from IL-1β-treated hMC, expression of both collagen IV and agrin increased in

A.

Diabetes-relevant stimulus	Collagen IV		Fibronectin		Laminin β1	
	Fold change	P-value	Fold change	P-value	Fold change	P-value
High glucose	1.05	ns	1.03	ns	**1.23**	**0.0056**
TNFα	0.96	ns	**0.75**	**0.0152**	**0.71**	**0.0014**
IL-1β	0.83	ns	0.84	ns	**0.71**	**0.0139**

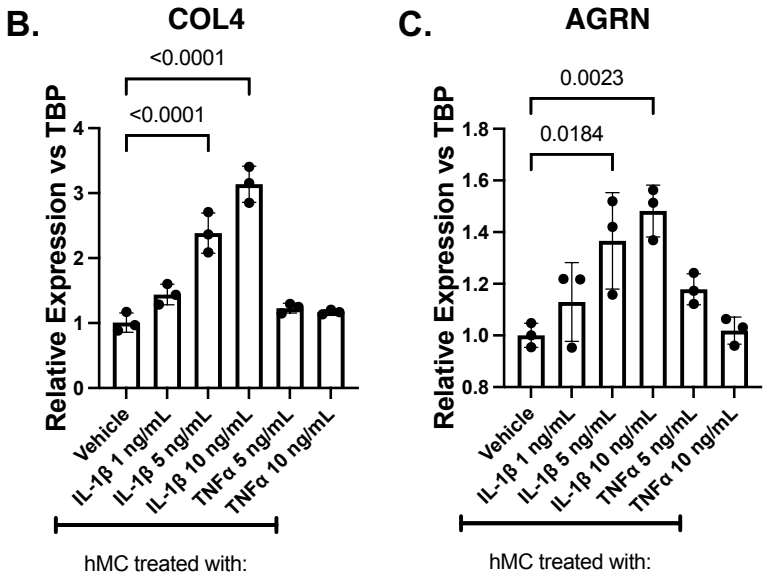

Figure 15: hMC-derived inflammation can influence hRMEC ECM expression. (A) ECM gene expression was measured using qRT-PCR. All statistics are t-tests between the DRS-treated group and its respective vehicle. Expression data are reported as fold induction over vehicle. Red cells highlight statistically significant decreases in expression; green cells highlight statistically significant increases in expression. (B) and (C) Conditioned media (CM) was collected from IL-1β- or TNFα-treated hMC. hRMEC were treated with CM from hMC and then collected and assayed for expression of collagen IV or agrin. Expression data are reported as fold induction over vehicle with bars representing mean +/- SD (n=3 for all groups).

a dose-dependent manner. At the highest dose, CM from IL-1β-treated hMC caused a 3.14-($p<0.0001$) and 1.48-fold ($p=0.0023$) increase in collagen IV and agrin expression, respectively (**Figure 15B-C**).

ECM conditioned by cytokine-treated hRMEC causes induction of adhesion molecules in naïve hRMEC

Numerous studies have demonstrated that changes in the constituency and/or biomechanics of vascular BM drive increased leukocyte adhesion to vascular endothelium.[171,174-176,178,179,260] Therefore, based on my finding that DR-relevant

cytokines significantly alter the expression of ECM constituents in retinal cells, I hypothesized that this inflammation-conditioned ECM contributes to the development of retinal leukostasis. To investigate how inflammation-induced changes in ECM could alter the behavior of naïve EC, I adopted previously described decellularization techniques. In these experiments (**Figure 6**), hRMEC are first treated with cytokines TNFα or IL-1β. Cultures are then decellularized, and naïve hRMEC are plated on the vehicle- or cytokine-conditioned ECM. Naïve hRMEC are subsequently collected to analyze expression of key leukocyte adhesion mo, E-selectin (gene name *SELE)*, ICAM-1, and VCAM-1, in naïve EC. The naïve hRMEC receive no treatment; the only difference between the control and experimental cultures is the conditioned ECM upon which they attach. When naïve hRMEC were grown on ECM derived from TNFα-treated hRMEC, 2.08- and 1.24-fold increases in E-selectin and VCAM-1 expression were observed, respectively; however, results did not reach statistical significance. When naïve hRMEC were plated on ECM derived from IL-1β-treated hRMEC, 4.30- ($p<0.0001$), 2.26- ($p<0.0001$), and 1.62-fold ($p<0.0001$) increases in E-selectin, ICAM-1, and VCAM-1 expression were observed, respectively, relative to hRMEC plated on ECM derived from non-treated hRMEC (**Figure 16A-C**).

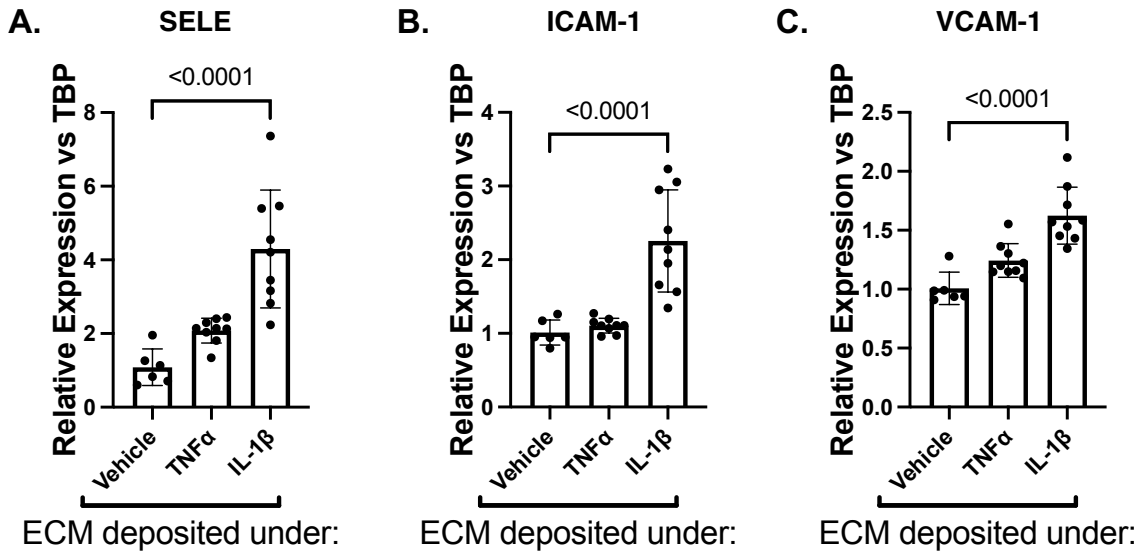

Figure 16: ECM conditioned by cytokine-treated hRMEC causes induction of adhesion molecules in naïve hRMEC. Naïve hRMEC were plated onto ECM derived from TNFα- or IL-1β-treated hRMEC. Cells were collected and assayed for expression of (A) E-selectin (gene name: SELE), (B) ICAM-1, or (C) VCAM-1. Expression data are reported as fold induction over vehicle with bars representing mean +/- SD (vehicle: n=6; TNFα: n=9; IL-1β: n=9).

Cytokine-conditioned matrix derived from hRMEC is sufficient to drive increased PBMC adhesion to naïve hRMEC

I next sought to determine if the changes seen in adhesion molecule expression resulted in corresponding changes in leukocyte adhesion behavior. To answer this question, I utilized static adhesion assays to test PBMC adhesion to monolayers grown on cytokine-conditioned ECM. When hRMEC monolayers were grown on TNFα-conditioned ECM, there was a 1.44-fold (p=0.0408) increase in PBMC adhesion to the

naïve hRMEC. Likewise, when monolayers were grown on IL-1β-conditioned ECM, there was a 1.89-fold ($p<0.0001$) increase in PBMC adhesion (**Figure 17**).

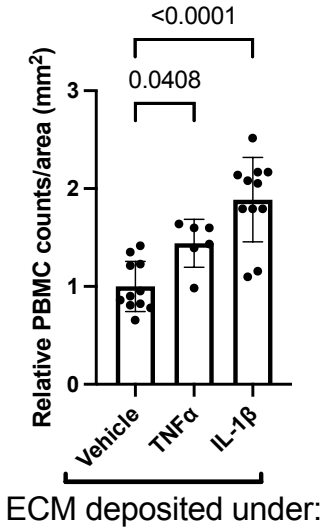

Figure 17: ECM derived from TNFα- or IL-1β-treated hRMEC causes increased PBMC adhesion. Naïve hRMEC monolayers were plated onto ECM derived from TNFα- or IL-1β-treated hRMEC. PBMC were added to naïve hRMEC, allowed to adhere, and washed to remove non-adherent cells. Adherent PBMC were counted in 3 regions per well and averaged. Average counts were then divided by count area. Data are reported as fold induction over vehicle with bars representing mean +/- SD (vehicle: n=11; TNFα: n=6; IL-1β: n=11).

I additionally sought to investigate changes in leukocyte behavior in the PPFC, as it is a more physiologically relevant assay than static adhesion. I measured adherent PBMC both before and after washing away lightly adherent cells. When hRMEC monolayers were grown on TNFα-conditioned ECM, there was a 2.76-fold (p=0.0310) increase in PBMC adhesion to the naïve hRMEC prior to wash. Likewise, when monolayers were grown on IL-1β-conditioned ECM, there was a 2.36-fold increase in PBMC adhesion (**Figure 18A**). After washing the monolayers, there was a 2.7-fold (p=0.0089) and 2.25-fold (p=0.0408) increase in PBMC adhesion to monolayers grown on TNFα-conditioned ECM and IL-1β-conditioned ECM, respectively (**Figure 18B)**.

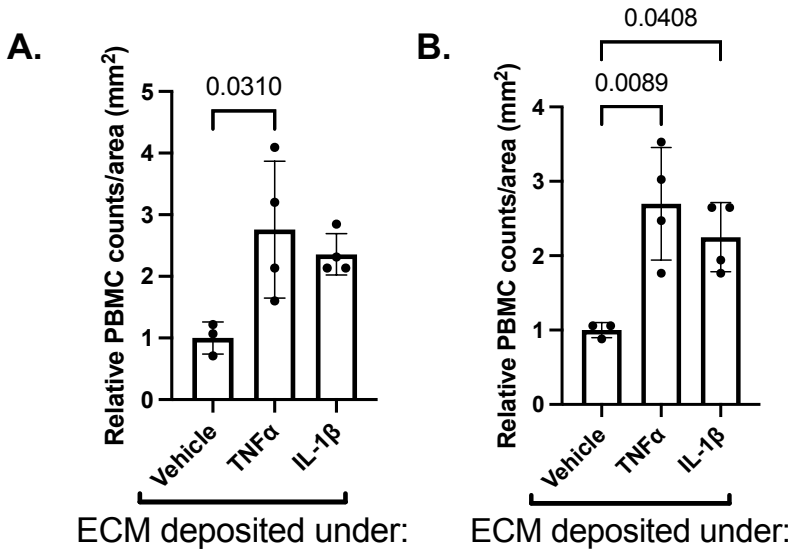

Figure 18: ECM derived from TNFα- or IL-1β-treated hRMEC causes increased PBMC adhesion in PPFC. Naïve hRMEC monolayers were plated onto ECM derived from TNFα- or IL-1β-treated hRMEC. Slides were placed in a PPFC, PBMC were flowed over the monolayers, and non-adherent cells were washed away. Adherent PBMC were counted in 8 fields per slide before (A) and after (B) wash and counts were averaged. Average counts were then divided by field area. Data are reported as fold induction over vehicle with bars representing mean +/- SD (n=3-4).

ECM derived from cytokine-treated hRP causes induction of hRMEC adhesion molecules

Based on my findings that hRP, similar to hRMEC, alter expression of ECM constituents under TNFα or IL-1β treatment, I investigated whether hRP-derived ECM could also alter EC-leukocyte behaviors (see experimental design in **Figure 6**). Naïve hRMEC were plated onto TNFα- or IL-1β-conditioned ECM deposited by hRP, and expression of E-selectin, ICAM-1, and VCAM-1 was measured. When naïve hRMEC were plated on ECM derived from TNFα-treated hRP, 3.57- (p=0.0181) and 1.79-fold (p=0.0317) increases in E-selectin and ICAM-1 expression were observed, respectively (**Figure 19A-C**). Likewise, when naïve hRMEC were plated on ECM derived from IL-1β-treated hRP, 20.08- (p<0.0001), 2.29- (p=0.0022), and 2.01-fold (p=0.0038) increases in E-selectin, ICAM-1, and VCAM-1 expression were observed, respectively.

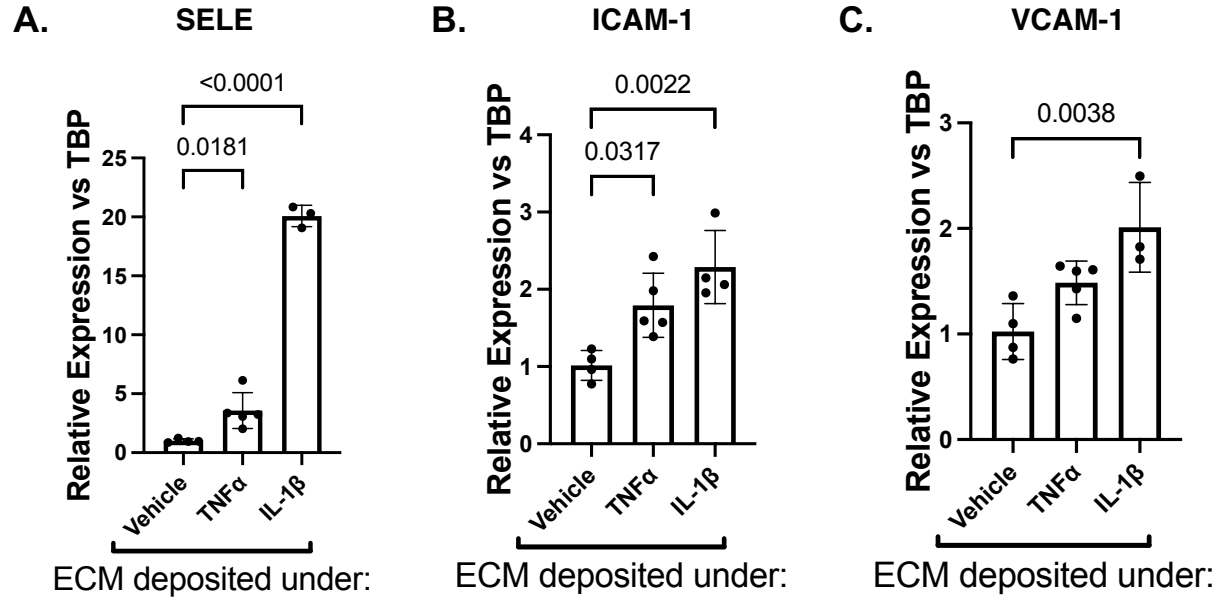

Figure 19: ECM derived from cytokine-treated hRP causes induction of hRMEC adhesion molecules. Naïve hRMEC were plated onto ECM derived from TNFα- or IL-1β-treated hRP. Cells were collected and assayed for expression of (A) E-selectin (gene name: SELE), (B) ICAM-1, or (C) VCAM-1. Expression data are reported as fold induction over vehicle with bars representing mean +/- SD (vehicle: n=4; TNFα: n=5; IL-1β: n=4).

Cytokine-conditioned matrix derived from hRP is sufficient to drive increased PBMC adhesion to naïve hRMEC

Finally, I sought to again investigate if the changes seen in adhesion molecule expression resulted in corresponding changes in leukocyte adhesion behavior utilizing static adhesion assays. When hRMEC monolayers were grown on TNFα-conditioned ECM derived from hRP, there was a 1.60-fold (p=0.0418) increase in PBMC adhesion to the naïve hRMEC (**Figure 20**). Likewise, when monolayers were grown on IL-1β-conditioned ECM derived from hRP, there was a 1.83-fold (p=0.0055) increase in PBMC adhesion.

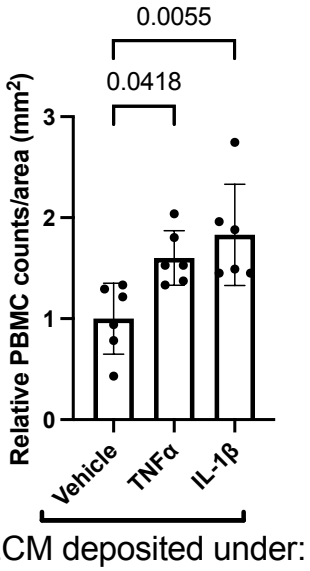

Figure 20: ECM derived from TNFα- or IL-1β-treated hRP causes increased PBMC adhesion. Naïve hRMEC monolayers were plated onto ECM derived from TNFα- or IL-1β-treated hRP. PBMC were added to naïve hRMEC, allowed to adhere, and washed to remove non-adherent cells. Adherent PBMC were counted in 3 regions per well and averaged. Average counts were then divided by count area. Data are reported as fold induction over vehicle with bars representing mean +/- SD (vehicle: n=6; TNFα: n=6; IL-1β: n=6).

Conclusions

In this chapter, I offer several new contributions to our understanding of BM thickening in DR. First, I demonstrate that conditions designed to mimic chronic inflammation (direct stimulation with inflammatory cytokines) caused larger alterations in expression of key ECM constituents by both hRMEC and hRP than did conditions that mimic hyperglycemia and dyslipidemia. Second, I demonstrate that the alterations in ECM that occur under these inflammatory conditions were alone sufficient to drive pathogenic behaviors in naïve EC. Third, I demonstrate that, similar to EC, pericytes both altered their expression of ECM constituents under inflammatory conditions and also deposited conditioned ECM that caused increased leukocyte adhesion to naïve EC, suggesting that pericytes may play a significant role in BM thickening.

To my knowledge, mine is the first systematic survey defining how different DRS affect retinal cell expression of ECM constituents. My qRT-PCR results demonstrate that, in both hRMEC and hRP, cytokines TNFα and IL-1β caused the largest changes in expression of key ECM constituents. The DRS designed to model diabetic hyperglycemia and dyslipidemia were either ineffective or far less effective in eliciting significant alterations than were TNFα or IL-1β. These findings are consistent with studies from our lab and others suggesting that chronic inflammation, particularly manifested via the cytokines TNFα and IL-1β, is a primary force behind the early pathogenic events in DR. [98,99,102,107,108,111,122,124-126] Therefore, in subsequent experiments, I focused my efforts on the role of inflammatory cytokines in driving ECM alterations. However, it is worth noting that the free fatty acids caused significant decreases in expression of fibronectin in hRMEC and both fibronectin and perlecan in

hRP. In particular, palmitic acid caused significant decreases in the expression of all five ECM constituents under study in hRP. Changes in the ratios of these constituents could represent major shifts in overall constituency, affecting stiffness of the vascular BM, thereby significantly contributing to altered cell-matrix interactions in DR. Although I chose to focus on cytokine-induced changes in the remainder of this study, future studies will focus on the potential contributions of these dyslipidemia-induced changes in ECM to DR pathology. Finally, I am aware that the failure of high glucose to stimulate altered expression of most ECM constituents in my experiments contradicts previously published studies.[162-166,168,169] However, previous studies had a number of limitations, including lack of an osmotic control for D-glucose treatment, ignoring the significant osmotic effects of high glucose, or use of rodent or non-retinal EC, despite hRMEC being known to be phenotypically unique from other common EC lines.[270-272]. In my studies, I was careful to utilize osmotic controls and primary human retinal microvascular cells. Furthermore, previous studies often treated EC with high glucose for long exposures (days or weeks); I chose relatively short exposure times (48 hours) to investigate more immediate expression changes in response to these stimuli. Although I did not find high glucose to cause notable changes in ECM expression during this time window, I do not mean to suggest that hyperglycemia plays no role in promoting retinal BM thickening. The diabetic environment offers a complex mixture of stimuli, with no single stimulus acting at one time. We have previously demonstrated that human Müller cells exhibit higher inflammatory responsivity to palmitic acid treatment when pre-treated with high glucose, suggesting an interplay between multiple

DRS.[51] High glucose could play a similar role in promoting BM thickening and future studies will investigate combinations of high glucose and free fatty acids.

Existing data have focused almost exclusively on the role of EC in the development of BM thickening, ignoring the potential contributions of other retinal cell types in the neurovascular unit. Since pericytes are highly abundant in the retina and contribute to both normal and pathogenic deposition of BM in other systems,[174,177,256-259] I hypothesized that pericytes might also be critical contributors to BM thickening in DR. Only one other study has specifically addressed the potential of pericytes to contribute to retinal BM thickening, and it found that pericyte-derived matrices had ten-fold higher levels of fibronectin than EC-derived matrices.[169] Furthermore, a recent report utilizing RNA sequencing to study pericytes isolated from diabetic mice identified "Enhancers of ECM synthesis" as one of the top hits in a gene set enrichment analysis.[273] This study was the first to provide a detailed analysis of the pericyte transcriptome in diabetic animals and further supports my hypothesis that pericytes play a major role in retinal BM thickening. My results demonstrate that both TNFα and IL-1β caused increased expression of collagen IV, agrin, and perlecan and decreased expression of laminin β1 in hRP. Interestingly, TNFα-treated hRP demonstrated higher relative fold changes in both collagen IV and agrin expression than hRMEC. These data are the first evidence that retinal pericyte expression of ECM constituents is altered under DRS and suggest that pericytes contribute to the development of BM thickening. In addition to pericytes, I considered the potential contributions of hMC since Müller cells are also in direct contact with the vascular BM and limited evidence points to their role in depositing ECM.[251] I performed a brief survey with hMC utilizing a limited set of DRS. Although I

did note significant changes in the expression of laminin β1, I chose not to pursue hMC further in this study since, overall, the changes were minor compared to those seen in hRMEC and hRP. However, we and others have evidence that Müller cells act as a primary driver of chronic retinal inflammation and serve as the major source of retinal TNFα and IL-1β in diabetes.[50,52,53,99,102,223,268,269] Interestingly, when hRMEC were treated with conditioned media from hMC treated with IL-1β, significant increases in collagen IV and agrin expression were observed in a clear dose-dependent manner. These results suggest that although Müller cells may not directly contribute to BM thickening, Müller cell-dependent inflammation may contribute to the initiation and progression of retinal BM thickening in surrounding cells. Future studies will include more detailed investigations into this cellular interplay. Additionally, in **Chapter III**, I demonstrated that INCA-6 has significant efficacy in reducing hMC-derived inflammation. My conditioned media results here further support the therapeutic potential of NFAT inhibition by demonstrating one of numerous pathogenic events downstream of hMC inflammation that would be mitigated by INCA-6.

Despite an increasing focus on inflammation in DR progression,[5,62,248] few studies have assessed the effects of inflammation on retinal matrix deposition. My systematic analysis of DRS raises many questions but here I chose to focus on the implications of my results with cytokine stimulation. First, in my studies, both hRMEC and hRP demonstrated significantly increased expression of collagen IV in response to treatment with TNFα and IL-1β, results directly in line with multiple studies that have demonstrated increased collagen IV synthesis in *in vitro* and *in vivo* models of DR.[145,149,158-160,164-167] Second, the decreased perlecan expression seen in TNFα-treated

hRMEC is in line with the results of a mass spectrometry study comparing the constituencies of retinal vascular BM isolated from non-diabetic and diabetic donors, wherein perlecan was identified as a constituent that was more abundant in the non-diabetic BM than the diabetic BM.[153] I noted significant changes in agrin and perlecan expression under TNFα and IL-1β in both hRMEC and hRP. These findings have important implications for retinal cell-matrix interactions; indeed, I specifically chose to include agrin and perlecan in this study because heparan sulfate proteoglycans play such key roles in the structure and function of BM. Heparan sulfate proteoglycans provide important structural contributions to BM integrity, serve as depots of regulatory factors such as cytokines and growth factors, and facilitate the establishment of chemokine gradients for leukocyte recruitment and homing in tissues,[130,133] yet their role in retinal BM thickening has been largely overlooked. Finally, my findings that fibronectin expression either decreased (hRMEC) or remained unchanged (hRP) under DRS were surprising as multiple studies have identified increases in fibronectin in diabetic rodents and humans.[152,153,157,159,161,261] However, my studies only capture expression changes at a single time point, highlighting an important limitation of qRT-PCR studies. For this reason, in the next chapter, I have completed studies utilizing quantitative mass spectrometry to investigate changes in ECM deposition under both TNFα and IL-1β treatment. It is interesting to note that for both hRMEC and hRP, TNFα caused more potent changes in ECM expression than IL-1β. However, in the decellularization experiments, IL-1β-conditioned ECM caused more potent changes in adhesion molecule expression and leukocyte adhesion. These results suggested that important ECM properties are governed by more than my five key ECM constituents,

and further necessitates the quantitative mass spectrometry approach described in **Chapter V**.

Although vascular BM thickening has long been considered a characteristic event in early DR,[154] it has been overlooked for its potential to advance other events in the pathologic cascade. However, a series of *in vivo* studies in rodent models of diabetes demonstrated that antisense oligonucleotides targeting key BM constituents not only reduced capillary BM thickening but also reduced other early NPDR events, including pericyte loss, acellular capillaries, and vascular hyperpermeability.[155,156] Additionally, *in vitro* studies have demonstrated that high glucose-induced changes in ECM can alter EC permeability and apoptosis as well as pericyte apoptosis.[156,166,274,275] These studies provided clear evidence that BM thickening is an active participant in the DR pathologic cascade and invited further exploration into the ways in which BM alterations could elicit pathogenic vascular cell behavior. Leukostasis is an important and well-studied event in NPDR and is a consequence of increased endothelial expression of the leukocyte adhesion proteins E-selectin, ICAM-1, and VCAM-1. Adherent leukocytes can occlude capillaries leading to downstream ischemia or amplify local inflammation and release of pro-apoptotic factors.[5,60-62,64,94] Numerous studies have demonstrated that cell-matrix interactions can produce changes in leukocyte adhesion,[171,174,176,260] including two studies in retinal EC demonstrating that changes in ECM stiffness associated with high glucose treatment were sufficient to increase monocyte adhesion to EC.[178,179] Here, I demonstrated that when naïve hRMEC are grown on ECM deposited by IL-1β-treated hRMEC, they increase expression of leukocyte adhesion molecules, and this increased expression is sufficient to cause increased PBMC adhesion. My results from TNFα-

conditioned ECM showed increased trends in adhesion molecule expression that did not reach significance. Yet, increased PBMC adhesion was observed, suggesting that TNFα can also drive ECM alterations sufficient to promote pathogenic cell behavior. Furthermore, in the PPFC, both TNFα- and IL-1β-conditioned ECM caused increased PBMC adhesion to naïve hRMEC monolayers. I am the first to examine chronic retinal inflammation as a contributor to altered cell-matrix dynamics in retinal cells. Coupled with what is known about the effects of glucose on cell-matrix interactions,[178,179] these data suggest that the diabetic environment promotes significant alterations in cell-matrix dynamics that subsequently contribute to pathogenic cell behaviors.

Like EC-derived ECM, pericyte-derived ECM is known to alter cell behavior in a number of other systems.[174,177,256-259] Of particular relevance, alterations in ECM deposition by placental microvascular pericytes under pro-inflammatory conditions caused increased EC expression of ICAM-1 and neutrophil transmigration.[174] However, the potential role of pericyte-derived ECM in pathogenic retinal cell behavior has not previously been considered. When naïve hRMEC were grown on ECM deposited by TNFα- or IL-1β-treated hRP, significant increases in E-selectin, ICAM-1, and VCAM-1 expression were observed. Furthermore, naïve hRMEC monolayers showed increased PBMC adherence when grown on the TNFα- or IL-1β-conditioned hRP-derived ECM. These data demonstrate that, similar to EC, inflammation-induced changes in ECM derived from hRP alone are sufficient to elicit pathogenic leukocyte adhesion behavior. These studies are the first to demonstrate that hRP-derived matrices cause alterations in hRMEC behavior relevant to DR. These results are particularly exciting since there is increasing focus on the role of pericytes in vascular inflammation and leukocyte

extravasation.[276] Pericytes release leukocyte chemoattractants, express adhesion molecules, and control the direction of leukocyte motility through the vascular BM.[177,254,276-279] Therefore, it is of interest to explore how diabetes-relevant changes in ECM alter the path, timing, and success of leukocyte extravasation along pericytes processes and through the vascular BM. Understanding these complicated dynamics between pericytes, EC, vascular BM, and leukocytes will be key to fully elucidating the molecular mechanisms of early DR.

It is important to acknowledge the challenge of modeling a chronic disease that develops over decades using *in vitro* methods that take only hours or days, and the limitations inherent in the extrapolation of these methods to disease events. However, BM is a particularly difficult structure to study *in vivo*, particularly when multiple cells contribute to its construction and maintenance, and I believe that my *in vitro* environment offers a reasonable first step to identifying important cell-matrix relationships. I also recognize that the changes in expression of ECM constituents, expression of adhesion molecules, and leukocyte adhesion observed here are relatively modest. However, it is important to note that these changes were observed after short treatment times. DR is a disease that develops over years, allowing BM alterations ample time to develop, grow, and influence the behavior of the vascular endothelium. When these changes are extrapolated over time, one can appreciate how even slight changes can accumulate to create larger, clinically relevant problems. In summary, in this chapter, I provide evidence of a number of novel conclusions including the following: inflammation plays a key role in stimulating altered ECM constituent expression by hRMEC and hRP; inflammation-conditioned ECM alters hRMEC-

leukocyte interactions, and pericytes contribute significantly to the development of BM thickening and the subsequent altered cell-matrix dynamics.

Chapter V

Proteomic profiling of inflammation-related changes in the matrisome of retinal microvascular endothelial cells

Overview

Current understanding of the composition of normal retinal BM and thickened retinal BM in DR is primarily based in immunohistochemistry or mRNA studies of whole retina.[152,157-161] These studies have a number of drawbacks including their qualitative nature and/or contamination from other retinal ECM such as the inner limiting membrane. The insolubility of the ECM has historically made its study intractable; however, recent advances in proteomic techniques have made studies of whole ECM proteomes increasingly feasible. These techniques and studies have led to a greater understanding of the constituency of ECM, termed the matrisome, in a variety of organ and disease contexts, enabling the identification of cell type-specific roles in BM assembly, disease- and age-related shifts in constituency, and organ-specific information.[192,193,280-286] Importantly, a recent study established the proteome of the retinal vascular BM and subsequently compared the constituency of the retinal vascular BM in non-diabetics and diabetics with DR.[153,170] These two studies provided the first insight into the unique constituency of the retinal vascular BM and how it might be altered in DR. Although *in vivo* studies such as these provide the best insight into disease pathogenesis, utilizing *in vitro* methods to establish ECM transcriptomes or proteomes can provide a number of advantages over the *in vivo* preparations, including

eliminating the complexities of extracting intact ECM from tissues and allowing for the assignment of ECM production to specific cell types. Furthermore, *in vitro* ECM provides a tractable three-dimensional system in which to answer mechanistic questions while still maintaining features relevant to tissue physiology and cell behavior *in vivo*.[192,287,288] For instance, proteomic analysis of cell-derived ECM *in vitro* enabled the identification and characterization of two novel fibrotic liver components that were later validated *in vivo*.[193] However, similar *in vitro* analyses have not yet been performed in retinal vascular cells.

In **Chapter IV**, I identified the inflammatory cytokines TNFα and IL-1β as having the most consistent and potent effect on ECM expression by retinal cells. Therefore, in this chapter, I undertook studies to investigate the matrisome derived from hRMEC under normal and diabetes-relevant inflammatory conditions. Utilizing quantitative mass spectrometry (qMS), I investigated how the matrisome of hRMEC is altered under the influence of TNFα and IL-1β. I had four goals in undertaking the experiments discussed in this chapter: first, to validate whether expression changes seen in qRT-PCR results translated to changes in protein deposition; second, to identify the cell-specific matrisome deposited by hRMEC; third, to understand how the composition of the ECM was changing under cytokine treatment; and finally, to determine, based on published studies, whether this system represented an effective model of the retinal vascular BM.

Results

Identification of new growth substrate compatible with MS of matrisome

I sought to utilize qMS to compare the constituencies of the matrisomes deposited by hRMEC under normal growth conditions and cytokine treatment. However, the attachment factor on which we typically grow hRMEC contains human ECM proteins and therefore had the potential to confound the qMS analysis. Therefore, I identified a porcine gelatin with a mix of porcine ECM proteins similar to the constituency of attachment factor. I confirmed that hRMEC behaved in a similar manner on this new cell substrate in two experimental contexts: (1) long exposure to TNFα or IL-1β with a qRT-PCR readout for ECM proteins and (2) short exposure to TNFα or IL-1β with a qRT-PCR readout for adhesion proteins (**Figure 21**).

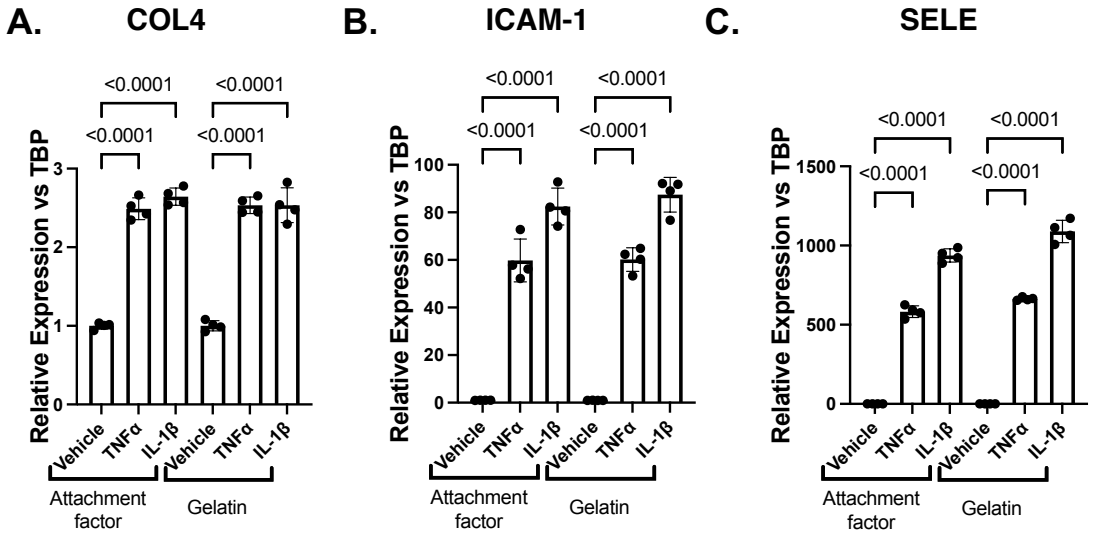

Figure 21: hRMEC behave similarly in multiple inflammatory contexts on both cell substrates. hRMEC were grown on attachment factor- or gelatin-coated dishes and then treated for (A) 48hrs with 10ng/mL TNFα or IL-1β to assay expression of ECM proteins or (B)(C) 2hrs with 1ng/mL TNFα or IL-1β to assay expression of adhesion proteins. Expression data are reported as fold induction over vehicle with bars representing mean +/- SD (n=4).

Quantitative MS identifies key differences in hRMEC matrisome under inflammatory conditions

To investigate how diabetes-relevant inflammatory conditions alter the constituency of the hRMEC matrisome, I treated hRMEC with either TNFα or IL-1β for 48 hours, decellularized and solubilized the underlying ECM, and submitted these samples for qMS analysis. Prior to submission, I measured the total protein concentration of the ECM samples and noted a significant increase in total protein deposited under both inflammatory conditions (**Figure 22**), supporting my hypothesis that inflammatory conditions drive increased ECM deposition. After MS data were collected, the online resources available through the Matrisome Project were used to annotate the identified list of proteins with matrisome labels.[196] 95 matrisome proteins were identified, including 14 collagens, 37 ECM glycoproteins, 24 ECM regulators, 10 ECM-affiliated proteins, 2 proteoglycans, and 8 secreted factors. 53 of these proteins

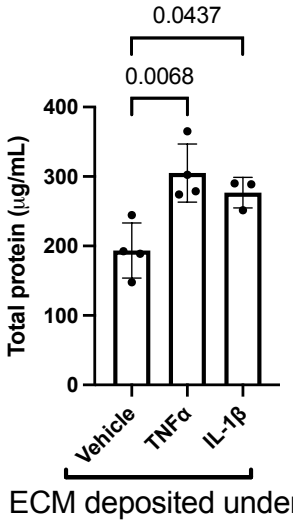

Figure 22: Cytokine-induced changes in total protein deposition by hRMEC. hRMEC were treated for 48hrs with 10ng/mL TNFα or IL-1β before collection for qMS analysis. Prior to qMS analysis, total protein concentration was assayed. Data are presented as total protein quantified (μg/mL) (n=3-4).

are considered core matrisome proteins and 42 are considered matrisome-associated (**Figure 23**). The full list of matrisome proteins identified in the hRMEC-derived samples can be found in **Appendix B**.

Overall, both TNFα and IL-1β caused significant alterations in the constituency of hRMEC-derived ECM (**Figure 24**). Label-free quantification was performed in Skyline (https://skyline.ms/project/home/software/Skyline) to compare the constituencies of the TNFα-conditioned ECM relative to vehicle. 23 matrisome proteins of interest were identified as significantly changed between the vehicle and TNFα-conditioned ECM, with 16 proteins meeting both the p-value and fold change thresholds (**Figure 25**). Within the significant changes in the TNFα-conditioned ECM, 11 proteins demonstrated increased deposition when compared with the vehicle-conditioned ECM, while 12 proteins demonstrated decreased deposition when compared with the vehicle-conditioned ECM. Of particular note, TNFα caused a 2-fold increase (p=0.023) in agrin

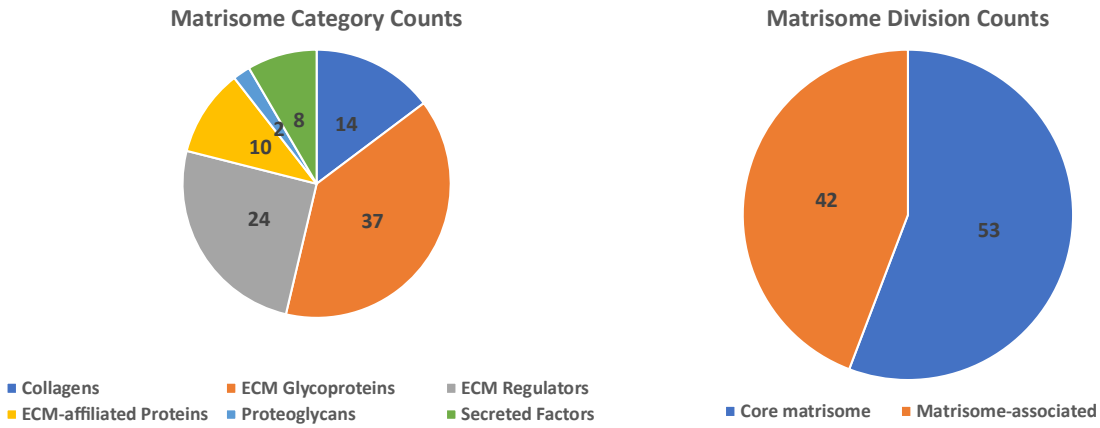

Figure 23: Matrisome proteins identified in MS results. Identified proteins were annotated based on (A) matrisome categories or (B) matrisome divisions determined by the Matrisome Project (*Characterization of the extracellular matrix of normal and diseased tissues using proteomics.* Naba et al. 2017).

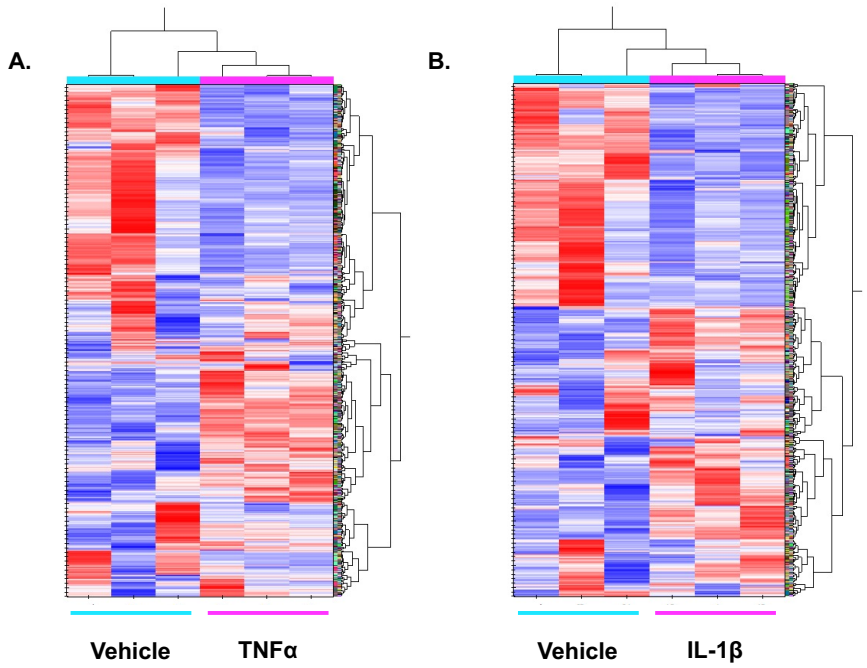

Figure 24: Cytokine treatment causes significant alterations in hRMEC-derived ECM. (A) Heat map of hierarchical clustering analysis of the TNFα- and vehicle-conditioned ECM. (B) Heat map of hierarchical clustering analysis of the IL-1β- and vehicle-conditioned ECM. HCA analysis was performed in Skyline; data were hierarchically clustered on the basis of Pearson correlation.

deposition. TNFα also caused increased expression in laminin γ2 (2.98-fold, p=0.0209) and laminin β3 (3.28-fold, p=0.0086). Interestingly, two of the greatest increases in deposition seen in the TNFα-conditioned ECM were degradation enzymes: urokinase deposition increased 3.41-fold (p=0.0352) and cathepsin S deposition increased 5.31-fold (p=0.0289).

Label-free quantification was also used to compare the constituencies of the IL-1β-conditioned ECM relative to vehicle. 30 matrisome proteins were identified as significantly changed between the vehicle- and IL-1β-conditioned ECM, with 21 proteins meeting both the p-value and fold change thresholds (**Figure 26**). Within the significant changes in the IL-1β-conditioned ECM, 16 proteins demonstrated increased deposition

when compared with the vehicle-conditioned ECM, while 14 proteins demonstrated decreased deposition when compared with the vehicle-conditioned ECM.

A.

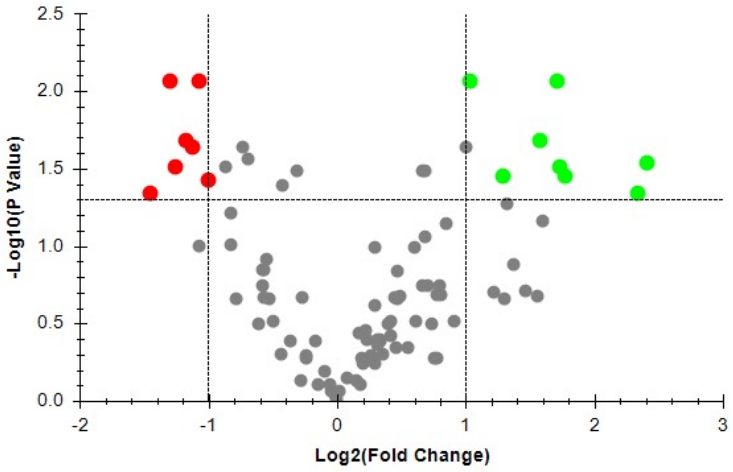

B.

Gene name (gene symbol)	UnitProt accession number	log2 (FC)	Adjusted P-value
C1q and tumor necrosis factor related protein 5(C1QTNF5)	Q9BXJ0	-1.47	0.0458
microfibrillar associated protein 2(MFAP2)	P55001	-1.32	0.0086
netrin 4(NTN4)	Q9HB63	-1.25	0.031
HtrA serine peptidase 3(HTRA3)	P83110	-1.18	0.0209
EGF containing fibulin like extracellular matrix protein 1(EFEMP1)	Q12805	-1.12	0.023
fibrillin 2(FBN2)	P35556	-1.06	0.0086
C-type lectin domain family 14 member A(CLEC14A)	Q86T13	-1.00	0.0377
multimerin 1(MMRN1)	Q13201	-0.86	0.031
connective tissue growth factor(CTGF)	P29279	-0.74	0.023
bone morphogenetic protein 6(BMP6)	P22004	-0.69	0.0272
fibrillin 1(FBN1)	P35555	-0.42	0.0404
sushi repeat containing protein, X-linked(SRPX)	P78539	-0.32	0.0327
insulin like growth factor binding protein 7(IGFBP7)	Q16270	0.66	0.0327
galectin 8(LGALS8)	O00214	0.68	0.0327
agrin(AGRN)	O00468	1.00	0.023
peroxidasin(PXDN)	Q92626	1.04	0.0086
bone morphogenetic protein 1(BMP1)	P13497	1.29	0.0352
laminin subunit gamma 2(LAMC2)	Q13753	1.58	0.0209
laminin subunit beta 3(LAMB3)	Q13751	1.71	0.0086
galectin 9(LGALS9)	O00182	1.73	0.031
plasminogen activator, urokinase(PLAU)	P00749	1.77	0.0352
C1q and tumor necrosis factor related protein 1(C1QTNF1)	Q9BXJ1	2.33	0.0458
cathepsin S(CTSS)	P25774	2.41	0.0289

Figure 25: Matrisome proteins with significant differences between TNFα- and vehicle-conditioned ECM. (A) Volcano plot comparing TNFα- and vehicle-conditioned ECM. Red and green dots indicate proteins that met both the fold change and p-value thresholds. (B) Matrisome proteins with significant differences ($p<0.05$) between TNFα- and vehicle-conditioned ECM. Bold lines indicate log2(FC) thresholds.

A.

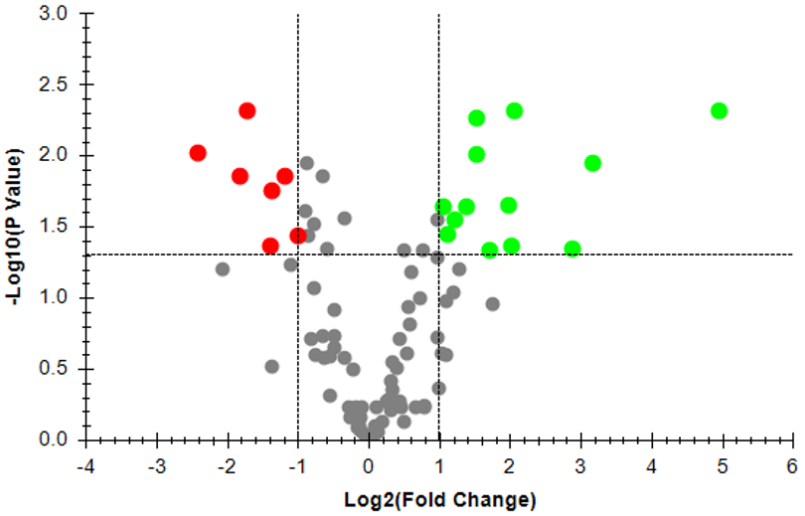

B.

Gene name (gene symbol)	UnitProt Accession Number	log2 (FC)	Adjusted P-value
netrin 4(NTN4)	Q9HB63	-2.40	0.0095
C-type lectin domain family 14 member A(CLEC14A)	Q86T13	-1.84	0.014
EGF containing fibulin like extracellular matrix protein 1(EFEMP1)	Q12805	-1.69	0.0049
von Willebrand factor(VWF)	P04275	-1.40	0.0432
HtrA serine peptidase 3(HTRA3)	P83110	-1.36	0.0177
microfibrillar associated protein 2(MFAP2)	P55001	-1.18	0.014
tubulointerstitial nephritis antigen like 1(TINAGL1)	Q9GZM7	-1.00	0.0368
fibrillin 2(FBN2)	P35556	-0.89	0.0113
fibulin 1(FBLN1)	P23142	-0.89	0.0246
multimerin 1(MMRN1)	Q13201	-0.86	0.0368
lysyl oxidase like 2(LOXL2)	Q9Y4K0	-0.79	0.0301
fibrillin 1(FBN1)	P35555	-0.64	0.014
bone morphogenetic protein 6(BMP6)	P22004	-0.60	0.0457
collagen type V alpha 2 chain(COL5A2)	P05997	-0.34	0.0277
laminin subunit gamma 1(LAMC1)	P11047	0.50	0.0465
agrin(AGRN)	O00468	0.77	0.0465
laminin subunit beta 2(LAMB2)	P55268	0.97	0.0285
peroxidasin(PXDN)	Q92626	1.06	0.0231
galectin 9(LGALS9)	O00182	1.11	0.0359
sushi repeat containing protein, X-linked 2(SRPX2)	O60687	1.21	0.0285
bone morphogenetic protein 1(BMP1)	P13497	1.38	0.0231
insulin like growth factor binding protein 7(IGFBP7)	Q16270	1.53	0.0054
laminin subunit gamma 2(LAMC2)	Q13753	1.54	0.0099
serpin family H member 1(SERPINH1)	P50454	1.72	0.0465
collagen type VIII alpha 1 chain(COL8A1)	P27658	1.97	0.0223
hyaluronan and proteoglycan link protein 3(HAPLN3)	Q96S86	2.02	0.0432
laminin subunit beta 3(LAMB3)	Q13751	2.06	0.0049
C1q and tumor necrosis factor related protein 1(C1QTNF1)	Q9BXJ1	2.88	0.0457
cathepsin S(CTSS)	P25774	3.17	0.0113
inter-alpha-trypsin inhibitor heavy chain 2(ITIH2)	P19823	4.95	0.0049

Figure 26: Matrisome proteins with significant differences between IL-1β- and vehicle-conditioned ECM. (A) Volcano plot comparing IL-1β- and vehicle-conditioned ECM. Red and green dots indicate proteins that met both the fold change and p-value thresholds. (B) Matrisome proteins with significant differences ($p<0.05$) between IL-1β- and vehicle-conditioned ECM. Bold lines indicate log2(FC) thresholds.

IL-1β caused a 1.7-fold increase (p=0.0465) in agrin deposition. IL-1β also caused increased expression in four laminin chains, laminin γ1 (1.41-fold, p=0.0465), laminin β2 (1.96-fold, p=0.0285), laminin γ2 (2.9-fold, p=0.0099), and laminin β3 (4.17-fold, p=0.0049). Changes in degradation enzymes were also observed in IL-1β-conditioned ECM: IL-1β caused a 9.01-fold (p=0.0113) increase in cathepsin S deposition and a 0.39-fold decrease (p=0.0177) in HtrA serine peptidase 3 deposition.

Label-free quantification was also used to compare the IL-1β-conditioned and TNFα-conditioned ECM; only 2 proteins were identified as significantly changed between the two cytokine-conditioned matrices (**Table 4**). Inter-alpha-trypsin inhibitor heavy chain 2 deposition increased 19.1-fold (p=0.0122) in the IL-1β-conditioned ECM when compared with the TNFα-conditioned ECM, while lysyl oxidase like 2 (LOXL2) showed a 0.7-fold decrease (p=0.0541).

Gene name (gene symbol)	UnitProt Accession Number	log2 (FC)	Adjusted P-value
inter-alpha-trypsin inhibitor heavy chain 2(ITIH2)	P19823	4.26	0.0122
lysyl oxidase like 2(LOXL2)	Q9Y4K0	-0.51	0.0541

Table 4: Matrisome proteins with significant differences between TNFα- and IL-1β-conditioned ECM.

Conclusions

Here I present for the first time the cell-specific composition of the ECM deposited by human retinal microvascular endothelial cells. I examined how this constituency changes under inflammatory stimuli, identifying a number of proteins worthy of further study into their contributions to disease pathogenesis. By comparing these data to my previous expression studies in **Chapter IV** and to other published

matrisome datasets, I am also able to demonstrate that this system represents an effective model of the retinal vascular BM.

In recent years there has been an increasing focus on the role chronic inflammation plays in driving DR pathogenesis, representing a shift away from hyperglycemia as the singular, driving force of DR pathology.[5,62,98,99,107,108,248] In **Chapter IV**, I provided further support of this shift by demonstrating that cytokines were more potent inducers of ECM expression changes than conditions designed to mimic diabetic hyperglycemia or dyslipidemia. Therefore, here I endeavored to identify cytokine-induced changes in the constituency of the hRMEC-derived matrisome. My results clearly demonstrate that both TNFα and IL-1β cause major alterations in the constituency of hRMEC-derived ECM. I noted many interesting findings in this survey which will provide the basis for future studies, but here I chose to narrow my focus to the implications of a few particularly compelling findings. First, and most broadly, I observed both increased and decreased deposition of ECM proteins under cytokine treatment, similar to the contrasting expression changes observed in my qRT-PCR results. Contrasting changes in the deposition of ECM constituents would further amplify differences in the ratios of constituents in diabetic retinal BM. Evidence in other systems has demonstrated that pathogenic cell behavior is initiated by variations in the ratios of ECM constituents, either through altered cell-matrix binding influencing cell signaling or through altered biophysical properties.[178,179,289,290] Second, I also observed increased deposition of laminin γ2 and laminin β3 in TNFα-conditioned ECM and laminin γ1, laminin β2, laminin γ2, and laminin β3 in IL-1β-conditioned ECM. Shifts in or complete loss of specific laminin subunits have been shown to alter cell behavior,[175,291-294]

including vascular permeability and leukostasis, two behaviors known to be involved in DR. Therefore, these shifts in the laminin chains deposited in the retinal ECM could contribute to pathogenic behavior in DR. Third, significant increases in agrin deposition were observed in both the TNFα- and IL-1β-conditioned ECM. Heparan sulfate proteoglycans such as agrin have a number of essential roles in vascular BM, including providing structural support and serving as depots of regulatory factors such as cytokines and growth factors. Through its role as a depot of cell signaling molecules, agrin facilitates the establishment of chemokine gradients for leukocyte recruitment and homing in tissues.[130,133,295] Despite these essential roles in BM function and inflammatory responses, agrin's role in retinal BM thickening has not been previously studied; however, these results suggest that it likely plays an important role in diabetes-induced alterations in cell-matrix interactions. Finally, I previously identified that collagen IV expression was increased under cytokine treatment. Both collagen IV α1 and collagen IV α2, the two predominant retinal vascular collagen IV isoforms, demonstrated increased fold change in the qMS results. However, neither met the threshold for significance, likely due to variability in identification at the peptide level. This variability is likely due to the fact that collagen IV has high levels of post-translational modifications that increase the difficulty of detecting various fragments using MS. Indeed, in these data, SERPINH1, a collagen chaperone protein involved in regulation of collagen biosynthesis, showed increased deposition in the IL-1β-conditioned ECM. This increase suggests that cytokine treatment could alter collagen IV biosynthesis, further complicating the identification and subsequent quantification of this protein via MS. Therefore, although collagen IV increases did not meet the threshold for significance, I

am encouraged that these positive trends reflect meaningful increases in collagen IV deposition. Since collagen family members provide significant structural and tensile strength to any ECM, this shift could represent changes in the stiffness of cytokine-conditioned ECM. Future studies will investigate how collagen IV post-translational modifications shift under cytokine treatment and interrogate collagen IV deposition at a more detailed, peptide level of assessment. Overall, both the TNFα- and IL-1β-conditioned ECM demonstrated significant changes not only in the deposition of individual constituents but also in the global constituency. These data suggests that in the diabetic environment, retinal endothelial cells are exposed to significantly altered cell-matrix interactions that could be driving pathogenic behavior.

There are two studies that served as important comparators to assess the efficacy of my qMS studies and the validity of this model system: my previous study utilizing qRT-PCR to examine cytokine-induced changes in expression of five key ECM constituents (**Chapter IV**) and one published study wherein MS was utilized to analyze retinal vascular BM isolated from non-diabetic and diabetic human eyes.[3] There were several key similarities between my qRT-PCR results and qMS results. First, agrin showed both significantly increased expression and deposition under TNFα and IL-1β treatment. Laminin β1 deposition also matched the expression studies, showing no significant changes in the qMS results. For the other proteins of interest, the trends in the qMS results were generally consistent with the patterns of expression found in my qRT-PCR study, though results did not reach significance. In the study of human retinal vascular BM, 28 proteins were identified as the common matrisome in all three of the control human eyes; the hRMEC-derived ECM identified 20 of those 28 proteins,

suggesting that this experimental platform serves as a good model for *in vivo* BM constituency. Furthermore, there were also key similarities in the trends seen in the diabetic vs non-diabetic eyes compared to my vehicle vs cytokine-conditioned ECM. The ECM glycoprotein, tubulointerstitial nephritis antigen (TINAG), was identified as more abundant in the non-diabetic BM than in the diabetic BM, suggesting a decreased deposition. This finding was similar to my qMS results, where I observed that TINAG content was significantly decreased in the IL-1β-conditioned ECM. Similar to my results, the *in vivo* study did not see statistically significant changes in collagen IV but identified an overall increase in the relative abundance of collagen IV. The human diabetic BM also showed decreased perlecan content, a trend I also observed in my qMS results. However, in my qRT-PCR studies, I observed significant decreases in fibronectin expression in response to cytokine treatment, and although the results did not reach significance here, fibronectin showed decreased trends in deposition in both cytokine-treated ECMs. This is in direct contrast to the human diabetic BM study, and several other published studies, which have found increased fibronectin in the diabetic retinal vascular BM.[152,153,157,159,161,261] These results suggest that some other element of the diabetic environment is driving increased fibronectin deposition and thus represent a drawback to my model. A number of issues may explain why my results do not exactly match those seen from the human proteomic studies. First, the methods required for isolating ECM from an *in vitro* system vary significantly from those required to isolate vascular BM from a complex tissue like the retina. Vascular BM extraction from human eyes requires additional steps and more stringent and aggressive purification and solubilization, offering more opportunities for alterations in BM constituency. Second,

the *in vivo* vascular BM is deposited by multiple cell types while my goal here was to identify the cell-specific constituency deposited by retinal endothelial cells. Thus, it is likely that differences observed here, such as the inconsistency in fibronectin deposition, reflect ECM deposition changes from other cell types *in vivo*. Overall, the evidence suggests that this experimental platform serves as a good model system for understanding vascular BM changes and, since it is *in vitro,* represents a more tractable environment to investigate the mechanisms by which BM thickening are contributing to DR.

I again acknowledge the challenges of modeling a chronic disease that develops over decades using short-term *in vitro* methods, as well as the limitations inherent in extrapolating these methods to NPDR events. However, isolation of intact ECM from tissues is labor intensive and requires access to expensive samples from animals or humans. Utilizing ECM extracted from cell culture models avoids these obstacles while also providing unique cell-specific information about ECM deposition. Likewise, *in vitro* systems represent a far more tractable experimental system, allowing for specific mechanistic questions to be asked which would not be feasible in an *in vivo* setting. Previous studies in other tissues have demonstrated that cell culture-derived ECM represents an excellent model system of *in vivo* ECM, even leading to therapeutic target identification in multiple disease models.[192,193] However, this validation of *in vitro* ECM has not occurred for retinal vascular BM. My studies demonstrate a model system that represents a powerful and tractable *in vitro* environment to investigate cell-type specific deposition profiles and analyze how cytokine-induced alterations in ECM composition affect retinal cell behavior.

Identifying disease-specific ECM signatures can improve multiple areas of translational research, including tissue bioengineering for regenerative medicine and cell culture models used for drug screening applications.[296] For instance, recent studies have utilized nanobodies targeted to ECM molecules known to be upregulated in tumors to enhance non-invasive imaging of tumors and to increase the efficacy of therapies by directing enhanced localization at the tumor site.[297,298] Another study used coupling to the ECM molecule lumican to increase retention of cytokines delivered to tumor sites.[299] Therefore, a better understanding of the constituency of the retinal BM will also enhance efforts to design future experimental systems and therapies in DR. Future studies will investigate the functional implications of the cytokine-induced changes in matrisome constituency identified here and attempt to isolate which ECM alterations cause the greatest changes in retinal cell behavior and thus have the greatest therapeutic potential. Overall, I have demonstrated for the first time the unique constituency of hRMEC-derived ECM as well as investigated how the constituency of the hRMEC-derived matrisome changes under cytokine treatment, highlighting a number of potential targets for future study.

CHAPTER VI

CONCLUSIONS AND FUTURE DIRECTIONS

The work presented in this dissertation relates to the role of inflammation in driving NPDR pathology, particularly as it relates to the development and contributions of vascular BM thickening. In **Chapter I**, I introduced the reader to diabetic retinopathy pathology and the emerging roles that chronic inflammation and retinal BM thickening play in driving retinal pathology. In **Chapter II**, I described the methodology utilized to complete the project. In **Chapter III**, I demonstrated the efficacy of the small molecule NFAT inhibitor, INCA-6, in reducing pathogenic cell responses, including inflammation, hyperpermeability, and leukostasis, downstream of IL-1β. The work described in **Chapter IV** focuses on the role of chronic retinal inflammation and retinal pericytes in altered ECM expression – topics that have been somewhat neglected as contributors to the development of BM thickening. Additionally, I demonstrated that cytokine-induced changes in retinal ECM are alone sufficient to drive pathogenic leukocyte-endothelial cell adhesion. Finally, in **Chapter V**, I utilized quantitative mass spectrometry (qMS) to identify, for the first time, the unique constituency of hRMEC ECM and how that constituency changes under cytokine treatment, thereby modeling how retinal inflammation contributes to BM thickening *in vivo.*

Across all chapters, this work emphasizes the importance of inflammation as a driving force behind NPDR pathology. My comprehensive assessment of the effects of diabetes-relevant stimuli on ECM expression by retinal cells in **Chapter IV** emphasized

the importance of both TNFα and IL-1β in early NPDR by demonstrating that these cytokines cause significant alterations of ECM expression in retinal endothelial cells and pericytes. Furthermore, all data support our lab's previous hypothesis that IL-1β acts as a "master regulator" of retinal inflammation. For example, in **Chapter III**, I demonstrated that IL-1β treatment causes significant increases in both Müller cell and endothelial cell inflammation and that it can model DR-relevant vascular hyperpermeability and leukostasis *in vitro* and *in vivo.* In **Chapter IV**, IL-1β-conditioned ECM caused greater increases in adhesion molecule expression and leukocyte adhesion than TNFα-conditioned ECM. Additionally, I observed that when hRMEC were treated with IL-1β conditioned media (CM) from hMC, significant increases in collagen IV and agrin expression were observed. Notably, CM generated from TNFα-treated hMC did not cause any significant changes in hRMEC ECM expression. These results are consistent with previous findings from our lab demonstrating that IL-1β is a more potent inducer of inflammation in hMC than TNFα. Finally, in **Chapter V**, my qMS findings demonstrated that IL-1β caused more significant alterations in the constituency of hRMEC-derived ECM than did TNFα. As discussed in **Chapter I**, historically, the DR field has been focused primarily on understanding and addressing retinal changes downstream of hyperglycemia. However, our lab has led a shift in emphasis towards the contributions to and propagation of DR pathologies by chronic inflammation. The data presented in this dissertation build on our existing evidence to further expand the list of pathogenic cell behaviors affected by inflammation, underscoring the need to develop new anti-inflammatory therapeutic strategies.

The most important finding in **Chapter III** is that INCA-6 is efficacious against the propagation of inflammation by both hMC and hRMEC; this finding holds significant implications for the therapeutic value of NFAT inhibition, or other anti-inflammatory strategies, to slow the progression of NPDR pathology. These data indicate that not only can NFAT inhibition directly mitigate pathogenic endothelial cell behaviors, like permeability or leukostasis as demonstrated in **Figures 12** and **14,** but it will likely also slow pathology through its inhibitory effects on cytokine expression since inflammation has been shown to drive all pathogenic events in NPDR, including BM thickening as proven in **Chapters IV** and **V**. For instance, I observed that CM from IL-1β-treated hMC caused significant increases in collagen IV and agrin expression in hRMEC (**Figure 15**). Indeed, the levels of induction from CM were equivalent to those seen from direct stimulation with cytokines. Thus, if NFAT inhibition attenuates secretion of inflammatory cytokines by hMC, it would consequently reduce downstream hRMEC ECM induction. Future studies will include NFAT inhibition in hMC CM experiments to directly test whether the expected attenuation of hMC-derived inflammation can prevent inflammation-induced ECM expression increases in hRMEC. However, overall, my NFAT inhibitory strategy shows significant therapeutic promise for slowing retinal inflammation and associated downstream pathogenic events.

A number of important questions remain regarding the therapeutic utility of NFAT inhibition. For instance, since INCA-6 prevents the binding of NFAT to the activating phosphatase CN, INCA-6 inhibits the action of all four calcium-dependent NFAT isoforms. However, we have demonstrated that distinct NFAT isoforms can oppose each other in their control of inflammatory gene expression by retinal cells. Indeed, we

have previously demonstrated that NFATc2 knockdown prevented TNFα-induced inflammatory responses in hRMEC while NFATc3 increased them.[108] Therefore, it is possible that greater efficacy could be achieved by identifying the isoform(s) responsible for pathogenic retinal events, which would then compel the development of isoform-specific therapies. Future studies will involve investigation of the isoform-specific roles that regulate each pathogenic behavior with the hopes of developing an NFAT-directed therapeutic strategy with enhanced efficacy. Although NFAT inhibitors have only been tested in pre-clinical settings, CN inhibitors are approved for clinical use and are used in post-kidney transplant and chemotherapy regimens,[208,300] suggesting that therapeutic targeting of this signaling axis is tolerated in humans.

The data presented in **Chapter IV** provide a new perspective to our current understanding of how BM thickening develops, namely that pericytes contribute significantly to this process and that chronic retinal inflammation is likely a major driver of this event. First, I demonstrated in both hRMEC and hRP that conditions designed to mimic chronic retinal inflammation yielded more consistent and potent alterations in ECM expression than those designed to mimic hyperglycemia or dyslipidemia. These results emphasized the importance of chronic retinal inflammation in promoting early DR pathology. My findings also demonstrate, for the first time, that pericytes contribute to BM thickening. Previous studies have focused almost exclusively on the role of endothelial cells in increased retinal BM deposition. However, my results demonstrate that hRP respond with similar, if not higher, levels of induction of expression of major ECM constituents in response to diabetes-relevant cytokine treatment. Finally, I also demonstrated that cytokine-induced changes in retinal vascular ECM are sufficient to

elicit increased leukocyte adhesion to naïve hRMEC monolayers. These results highlighted a novel role for both chronic retinal inflammation and hRP-derived ECM in promoting altered cell-matrix dynamics in retinal cells. Cumulatively, the data presented in **Chapter IV** support growing evidence in the literature that vascular BM thickening is an active contributor to the DR pathogenic cascade. Since retinal cells are in constant contact with vascular BM, the emerging role of BM thickening in the DR pathogenic cascade has important implications for the development of DR therapeutics. For instance, even if a novel therapy could address pathogenic behavior on the cellular level, by stopping endothelial cell dysfunction or pericyte apoptosis for example, the altered vascular BM would remain as a pathogenic stimulus. The altered vascular BM would continue to instigate and propagate pathogenic cell behaviors through aberrant cell-matrix interactions. Therefore, it will be important to continue to expand our understanding of the role of vascular BM thickening in DR if we hope to develop therapies designed to attenuate this event.

Of particular interest to me was the finding that hRP-derived ECM could drive changes in leukocyte-endothelial cell adhesion since pericytes are increasingly considered a key mediator of the leukocyte adhesion cascade. Similar to EC, pericytes release leukocyte chemoattractants and express adhesion molecules to facilitate leukocyte binding and control the direction of leukocyte motility during transmigration and migration within the BM.[276-278] A series of papers demonstrated that, across multiple tissues, venular BM has matrix protein low expression regions (LER) that are the preferential sites of neutrophil extravasation.[177,254,279,301] These LER were frequently co-localized with pericytes, in fact the size of the gaps between pericytes and the size of

LER were similar, strongly suggesting that pericyte-derived ECM plays a major role in leukocyte extravasation. Therefore, it would be of great interest to explore how diabetes-relevant changes in ECM alter the path, timing, and success of leukocyte extravasation along LER and pericytes. Future studies should endeavor to understand these dynamic relationships between pericytes, EC, vascular BM, and leukocytes, thereby enabling a deeper understanding of the complex molecular mechanisms of NPDR.

It has long been known from studies performed in non-ocular tissues that chronic inflammation leads to significant alterations in the constituency and functionality of ECM.[171] Therefore, it was not surprising when I found that inflammatory cytokines caused consistent changes in ECM expression in retinal cells and that cytokine-conditioned ECM elicited associated changes in endothelial cell behavior. As discussed in **Chapter IV**, my findings point to a number of areas for future investigation that were outside the scope of this dissertation. Included are: how inflammation-induced changes in ECM alter matrix stiffness, how dyslipidemia contributes to BM thickening, and how dyslipidemia and hyperglycemia may interact to further potentiate BM thickening. Additionally, the experimental platform described and utilized in **Chapter IV** could be further utilized to interrogate the contribution of BM thickening to other NPDR events and whether similar mechanisms of action underlie these other events. Significant questions remain concerning the mechanisms by which BM thickening might contribute to vascular hyperpermeability, endothelial cell or pericyte apoptosis, or propagation of local inflammation by retinal cells. Indeed, changes in ECM constituency have been shown to drive changes in each of these behaviors in other tissues and pathological

conditions. For instance, exposure to advanced glycation end products, which accumulate in retinal BM in diabetes, caused pericytes to undergo anoikis, a form of cell death initiated by loss of cell-matrix interactions.[302,303] As further evidence to indicate altered pericyte-matrix interactions in the diabetic environment, pericytes demonstrated increased apoptosis when grown on ECM deposited by high glucose-treated endothelial cells.[275] Of particular interest would be to determine if cytokine-induced changes in retinal ECM could drive Müller cell inflammation. Müller cell processes are in direct contact with the vascular BM and thus could also sense biophysical or constituency shifts in the vascular BM in ways that might propagate inflammation. Overall, much remains to be understood about the mechanisms by which aberrant cell-matrix interactions contribute to DR pathology.

Future studies will also endeavor to identify the molecular, biochemical, or biophysical property shifts in ECM deposited under inflammatory conditions that underlie the shifts in EC/leukocyte adhesion behavior identified here. There are a number of possible contributors. Previous studies have demonstrated that alterations of the constituency of ECM, particularly in the ratios of key proteins, can cause changes in the behavior of neighboring cells.[174,176,289] In a number of cases, I observed contrasting changes in expression between different ECM constituents. For instance, TNFα caused increased agrin, but decreased perlecan, expression in hRMEC. Contrasting expression changes can amplify differences in the ratios of constituents in diabetic retinal BM, fundamentally altering its architecture and therefore its functionality.[289,290] Furthermore, alterations in the ratios and constituency of BM constituents can cause significant changes in ECM stiffness. Changes in BM stiffness profoundly alter the behavior of

adjacent cells, in turn accelerating disease pathology.[176,290,304] Of particular relevance, previous studies have demonstrated that changes in ECM stiffness cause increased leukocyte adherence.[178,179] Therefore, it would be of value to measure stiffness alterations in my cytokine-conditioned ECM. Finally, the ECM can serve as a reservoir of secreted and trapped cytokines and growth factors, so it is possible that these matrix-associated proteins contribute to pathogenic retinal events. Although no increases in inflammatory mediators were observed in the *in vitro* qMS studies, it remains a possibility in the more complex *in vivo* retinal BM. Consequently, a more global and detailed understanding of how ECM deposition is altered under inflammatory conditions will be necessary to elucidate the mechanisms of action underlying the changes I have observed in naïve EC.

To this end, in **Chapter V**, I utilized quantitative mass spectrometry (qMS) to establish the constituency of hRMEC-derived ECM and characterize how this constituency is altered under TNFα or IL-1β treatment, in order to identify targets and direct future mechanisms of action studies. Identification of alterations in the deposition of specific ECM proteins under disease conditions is important to the elucidation of the mechanisms by which ECM changes cell behavior and the subsequent development of therapeutics. For instance, in a recent study, matrisome proteomics were used to identify collagen VI as novel driver of tumor cell invasion in breast cancer.[283] The qMS data presented here provide a wealth of novel, cell-specific information to inform which ECM constituents drive pathogenic behaviors in retinal cells, such as the increased leukocyte adhesion seen in **Chapter IV**. For example, I observed a significant increase in agrin deposition as well as a shift in the isoforms of laminin deposited under both

TNFα and IL-1β treatment. As discussed in **Chapter V**, both increased HSPG content and altered laminin trimers have been known to cause altered behavior in other tissues and diseases, indicating that these proteins are interesting candidates for future mechanism of action studies.[130,133,175,291-295] Overall, the data presented in **Chapter V** provide a number of interesting candidates that warrant further investigation.

In addition to specific ECM proteins being responsible for shifts in cell behavior, another potential contributor is ECM stiffness. I have not yet explored how the molecular changes in constituency observed in the qMS results might alter the biophysical properties of the cytokine-conditioned ECM. However, as mentioned above, much is known about the influence of biophysical properties on the behavior of neighboring cell populations and the importance of BM stiffness in pathogenesis.[176,290,304] For instance, recent evidence has elucidated the importance of collagen cross-linking enzymes in DR. Studies have demonstrated increased lysyl oxidase (LOX) expression, protein levels, and activity in high glucose-treated endothelial cells as well as increased LOX levels in the retinas of diabetic rats.[178,305-307] Additionally, inhibiting LOX through siRNA, genetic deletion, or pharmacological inhibition attenuated the development of acellular capillaries, pericyte loss, and vascular hyperpermeability in diabetic rats and high glucose cell cultures.[305-307] The increased LOX levels seen in high glucose-treated endothelial cells were also associated with an increase in ECM stiffness; pharmacological inhibition of LOX activity both reduced ECM stiffness and high glucose-induced monocyte adhesion to endothelial cell monolayers.[178] In my qMS study, I identified two candidates that suggested an important shift in the biophysical properties of the cytokine-conditioned ECM. First, lysyl oxidase homolog 2 (LOXL2) was

significantly decreased in the IL-1β-conditioned ECM. LOLX2 is a copper-dependent amino-oxidase in the LOX family of proteins. LOXL2 covalently cross-links collagen and elastin, providing structural integrity and tensile strength to the ECM. Evidence suggests that LOXL2 may preferentially cross-link collagen IV compared to LOXL1 or LOX.[308] Dysregulation of LOX family expression and activity have been implicated in many diseases, in particular in fibrotic diseases including some forms of cancer.[309] Additionally, evidence demonstrates that, through its control of the collagen IV scaffold, LOXL2 is an important regulator of angiogenesis.[310] LOLXL2 has also been shown to have key regulatory roles in kidney fibrosis and glomerular BM structure in a mouse model of Alport syndrome.[311] Second, I also identified peroxidasin (PXDN) as significantly increased in both the TNFα and IL-1β datasets. PXDN catalyzes sulfilimine bonds between collagen IV, providing important structural integrity to the collagen IV network.[312,313] Studies have shown that PXDN and its downstream network formation are essential to endothelial cell survival and growth.[313] Combined with the existing data on LOX, these new data on cytokine-induced changes in LOXL2 and PXDN deposition support an emerging role for cross-linking enzymes and their downstream biophysical influences on DR pathology. Therefore, it will be important to investigate how the biophysical properties of cytokine-conditioned ECM shift, since targeting these cross-linking enzymes could have significant therapeutic potential.

Notably, it remains unclear if BM thickening is solely a result of excessive ECM deposition. It is entirely possible that insufficient matrix degradation, or some combination of both dysregulated deposition and degradation, could also contribute. However, previous studies in DR have primarily focused on the role of increased

deposition of ECM constituents, with little interrogation of the role of degradation enzymes in BM thickening. The degradation of BM is a complex and delicately balanced process that ensures that the ECM remodeling needed for normal BM homeostasis and maintenance occurs. I did not consider the potential relationship between ECM degradation and BM thickening here. However, a number of interesting findings from my work provide evidence that investigations into ECM degradation and turnover are warranted. First, in both hRMEC and hRP treated with either TNFα or IL-1β, high levels of MMP9 induction were observed, though no changes were observed in MMP2 expression (**Appendix C** and **D**). Additionally, in **Chapter V**, three of the most highly significant proteins in the TNFα dataset and two of the most highly significant proteins in the IL-1β dataset were ECM degradation enzymes. Specifically, HtrA serine peptidase 3 (HTRA3) deposition was significantly decreased in both datasets while cathepsin S deposition was increased. Urokinase showed the third highest levels of induction in the TNFα dataset. Each of these proteins plays essential roles in regulating ECM turnover and homeostasis. For instance, although urokinase does not directly act on key network ECM proteins like collagen or laminin, it is responsible for activating plasmin, which in turn can both activate MMPs and itself degrade ECM proteins.[314] Urokinase has also been implicated in the activation of neutrophils, suggesting a role in the inflammation cascade.[315] Cathepsin S is known to degrade a broad range of ECM proteins, including fibronectin, nidogen, collagen IV, and laminin.[316] Its elevation and subsequent dysregulation of ECM degradation has been implicated in a range of inflammation-related diseases, including osteoarthritis, liver fibrosis, and atherosclerosis.[316] Additionally, its cleavage of ECM proteins has demonstrated pro-angiogenic effects

which supported tumor growth.[317] Finally, less is known about the substrates of HTRA3, however evidence suggests a role in degrading ECM proteoglycans, including fibronectin, as well as a role in controlling TGF-β signaling, possibly through digestion of ECM components.[318] Combined with the MMP9 expression results, the appearance of these important degradation enzymes in the significant hits of the qMS data suggests that alterations of BM degradation may contribute more to BM thickening than previously thought. Future work should focus on identifying how ECM turnover is altered under the diabetes-relevant cytokine treatment.

Quantitative MS is a powerful tool that is rapidly advancing our understanding of matrisome constituencies in health and disease. Although my results represent a major step in understanding and modeling retinal vascular BM, many important applications of this technology remain. Future studies will include investigations of whether co-culture models, utilizing pericytes and endothelial cells, provide a superior *in vitro* model. Recent studies of glomerular BM have elucidated not only the BM constituency but also identified cell-type specific deposition profiles. These data facilitated the comparison of human tissue-derived glomerular BM and the BM deposited by glomerular endothelial cells and podocytes in single cultures and co-cultures; thereby identifying cell-type specific differences in *in vitro* ECM composition and providing indications of cell type-specific roles in BM assembly.[192] Based on my results in **Chapter IV** and the importance of pericyte-derived ECM in other disease states,[252-256,319] I sought to complete qMS analysis of the matrisome deposited by hRP under both TNFα and IL-1β treatment as well. Similar to hRMEC, I found that the total ECM protein deposited by hRP under cytokine treatment was significantly increased (**Appendix E**). I have

collected the MS data from the hRP samples, however the matrisome samples from vehicle-treated pericytes proved to be more fundamentally different from the cytokine-treated samples than what I observed in hRMEC. Although this is in line with my findings in **Chapter IV**, where hRP showed greater induction of ECM expression compared to hRMEC, it rendered the proteomic analysis more complex, and thus my qMS work on pericytes is still ongoing. However, once completed, these results will enable us to compare the matrisome constituencies of hRMEC and hRP. Furthermore, I will be able to understand how these cell-specific signatures shift under diabetes-relevant cytokine treatment, leading to a deeper and more nuanced understanding of the development of BM thickening.

In summary, I have demonstrated that NFAT inhibition has strong therapeutic potential to mitigate diabetes-related retinal inflammation, that inflammation drives significant changes in retinal vascular ECM, that these changes in retinal vascular ECM promote pathogenic changes in leukocyte adhesion behavior, and that retinal pericytes are likely equal contributors to the development of vascular BM thickening. Taken together, this work represents a significant step in our understanding of early DR pathogenesis and the potential of anti-inflammatory agents to slow the disease.

Appendix A

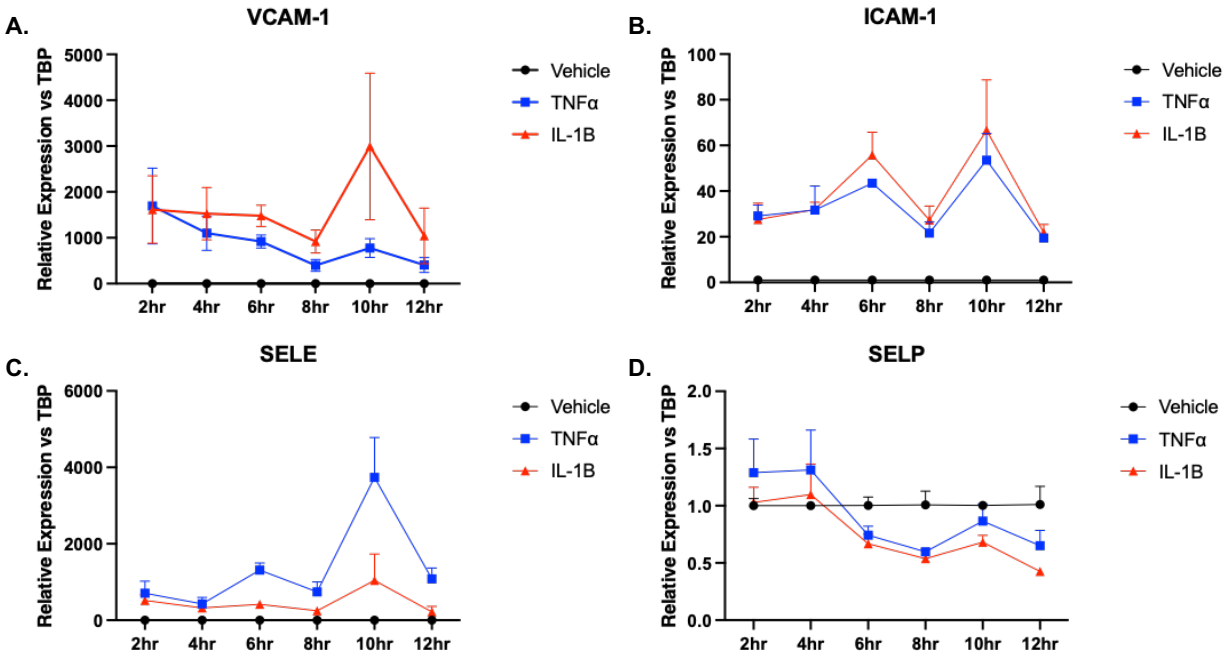

Time course of TNFα- and IL-1β-induced adhesion molecule expression in hRMEC. hRMEC were treated with 1ng/mL TNFα or IL-1β. Cells were collected and assayed for expression of (A) VCAM-1, (B) ICAM-1, (C) E-selectin (gene name: SELE), or (D) P-selectin (gene name: SELP). Expression data are reported as fold induction over vehicle with bars representing mean +/- SD (n=3).

Appendix B

Matrisome Category	Matrisome Division	Gene name (gene symbol)	UnitProt	Vehicle vs TNFα		Vehicle vs IL-1β	
				Fold Change	Adjusted P-Value	Fold Change	Adjusted P-Value
Collagens	Core matrisome	collagen type I alpha 1 chain(COL1A1)	P02452	0.65	0.3149	0.65	0.2622
Collagens	Core matrisome	collagen type III alpha 1 chain(COL3A1)	P02461	0.74	0.5015	0.69	0.4856
Collagens	Core matrisome	collagen type IV alpha 1 chain(COL4A1)	P02462	1.24	0.4049	1.5	0.1552
Collagens	Core matrisome	collagen type V alpha 2 chain(COL5A2)	P05997	0.89	0.4077	0.79	0.0277
Collagens	Core matrisome	collagen type I alpha 2 chain(COL1A2)	P08123	0.67	0.2132	0.64	0.1852
Collagens	Core matrisome	collagen type IV alpha 2 chain(COL4A2)	P08572	1.26	0.4117	1.45	0.2461
Collagens	Core matrisome	collagen type VI alpha 1 chain(COL6A1)	P12109	0.85	0.5062	0.91	0.7877
Collagens	Core matrisome	collagen type VI alpha 2 chain(COL6A2)	P12110	1.2	0.5044	1.2	0.5237
Collagens	Core matrisome	collagen type VI alpha 3 chain(COL6A3)	P12111	0.69	0.2205	0.88	0.5883
Collagens	Core matrisome	collagen type V alpha 1 chain(COL5A1)	P20908	1.22	0.1017	0.94	0.5883
Collagens	Core matrisome	collagen type VIII alpha 1 chain(COL8A1)	P27658	1.75	0.2051	3.93	0.0223
Collagens	Core matrisome	collagen type XVIII alpha 1 chain(COL18A1)	P39060	0.99	0.9195	1.06	0.8367
Collagens	Core matrisome	collagen type XIII alpha 1 chain(COL13A1)	Q5TAT6	0.78	0.4117	1	0.9981
Collagens	Core matrisome	collagen type XII alpha 1 chain(COL12A1)	Q99715	1.38	0.2205	1.32	0.3101
ECM Glycoproteins	Core matrisome	agrin(AGRN)	O00468	2	0.023	1.7	0.0465
ECM Glycoproteins	Core matrisome	cysteine rich angiogenic inducer 61(CYR61)	O00622	1.01	0.8566	1.08	0.5927
ECM Glycoproteins	Core matrisome	laminin subunit alpha 5(LAMA5)	O15230	1.33	0.3797	1.35	0.5342
ECM Glycoproteins	Core matrisome	EGF like repeats and discoidin domains 3(EDIL3)	O43854	1.18	0.4	0.93	0.699
ECM Glycoproteins	Core matrisome	sushi repeat containing protein, X-linked 2(SRPX2)	O60687	1.15	0.5757	2.31	0.0285
ECM Glycoproteins	Core matrisome	fibronectin 1(FN1)	P02751	0.67	0.178	0.71	0.226
ECM Glycoproteins	Core matrisome	vitronectin(VTN)	P04004	1.22	0.5757	1.24	0.6122
ECM Glycoproteins	Core matrisome	von Willebrand factor(VWF)	P04275	0.56	0.0986	0.38	0.0432
ECM Glycoproteins	Core matrisome	laminin subunit beta 1(LAMB1)	P07942	1.14	0.5292	1.47	0.1156
ECM Glycoproteins	Core matrisome	thrombospondin 1(THBS1)	P07996	0.58	0.2205	0.59	0.2552
ECM Glycoproteins	Core matrisome	laminin subunit gamma 1(LAMC1)	P11047	1.12	0.3656	1.41	0.0465
ECM Glycoproteins	Core matrisome	nidogen 1(NID1)	P14543	0.94	0.643	1.24	0.3827
ECM Glycoproteins	Core matrisome	fibulin 1(FBLN1)	P23142	0.67	0.1416	0.54	0.0246
ECM Glycoproteins	Core matrisome	tenascin C(TNC)	P24821	1.52	0.3063	1.38	0.5927
ECM Glycoproteins	Core matrisome	connective tissue growth factor(CTGF)	P29279	0.6	0.023	0.59	0.0854
ECM Glycoproteins	Core matrisome	fibrillin 1(FBN1)	P35555	0.75	0.0404	0.64	0.014
ECM Glycoproteins	Core matrisome	fibrillin 2(FBN2)	P35556	0.48	0.0086	0.54	0.0113
ECM Glycoproteins	Core matrisome	microfibrillar associated protein 2(MFAP2)	P55001	0.4	0.0086	0.44	0.014
ECM Glycoproteins	Core matrisome	laminin subunit beta 2(LAMB2)	P55268	1.4	0.2091	1.96	0.0285
ECM Glycoproteins	Core matrisome	sushi repeat containing protein, X-linked(SRPX)	P78539	0.8	0.0327	0.86	0.3174
ECM Glycoproteins	Core matrisome	EGF containing fibulin like extracellular matrix protein 1(EFEMP1)	Q12805	0.46	0.023	0.31	0.0049
ECM Glycoproteins	Core matrisome	multimerin 1(MMRN1)	Q13201	0.55	0.031	0.55	0.0368
ECM Glycoproteins	Core matrisome	laminin subunit beta 3(LAMB3)	Q13751	3.28	0.0086	4.17	0.0049
ECM Glycoproteins	Core matrisome	laminin subunit gamma 2(LAMC2)	Q13753	2.98	0.0209	2.9	0.0099
ECM Glycoproteins	Core matrisome	nidogen 2(NID2)	Q14112	1.74	0.178	2.28	0.0919
ECM Glycoproteins	Core matrisome	latent transforming growth factor beta binding protein 1(LTBP1)	Q14766	0.71	0.3063	0.68	0.2572
ECM Glycoproteins	Core matrisome	latent transforming growth factor beta binding protein 2(LTBP2)	Q14767	0.96	0.7894	1.04	0.9054
ECM Glycoproteins	Core matrisome	transforming growth factor beta induced(TGFBI)	Q15582	1.13	0.7841	1	0.9981
ECM Glycoproteins	Core matrisome	insulin like growth factor binding protein 7(IGFBP7)	Q16270	1.58	0.0327	2.88	0.0054
ECM Glycoproteins	Core matrisome	laminin subunit alpha 4(LAMA4)	Q16363	1.17	0.3497	1.52	0.0661
ECM Glycoproteins	Core matrisome	laminin subunit alpha 3(LAMA3)	Q16787	1.27	0.4974	0.9	0.8272
ECM Glycoproteins	Core matrisome	thrombospondin type 1 domain containing 4(THSD4)	Q6ZMP0	1.39	0.1443	1.35	0.1949
ECM Glycoproteins	Core matrisome	peroxidasin(PXDN)	Q92626	2.05	0.0086	2.09	0.0231
ECM Glycoproteins	Core matrisome	collagen triple helix repeat containing 1(CTHRC1)	Q96CG8	1.22	0.2417	1.03	0.9054
ECM Glycoproteins	Core matrisome	tubulointerstitial nephritis antigen like 1(TINAGL1)	Q9GZM7	0.57	0.0612	0.5	0.0368
ECM Glycoproteins	Core matrisome	multimerin 2(MMRN2)	Q9H8L6	0.67	0.1416	0.71	0.1852
ECM Glycoproteins	Core matrisome	netrin 4(NTN4)	Q9HB63	0.42	0.031	0.19	0.0095

Full matrisome identified in qMS. All matrisome proteins identified in the qMS results are listed here. Additionally, information is provided on the matrisome category, matrisome division, and the fold change and adjusted p-value for both the vehicle vs TNFα and vehicle vs IL-1β comparisons (table continued on second page).

Matrisome Category	Matrisome Division	Gene name (gene symbol)	UnitProt	Vehicle vs TNFα		Vehicle vs IL-1β	
				Fold Change	Adjusted P-Value	Fold Change	Adjusted P-Value
ECM Regulators	Matrisome-associated	procollagen-lysine,2-oxoglutarate 5-dioxygenase 2(PLOD2)	O00469	2.46	0.2205	2.15	0.2536
ECM Regulators	Matrisome-associated	ADAM metallopeptidase with thrombospondin type 1 motif 4(ADAMTS4)	O75173	1.24	0.4359	2.13	0.1051
ECM Regulators	Matrisome-associated	coagulation factor II, thrombin(F2)	P00734	1.26	0.4049	1.19	0.5342
ECM Regulators	Matrisome-associated	plasminogen activator, urokinase(PLAU)	P00749	3.41	0.0352	2.42	0.0622
ECM Regulators	Matrisome-associated	plasminogen activator, tissue type(PLAT)	P00750	1.38	0.4549	1.07	0.8911
ECM Regulators	Matrisome-associated	serpin family C member 1(SERPINC1)	P01008	1.36	0.2132	1.27	0.4407
ECM Regulators	Matrisome-associated	cystatin B(CSTB)	P04080	2.32	0.1967	2.06	0.2439
ECM Regulators	Matrisome-associated	serpin family B member 2(SERPINB2)	P05120	2.76	0.1953	1.99	0.4383
ECM Regulators	Matrisome-associated	serpin family E member 1(SERPINE1)	P05121	1.11	0.7392	1.14	0.7536
ECM Regulators	Matrisome-associated	cathepsin B(CTSB)	P07858	2.5	0.0528	1.96	0.1911
ECM Regulators	Matrisome-associated	matrix metallopeptidase 2(MMP2)	P08253	0.99	0.9787	0.97	0.9228
ECM Regulators	Matrisome-associated	bone morphogenetic protein 1(BMP1)	P13497	2.44	0.0352	2.61	0.0231
ECM Regulators	Matrisome-associated	inter-alpha-trypsin inhibitor heavy chain 2(ITIH2)	P19823	1.8	0.0721	30.94	0.0049
ECM Regulators	Matrisome-associated	transglutaminase 2(TGM2)	P21980	0.9	0.7834	0.84	0.699
ECM Regulators	Matrisome-associated	cathepsin S(CTSS)	P25774	5.31	0.0289	9.01	0.0113
ECM Regulators	Matrisome-associated	serpin family H member 1(SERPINH1)	P50454	3.01	0.0691	3.29	0.0465
ECM Regulators	Matrisome-associated	cathepsin C(CTSC)	P53634	0.97	0.8566	0.57	0.1949
ECM Regulators	Matrisome-associated	HtrA serine peptidase 3(HTRA3)	P83110	0.44	0.0209	0.39	0.0177
ECM Regulators	Matrisome-associated	procollagen-lysine,2-oxoglutarate 5-dioxygenase 1(PLOD1)	Q02809	2.58	0.1312	1.59	0.5883
ECM Regulators	Matrisome-associated	inter-alpha-trypsin inhibitor heavy chain 3(ITIH3)	Q06033	1.88	0.3072	3.37	0.1104
ECM Regulators	Matrisome-associated	CD109 molecule(CD109)	Q6YHK3	1.59	0.178	0.92	0.8581
ECM Regulators	Matrisome-associated	ADAMTS like 1(ADAMTSL1)	Q8N6G6	1.05	0.7027	0.79	0.2665
ECM Regulators	Matrisome-associated	HtrA serine peptidase 1(HTRA1)	Q92743	0.48	0.1	0.47	0.0591
ECM Regulators	Matrisome-associated	lysyl oxidase like 2(LOXL2)	Q9Y4K0	0.83	0.2132	0.58	0.0301
ECM-affiliated Proteins	Matrisome-associated	galectin 9(LGALS9)	O00182	3.31	0.031	2.16	0.0359
ECM-affiliated Proteins	Matrisome-associated	galectin 8(LGALS8)	O00214	1.6	0.0327	1.26	0.2847
ECM-affiliated Proteins	Matrisome-associated	annexin A1(ANXA1)	P04083	1.69	0.5292	1.72	0.5883
ECM-affiliated Proteins	Matrisome-associated	annexin A2(ANXA2)	P07355	1.71	0.5333	1.42	0.7511
ECM-affiliated Proteins	Matrisome-associated	annexin A6(ANXA6)	P08133	2.93	0.2083	1.73	0.5689
ECM-affiliated Proteins	Matrisome-associated	galectin 1(LGALS1)	P09382	1.52	0.1017	1.07	0.8367
ECM-affiliated Proteins	Matrisome-associated	C-type lectin domain family 14 member A(CLEC14A)	Q86T13	0.5	0.0377	0.28	0.014
ECM-affiliated Proteins	Matrisome-associated	C1q and tumor necrosis factor related protein 6(C1QTNF6)	Q9BXI9	1.66	0.3149	1.97	0.0519
ECM-affiliated Proteins	Matrisome-associated	C1q and tumor necrosis factor related protein 5(C1QTNF5)	Q9BXJ0	0.36	0.0458	0.39	0.3062
ECM-affiliated Proteins	Matrisome-associated	C1q and tumor necrosis factor related protein 1(C1QTNF1)	Q9BXJ1	5.04	0.0458	7.34	0.0457
Proteoglycans	Core matrisome	heparan sulfate proteoglycan 2(HSPG2)	P98160	0.68	0.1203	0.71	0.1222
Proteoglycans	Core matrisome	hyaluronan and proteoglycan link protein 3(HAPLN3)	Q96S86	1.6	0.0878	4.06	0.0432
Secreted Factors	Matrisome-associated	angiopoietin 2(ANGPT2)	O15123	0.84	0.5292	0.24	0.0622
Secreted Factors	Matrisome-associated	S100 calcium binding protein A6(S100A6)	P06703	1.63	0.178	1.01	0.9742
Secreted Factors	Matrisome-associated	bone morphogenetic protein 6(BMP6)	P22004	0.62	0.0272	0.66	0.0457
Secreted Factors	Matrisome-associated	S100 calcium binding protein A11(S100A11)	P31949	1.46	0.4552	1.1	0.8794
Secreted Factors	Matrisome-associated	hornerin(HRNR)	Q86YZ3	0.82	0.7388	0.82	0.5927
Secreted Factors	Matrisome-associated	S100 calcium binding protein A16(S100A16)	Q96FQ6	1.33	0.3072	1.07	0.8044
Secreted Factors	Matrisome-associated	hedgehog interacting protein(HHIP)	Q96QV1	1.71	0.2073	1.07	0.9054
Secreted Factors	Matrisome-associated	growth differentiation factor 15(GDF15)	Q99988	1.31	0.3149	1.65	0.1014

Appendix C

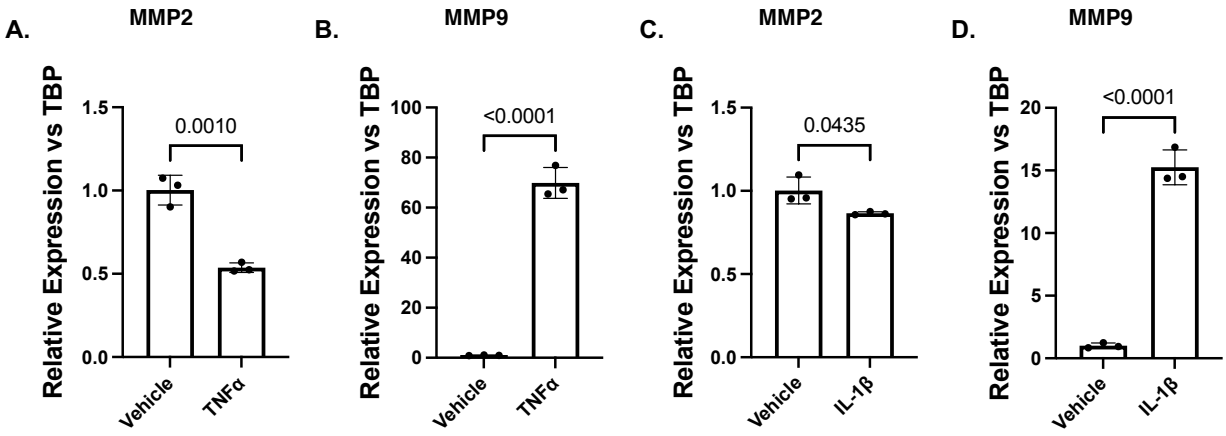

Cytokine-induced changes in MMP expression in hRMEC. Cells were treated as in Table 2 and assayed for expression of MMP2 (A)(C) or MMP9 (B)(D). Expression data are reported as fold induction over vehicle with bars representing mean +/- SD (n=3 for all groups).

Appendix D

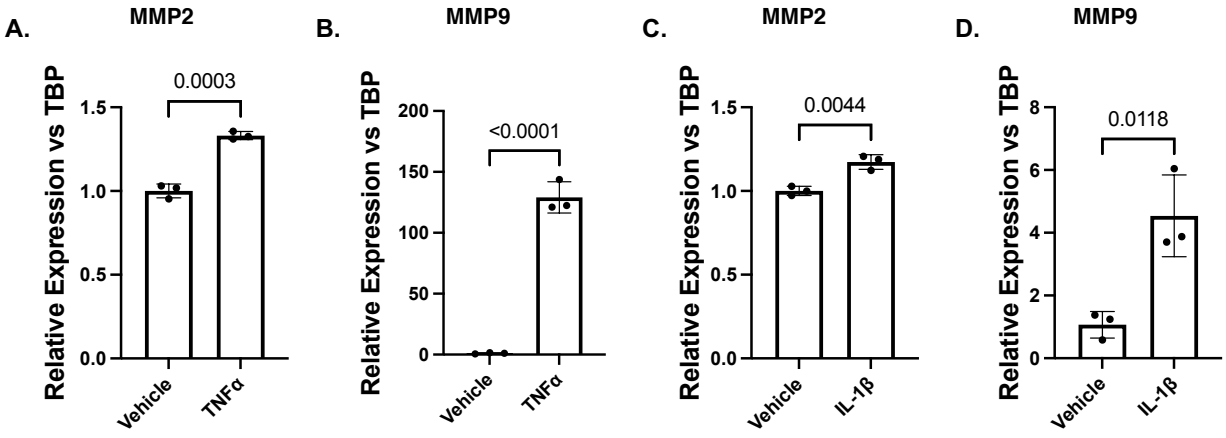

Cytokine-induced changes in MMP expression in hRP. Cells were treated as in Table 3 and assayed for expression of MMP2 (A)(C) or MMP9 (B)(D). Expression data are reported as fold induction over vehicle with bars representing mean +/- SD (n=3 for all groups).

Appendix E

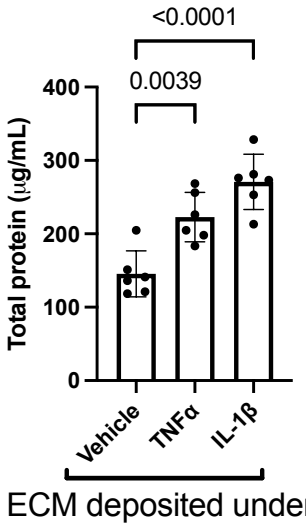

Cytokine-induced changes in total protein deposition by hRP. hRP were treated for 48hrs with 10ng/mL TNFα or IL-1β before collection for qMS analysis. Prior to qMS analysis, total protein concentration was assayed. Data are presented as total protein quantified (μg/mL) (n=6 for all groups).

REFERENCES

1 Tan, S. Y. *et al.* Type 1 and 2 diabetes mellitus: A review on current treatment approach and gene therapy as potential intervention. *Diabetes Metab Syndr* **13**, 364-372, doi:10.1016/j.dsx.2018.10.008 (2019).

2 Guariguata, L. *et al.* Global estimates of diabetes prevalence for 2013 and projections for 2035. *Diabetes Res Clin Pract* **103**, 137-149, doi:10.1016/j.diabres.2013.11.002 (2014).

3 Zimmet, P., Alberti, K. G., Magliano, D. J. & Bennett, P. H. Diabetes mellitus statistics on prevalence and mortality: facts and fallacies. *Nat Rev Endocrinol* **12**, 616-622, doi:10.1038/nrendo.2016.105 (2016).

4 Centers for Disease, C. & Prevention. Blindness caused by diabetes--Massachusetts, 1987-1994. *MMWR Morb Mortal Wkly Rep* **45**, 937-941 (1996).

5 Rubsam, A., Parikh, S. & Fort, P. E. Role of Inflammation in Diabetic Retinopathy. *Int J Mol Sci* **19**, doi:10.3390/ijms19040942 (2018).

6 Kempen, J. H. *et al.* The prevalence of diabetic retinopathy among adults in the United States. *Arch Ophthalmol* **122**, 552-563, doi:10.1001/archopht.122.4.552 (2004).

7 Zhang, X. *et al.* Prevalence of diabetic retinopathy in the United States, 2005-2008. *JAMA* **304**, 649-656, doi:10.1001/jama.2010.1111 (2010).

8 Antonetti, D. A., Klein, R. & Gardner, T. W. Diabetic retinopathy. *N Engl J Med* **366**, 1227-1239, doi:10.1056/NEJMra1005073 (2012).

9 Nathan, D. M. & Group, D. E. R. The diabetes control and complications trial/epidemiology of diabetes interventions and complications study at 30 years: overview. *Diabetes Care* **37**, 9-16, doi:10.2337/dc13-2112 (2014).

10 Intensive blood-glucose control with sulphonylureas or insulin compared with conventional treatment and risk of complications in patients with type 2 diabetes (UKPDS 33). UK Prospective Diabetes Study (UKPDS) Group. *Lancet* **352**, 837-853 (1998).

11 Aiello, L. P. & Group, D. E. R. Diabetic retinopathy and other ocular findings in the diabetes control and complications trial/epidemiology of diabetes interventions and complications study. *Diabetes Care* **37**, 17-23, doi:10.2337/dc13-2251 (2014).

12 Hirsch, I. B. & Brownlee, M. Beyond hemoglobin A1c--need for additional markers of risk for diabetic microvascular complications. *JAMA* **303**, 2291-2292, doi:10.1001/jama.2010.785 (2010).

13 Duh, E. J., Sun, J. K. & Stitt, A. W. Diabetic retinopathy: current understanding, mechanisms, and treatment strategies. *JCI Insight* **2**, doi:10.1172/jci.insight.93751 (2017).

14 Preliminary report on effects of photocoagulation therapy. The Diabetic Retinopathy Study Research Group. *Am J Ophthalmol* **81**, 383-396, doi:10.1016/0002-9394(76)90292-0 (1976).

15 Photocoagulation for diabetic macular edema. Early Treatment Diabetic Retinopathy Study report number 1. Early Treatment Diabetic Retinopathy Study research group. *Arch Ophthalmol* **103**, 1796-1806 (1985).

16 Diabetic Retinopathy Clinical Research, N. *et al.* Randomized trial evaluating ranibizumab plus prompt or deferred laser or triamcinolone plus prompt laser for diabetic macular edema. *Ophthalmology* **117**, 1064-1077 e1035, doi:10.1016/j.ophtha.2010.02.031 (2010).

17 Brown, D. M. *et al.* Long-term outcomes of ranibizumab therapy for diabetic macular edema: the 36-month results from two phase III trials: RISE and RIDE. *Ophthalmology* **120**, 2013-2022, doi:10.1016/j.ophtha.2013.02.034 (2013).

18 Heier, J. S. *et al.* Intravitreal Aflibercept for Diabetic Macular Edema: 148-Week Results from the VISTA and VIVID Studies. *Ophthalmology* **123**, 2376-2385, doi:10.1016/j.ophtha.2016.07.032 (2016).
19 Diabetic Retinopathy Clinical Research, N. *et al.* Aflibercept, bevacizumab, or ranibizumab for diabetic macular edema. *N Engl J Med* **372**, 1193-1203, doi:10.1056/NEJMoa1414264 (2015).
20 Wells, J. A. *et al.* Aflibercept, Bevacizumab, or Ranibizumab for Diabetic Macular Edema: Two-Year Results from a Comparative Effectiveness Randomized Clinical Trial. *Ophthalmology* **123**, 1351-1359, doi:10.1016/j.ophtha.2016.02.022 (2016).
21 Writing Committee for the Diabetic Retinopathy Clinical Research, N. *et al.* Panretinal Photocoagulation vs Intravitreous Ranibizumab for Proliferative Diabetic Retinopathy: A Randomized Clinical Trial. *JAMA* **314**, 2137-2146, doi:10.1001/jama.2015.15217 (2015).
22 Avery, R. L. *et al.* Intravitreal bevacizumab (Avastin) in the treatment of proliferative diabetic retinopathy. *Ophthalmology* **113**, 1695 e1691-1615, doi:10.1016/j.ophtha.2006.05.064 (2006).
23 Simo, R., Sundstrom, J. M. & Antonetti, D. A. Ocular Anti-VEGF therapy for diabetic retinopathy: the role of VEGF in the pathogenesis of diabetic retinopathy. *Diabetes Care* **37**, 893-899, doi:10.2337/dc13-2002 (2014).
24 Virgili, G., Parravano, M., Evans, J. R., Gordon, I. & Lucenteforte, E. Anti-vascular endothelial growth factor for diabetic macular oedema: a network meta-analysis. *Cochrane Database Syst Rev* **10**, CD007419, doi:10.1002/14651858.CD007419.pub6 (2018).
25 Lorenzi, M. & Gerhardinger, C. Early cellular and molecular changes induced by diabetes in the retina. *Diabetologia* **44**, 791-804, doi:10.1007/s001250100544 (2001).
26 Lieth, E., Gardner, T. W., Barber, A. J., Antonetti, D. A. & Penn State Retina Research, G. Retinal neurodegeneration: early pathology in diabetes. *Clin Exp Ophthalmol* **28**, 3-8, doi:10.1046/j.1442-9071.2000.00222.x (2000).
27 Barber, A. J. *et al.* Neural apoptosis in the retina during experimental and human diabetes. Early onset and effect of insulin. *J Clin Invest* **102**, 783-791, doi:10.1172/JCI2425 (1998).
28 Park, S. H. *et al.* Apoptotic death of photoreceptors in the streptozotocin-induced diabetic rat retina. *Diabetologia* **46**, 1260-1268, doi:10.1007/s00125-003-1177-6 (2003).
29 Carrasco, E. *et al.* Lower somatostatin expression is an early event in diabetic retinopathy and is associated with retinal neurodegeneration. *Diabetes Care* **30**, 2902-2908, doi:10.2337/dc07-0332 (2007).
30 Du, Y., Veenstra, A., Palczewski, K. & Kern, T. S. Photoreceptor cells are major contributors to diabetes-induced oxidative stress and local inflammation in the retina. *Proc Natl Acad Sci U S A* **110**, 16586-16591, doi:10.1073/pnas.1314575110 (2013).
31 Cerani, A. *et al.* Neuron-derived semaphorin 3A is an early inducer of vascular permeability in diabetic retinopathy via neuropilin-1. *Cell Metab* **18**, 505-518, doi:10.1016/j.cmet.2013.09.003 (2013).
32 Roy, M. S., Gunkel, R. D. & Podgor, M. J. Color vision defects in early diabetic retinopathy. *Arch Ophthalmol* **104**, 225-228, doi:10.1001/archopht.1986.01050140079024 (1986).
33 Sokol, S. *et al.* Contrast sensitivity in diabetics with and without background retinopathy. *Arch Ophthalmol* **103**, 51-54, doi:10.1001/archopht.1985.01050010055018 (1985).
34 Antonetti, D. A. *et al.* Diabetic retinopathy: seeing beyond glucose-induced microvascular disease. *Diabetes* **55**, 2401-2411, doi:10.2337/db05-1635 (2006).
35 Frost-Larsen, K., Larsen, H. W. & Simonsen, S. E. Oscillatory potential and nyctometry in insulin-dependent diabetics. *Acta Ophthalmol (Copenh)* **58**, 879-888 (1980).

36 Simonsen, S. E. The value of the oscillatory potential in selecting juvenile diabetics at risk of developing proliferative retinopathy. *Acta Ophthalmol (Copenh)* **58**, 865-878 (1980).
37 Bearse, M. A., Jr. *et al.* Local multifocal oscillatory potential abnormalities in diabetes and early diabetic retinopathy. *Investigative ophthalmology & visual science* **45**, 3259-3265, doi:10.1167/iovs.04-0308 (2004).
38 Parisi, V. & Uccioli, L. Visual electrophysiological responses in persons with type 1 diabetes. *Diabetes Metab Res Rev* **17**, 12-18 (2001).
39 Della Sala, S., Bertoni, G., Somazzi, L., Stubbe, F. & Wilkins, A. J. Impaired contrast sensitivity in diabetic patients with and without retinopathy: a new technique for rapid assessment. *Br J Ophthalmol* **69**, 136-142 (1985).
40 Dosso, A. A. *et al.* Contrast sensitivity in obese dyslipidemic patients with insulin resistance. *Arch Ophthalmol* **116**, 1316-1320 (1998).
41 Han, Y. *et al.* Multifocal electroretinogram delays predict sites of subsequent diabetic retinopathy. *Investigative ophthalmology & visual science* **45**, 948-954 (2004).
42 Realini, T., Lai, M. Q. & Barber, L. Impact of diabetes on glaucoma screening using frequency-doubling perimetry. *Ophthalmology* **111**, 2133-2136, doi:10.1016/j.ophtha.2004.05.024 (2004).
43 van Dijk, H. W. *et al.* Selective loss of inner retinal layer thickness in type 1 diabetic patients with minimal diabetic retinopathy. *Invest Ophthalmol Vis Sci* **50**, 3404-3409, doi:10.1167/iovs.08-3143 (2009).
44 van Dijk, H. W. *et al.* Decreased retinal ganglion cell layer thickness in patients with type 1 diabetes. *Invest Ophthalmol Vis Sci* **51**, 3660-3665, doi:10.1167/iovs.09-5041 (2010).
45 Mizutani, M., Gerhardinger, C. & Lorenzi, M. Muller cell changes in human diabetic retinopathy. *Diabetes* **47**, 445-449 (1998).
46 Abu-El-Asrar, A. M., Dralands, L., Missotten, L., Al-Jadaan, I. A. & Geboes, K. Expression of apoptosis markers in the retinas of human subjects with diabetes. *Invest Ophthalmol Vis Sci* **45**, 2760-2766, doi:10.1167/iovs.03-1392 (2004).
47 Hammes, H. P., Federoff, H. J. & Brownlee, M. Nerve growth factor prevents both neuroretinal programmed cell death and capillary pathology in experimental diabetes. *Mol Med* **1**, 527-534 (1995).
48 Zong, H. *et al.* Hyperglycaemia-induced pro-inflammatory responses by retinal Muller glia are regulated by the receptor for advanced glycation end-products (RAGE). *Diabetologia* **53**, 2656-2666, doi:10.1007/s00125-010-1900-z (2010).
49 Cuenca, N. *et al.* Cellular responses following retinal injuries and therapeutic approaches for neurodegenerative diseases. *Prog Retin Eye Res* **43**, 17-75, doi:10.1016/j.preteyeres.2014.07.001 (2014).
50 Abcouwer, S. F. Muller Cell-Microglia Cross Talk Drives Neuroinflammation in Diabetic Retinopathy. *Diabetes* **66**, 261-263, doi:10.2337/dbi16-0047 (2017).
51 Capozzi, M. E., Giblin, M. J. & Penn, J. S. Palmitic Acid Induces Muller Cell Inflammation that is Potentiated by Co-treatment with Glucose. *Sci Rep* **8**, 5459, doi:10.1038/s41598-018-23601-1 (2018).
52 Capozzi, M. E., McCollum, G. W., Cousins, D. B. & Penn, J. S. Linoleic Acid is a Diabetes-relevant Stimulator of Retinal Inflammation in Human Retinal Muller Cells and Microvascular Endothelial Cells. *J Diabetes Metab* **7**, doi:10.4172/2155-6156.1000718 (2016).
53 Coughlin, B. A., Feenstra, D. J. & Mohr, S. Muller cells and diabetic retinopathy. *Vision Res* **139**, 93-100, doi:10.1016/j.visres.2017.03.013 (2017).
54 Wang, J., Xu, X., Elliott, M. H., Zhu, M. & Le, Y. Z. Muller cell-derived VEGF is essential for diabetes-induced retinal inflammation and vascular leakage. *Diabetes* **59**, 2297-2305, doi:10.2337/db09-1420 (2010).

55 Beltramo, E. & Porta, M. Pericyte loss in diabetic retinopathy: mechanisms and consequences. *Curr Med Chem* **20**, 3218-3225 (2013).
56 Li, W., Yanoff, M., Liu, X. & Ye, X. Retinal capillary pericyte apoptosis in early human diabetic retinopathy. *Chin Med J (Engl)* **110**, 659-663 (1997).
57 Enge, M. *et al.* Endothelium-specific platelet-derived growth factor-B ablation mimics diabetic retinopathy. *EMBO J* **21**, 4307-4316, doi:10.1093/emboj/cdf418 (2002).
58 Feenstra, D. J., Yego, E. C. & Mohr, S. Modes of Retinal Cell Death in Diabetic Retinopathy. *J Clin Exp Ophthalmol* **4**, 298, doi:10.4172/2155-9570.1000298 (2013).
59 Campbell, M. & Humphries, P. The blood-retina barrier: tight junctions and barrier modulation. *Adv Exp Med Biol* **763**, 70-84 (2012).
60 Miyamoto, K. *et al.* Prevention of leukostasis and vascular leakage in streptozotocin-induced diabetic retinopathy via intercellular adhesion molecule-1 inhibition. *Proc Natl Acad Sci U S A* **96**, 10836-10841, doi:10.1073/pnas.96.19.10836 (1999).
61 Kim, S. Y. *et al.* Neutrophils are associated with capillary closure in spontaneously diabetic monkey retinas. *Diabetes* **54**, 1534-1542 (2005).
62 Joussen, A. M. *et al.* A central role for inflammation in the pathogenesis of diabetic retinopathy. *FASEB J* **18**, 1450-1452, doi:10.1096/fj.03-1476fje (2004).
63 Olivares, A. M. *et al.* Animal Models of Diabetic Retinopathy. *Curr Diab Rep* **17**, 93, doi:10.1007/s11892-017-0913-0 (2017).
64 Schroder, S., Palinski, W. & Schmid-Schonbein, G. W. Activated monocytes and granulocytes, capillary nonperfusion, and neovascularization in diabetic retinopathy. *Am J Pathol* **139**, 81-100 (1991).
65 McLeod, D. S., Lefer, D. J., Merges, C. & Lutty, G. A. Enhanced expression of intracellular adhesion molecule-1 and P-selectin in the diabetic human retina and choroid. *Am J Pathol* **147**, 642-653 (1995).
66 Joussen, A. M. *et al.* Leukocyte-mediated endothelial cell injury and death in the diabetic retina. *Am J Pathol* **158**, 147-152, doi:10.1016/S0002-9440(10)63952-1 (2001).
67 Tarr, J. M., Kaul, K., Chopra, M., Kohner, E. M. & Chibber, R. Pathophysiology of diabetic retinopathy. *ISRN Ophthalmol* **2013**, 343560, doi:10.1155/2013/343560 (2013).
68 Gui, F., You, Z., Fu, S., Wu, H. & Zhang, Y. Endothelial Dysfunction in Diabetic Retinopathy. *Front Endocrinol (Lausanne)* **11**, 591, doi:10.3389/fendo.2020.00591 (2020).
69 Robinson, R., Barathi, V. A., Chaurasia, S. S., Wong, T. Y. & Kern, T. S. Update on animal models of diabetic retinopathy: from molecular approaches to mice and higher mammals. *Dis Model Mech* **5**, 444-456, doi:10.1242/dmm.009597 (2012).
70 The effect of intensive treatment of diabetes on the development and progression of long-term complications in insulin-dependent diabetes mellitus. The Diabetes Control and Complications Trial Research Group. *N Engl J Med* **329**, 977-986, doi:10.1056/NEJM199309303291401 (1993).
71 Busik, J. V., Esselman, W. J. & Reid, G. E. Examining the role of lipid mediators in diabetic retinopathy. *Clin Lipidol* **7**, 661-675, doi:10.2217/clp.12.68 (2012).
72 Lyons, T. J. *et al.* Diabetic retinopathy and serum lipoprotein subclasses in the DCCT/EDIC cohort. *Invest Ophthalmol Vis Sci* **45**, 910-918 (2004).
73 Tikhonenko, M. *et al.* Remodeling of retinal Fatty acids in an animal model of diabetes: a decrease in long-chain polyunsaturated fatty acids is associated with a decrease in fatty acid elongases Elovl2 and Elovl4. *Diabetes* **59**, 219-227, doi:10.2337/db09-0728 (2010).
74 Chew, E. Y. *et al.* Association of elevated serum lipid levels with retinal hard exudate in diabetic retinopathy. Early Treatment Diabetic Retinopathy Study (ETDRS) Report 22. *Arch Ophthalmol* **114**, 1079-1084 (1996).
75 Yau, J. W. *et al.* Global prevalence and major risk factors of diabetic retinopathy. *Diabetes Care* **35**, 556-564, doi:10.2337/dc11-1909 (2012).

76 Chew, E. Y. & Ambrosius, W. T. Update of the ACCORD Eye Study. *N Engl J Med* **364**, 188-189, doi:10.1056/NEJMc1011499 (2011).
77 Ansquer, J. C., Crimet, D. & Foucher, C. Fibrates and statins in the treatment of diabetic retinopathy. *Curr Pharm Biotechnol* **12**, 396-405 (2011).
78 Group, A. S. *et al.* Effects of medical therapies on retinopathy progression in type 2 diabetes. *N Engl J Med* **363**, 233-244, doi:10.1056/NEJMoa1001288 (2010).
79 Keech, A. C. *et al.* Effect of fenofibrate on the need for laser treatment for diabetic retinopathy (FIELD study): a randomised controlled trial. *Lancet* **370**, 1687-1697, doi:10.1016/S0140-6736(07)61607-9 (2007).
80 Kern, T. S. Contributions of inflammatory processes to the development of the early stages of diabetic retinopathy. *Exp Diabetes Res* **2007**, 95103, doi:10.1155/2007/95103 (2007).
81 Zhang, W., Liu, H., Al-Shabrawey, M., Caldwell, R. W. & Caldwell, R. B. Inflammation and diabetic retinal microvascular complications. *J Cardiovasc Dis Res* **2**, 96-103, doi:10.4103/0975-3583.83035 (2011).
82 Mohammad, G., Mairaj Siddiquei, M., Imtiaz Nawaz, M. & Abu El-Asrar, A. M. The ERK1/2 Inhibitor U0126 Attenuates Diabetes-Induced Upregulation of MMP-9 and Biomarkers of Inflammation in the Retina. *J Diabetes Res* **2013**, 658548, doi:10.1155/2013/658548 (2013).
83 Yu, Z. *et al.* Dendrobium chrysotoxum Lindl. alleviates diabetic retinopathy by preventing retinal inflammation and tight junction protein decrease. *J Diabetes Res* **2015**, 518317, doi:10.1155/2015/518317 (2015).
84 Rangasamy, S. *et al.* Chemokine mediated monocyte trafficking into the retina: role of inflammation in alteration of the blood-retinal barrier in diabetic retinopathy. *PLoS One* **9**, e108508, doi:10.1371/journal.pone.0108508 (2014).
85 Schwartzman, M. L. *et al.* Profile of lipid and protein autacoids in diabetic vitreous correlates with the progression of diabetic retinopathy. *Diabetes* **59**, 1780-1788, doi:10.2337/db10-0110 (2010).
86 Suzuki, Y., Nakazawa, M., Suzuki, K., Yamazaki, H. & Miyagawa, Y. Expression profiles of cytokines and chemokines in vitreous fluid in diabetic retinopathy and central retinal vein occlusion. *Jpn J Ophthalmol* **55**, 256-263, doi:10.1007/s10384-011-0004-8 (2011).
87 Rangasamy, S., McGuire, P. G. & Das, A. Diabetic retinopathy and inflammation: novel therapeutic targets. *Middle East Afr J Ophthalmol* **19**, 52-59, doi:10.4103/0974-9233.92116 (2012).
88 McAuley, A. K. *et al.* Vitreous biomarkers in diabetic retinopathy: a systematic review and meta-analysis. *J Diabetes Complications* **28**, 419-425, doi:10.1016/j.jdiacomp.2013.09.010 (2014).
89 Vujosevic, S. *et al.* Proteome analysis of retinal glia cells-related inflammatory cytokines in the aqueous humour of diabetic patients. *Acta Ophthalmol* **94**, 56-64, doi:10.1111/aos.12812 (2016).
90 Funatsu, H., Noma, H., Mimura, T., Eguchi, S. & Hori, S. Association of vitreous inflammatory factors with diabetic macular edema. *Ophthalmology* **116**, 73-79, doi:10.1016/j.ophtha.2008.09.037 (2009).
91 Maier, R. *et al.* Multiplex bead analysis of vitreous and serum concentrations of inflammatory and proangiogenic factors in diabetic patients. *Mol Vis* **14**, 637-643 (2008).
92 Taghavi, Y., Hassanshahi, G., Kounis, N. G., Koniari, I. & Khorramdelazad, H. Monocyte chemoattractant protein-1 (MCP-1/CCL2) in diabetic retinopathy: latest evidence and clinical considerations. *J Cell Commun Signal* **13**, 451-462, doi:10.1007/s12079-018-00500-8 (2019).

93 Demircan, N., Safran, B. G., Soylu, M., Ozcan, A. A. & Sizmaz, S. Determination of vitreous interleukin-1 (IL-1) and tumour necrosis factor (TNF) levels in proliferative diabetic retinopathy. *Eye (Lond)* **20**, 1366-1369, doi:10.1038/sj.eye.6702138 (2006).
94 Tang, J. & Kern, T. S. Inflammation in diabetic retinopathy. *Prog Retin Eye Res* **30**, 343-358, doi:10.1016/j.preteyeres.2011.05.002 (2011).
95 Dong, N., Xu, B., Wang, B. & Chu, L. Study of 27 aqueous humor cytokines in patients with type 2 diabetes with or without retinopathy. *Mol Vis* **19**, 1734-1746 (2013).
96 Doganay, S. *et al.* Comparison of serum NO, TNF-alpha, IL-1beta, sIL-2R, IL-6 and IL-8 levels with grades of retinopathy in patients with diabetes mellitus. *Eye (Lond)* **16**, 163-170, doi:10.1038/sj/EYE/6700095 (2002).
97 Ferreira, R. *et al.* Neuropeptide Y inhibits interleukin-1 beta-induced microglia motility. *J Neurochem* **120**, 93-105, doi:10.1111/j.1471-4159.2011.07541.x (2012).
98 Giblin, M. J. *et al.* Nuclear factor of activated T-cells (NFAT) regulation of IL-1beta-induced retinal vascular inflammation. *Biochim Biophys Acta Mol Basis Dis*, 166238, doi:10.1016/j.bbadis.2021.166238 (2021).
99 Ontko, C. D., Capozzi, M. E., Kim, M. J., McCollum, G. W. & Penn, J. S. Cytochrome P450-epoxygenated fatty acids inhibit Muller glial inflammation. *Sci Rep* **11**, 9677, doi:10.1038/s41598-021-89000-1 (2021).
100 Liu, X. *et al.* IL-1beta Upregulates IL-8 Production in Human Muller Cells Through Activation of the p38 MAPK and ERK1/2 Signaling Pathways. *Inflammation* **37**, 1486-1495, doi:10.1007/s10753-014-9874-5 (2014).
101 Liu, X. *et al.* IL-1beta induces IL-6 production in retinal Muller cells predominantly through the activation of p38 MAPK/NF-kappaB signaling pathway. *Exp Cell Res* **331**, 223-231, doi:10.1016/j.yexcr.2014.08.040 (2015).
102 Liu, Y., Biarnes Costa, M. & Gerhardinger, C. IL-1beta is upregulated in the diabetic retina and retinal vessels: cell-specific effect of high glucose and IL-1beta autostimulation. *PLoS One* **7**, e36949, doi:10.1371/journal.pone.0036949 (2012).
103 Kowluru, R. A. & Odenbach, S. Role of interleukin-1beta in the pathogenesis of diabetic retinopathy. *Br J Ophthalmol* **88**, 1343-1347, doi:10.1136/bjo.2003.038133 (2004).
104 Luna, J. D. *et al.* Blood-retinal barrier (BRB) breakdown in experimental autoimmune uveoretinitis: comparison with vascular endothelial growth factor, tumor necrosis factor alpha, and interleukin-1beta-mediated breakdown. *J Neurosci Res* **49**, 268-280, doi:10.1002/(sici)1097-4547(19970801)49:3<268::aid-jnr2>3.0.co;2-a. (1997).
105 Takeda, K. *et al.* Brain-Derived Neurotrophic Factor Inhibits Intercellular Adhesion Molecule-1 Expression in Interleukin-1beta-Treated Endothelial Cells. *Cell Biochem Biophys* **74**, 399-406, doi:10.1007/s12013-016-0749-2 (2016).
106 Bamforth, S. D., Lightman, S. L. & Greenwood, J. Ultrastructural analysis of interleukin-1 beta-induced leukocyte recruitment to the rat retina. *Invest Ophthalmol Vis Sci* **38**, 25-35 (1997).
107 Capozzi, M. E., Hammer, S. S., McCollum, G. W. & Penn, J. S. Epoxygenated Fatty Acids Inhibit Retinal Vascular Inflammation. *Sci Rep* **6**, 39211, doi:10.1038/srep39211 (2016).
108 Bretz, C. A., Savage, S. R., Capozzi, M. E., Suarez, S. & Penn, J. S. NFAT isoforms play distinct roles in TNFalpha-induced retinal leukostasis. *Sci Rep* **5**, 14963, doi:10.1038/srep14963 (2015).
109 Powell, E. D. & Field, R. A. Diabetic Retinopathy and Rheumatoid Arthritis. *Lancet* **2**, 17-18 (1964).
110 Cukras, C. A., Petrou, P., Chew, E. Y., Meyerle, C. B. & Wong, W. T. Oral minocycline for the treatment of diabetic macular edema (DME): results of a phase I/II clinical study. *Invest Ophthalmol Vis Sci* **53**, 3865-3874, doi:10.1167/iovs.11-9413 (2012).

111 Joussen, A. M. *et al.* Nonsteroidal anti-inflammatory drugs prevent early diabetic retinopathy via TNF-alpha suppression. *FASEB J* **16**, 438-440, doi:10.1096/fj.01-0707fje (2002).
112 Du, Y., Sarthy, V. P. & Kern, T. S. Interaction between NO and COX pathways in retinal cells exposed to elevated glucose and retina of diabetic rats. *American journal of physiology. Regulatory, integrative and comparative physiology* **287**, R735-741, doi:10.1152/ajpregu.00080.2003 (2004).
113 Ayalasomayajula, S. P. & Kompella, U. B. Celecoxib, a selective cyclooxygenase-2 inhibitor, inhibits retinal vascular endothelial growth factor expression and vascular leakage in a streptozotocin-induced diabetic rat model. *Eur J Pharmacol* **458**, 283-289 (2003).
114 Sun, W., Gerhardinger, C., Dagher, Z., Hoehn, T. & Lorenzi, M. Aspirin at low-intermediate concentrations protects retinal vessels in experimental diabetic retinopathy through non-platelet-mediated effects. *Diabetes* **54**, 3418-3426 (2005).
115 Zhang, W., Liu, H., Rojas, M., Caldwell, R. W. & Caldwell, R. B. Anti-inflammatory therapy for diabetic retinopathy. *Immunotherapy* **3**, 609-628, doi:10.2217/imt.11.24 (2011).
116 Effects of aspirin treatment on diabetic retinopathy. ETDRS report number 8. Early Treatment Diabetic Retinopathy Study Research Group. *Ophthalmology* **98**, 757-765 (1991).
117 Effect of aspirin alone and aspirin plus dipyridamole in early diabetic retinopathy. A multicenter randomized controlled clinical trial. The DAMAD Study Group. *Diabetes* **38**, 491-498 (1989).
118 Tamura, H. *et al.* Intravitreal injection of corticosteroid attenuates leukostasis and vascular leakage in experimental diabetic retina. *Investigative ophthalmology & visual science* **46**, 1440-1444, doi:10.1167/iovs.04-0905 (2005).
119 Jonas, J. B. Intravitreal triamcinolone acetonide for diabetic retinopathy. *Dev Ophthalmol* **39**, 96-110, doi:10.1159/000098502 (2007).
120 Sahni, J. *et al.* Simultaneous Inhibition of Angiopoietin-2 and Vascular Endothelial Growth Factor-A with Faricimab in Diabetic Macular Edema: BOULEVARD Phase 2 Randomized Trial. *Ophthalmology* **126**, 1155-1170, doi:10.1016/j.ophtha.2019.03.023 (2019).
121 Beckmann, R. *et al.* DutaFabs are engineered therapeutic Fab fragments that can bind two targets simultaneously. *Nat Commun* **12**, 708, doi:10.1038/s41467-021-20949-3 (2021).
122 Joussen, A. M. *et al.* TNF-alpha mediated apoptosis plays an important role in the development of early diabetic retinopathy and long-term histopathological alterations. *Mol Vis* **15**, 1418-1428 (2009).
123 Behl, Y. *et al.* Diabetes-enhanced tumor necrosis factor-alpha production promotes apoptosis and the loss of retinal microvascular cells in type 1 and type 2 models of diabetic retinopathy. *Am J Pathol* **172**, 1411-1418, doi:10.2353/ajpath.2008.071070 (2008).
124 Behl, Y., Krothapalli, P., Desta, T., Roy, S. & Graves, D. T. FOXO1 plays an important role in enhanced microvascular cell apoptosis and microvascular cell loss in type 1 and type 2 diabetic rats. *Diabetes* **58**, 917-925, doi:10.2337/db08-0537 (2009).
125 Huang, H. *et al.* TNFalpha is required for late BRB breakdown in diabetic retinopathy, and its inhibition prevents leukostasis and protects vessels and neurons from apoptosis. *Invest Ophthalmol Vis Sci* **52**, 1336-1344, doi:10.1167/iovs.10-5768 (2011).
126 Vincent, J. A. & Mohr, S. Inhibition of caspase-1/interleukin-1beta signaling prevents degeneration of retinal capillaries in diabetes and galactosemia. *Diabetes* **56**, 224-230, doi:10.2337/db06-0427 (2007).

127 Roy, S., Bae, E., Amin, S. & Kim, D. Extracellular matrix, gap junctions, and retinal vascular homeostasis in diabetic retinopathy. *Exp Eye Res* **133**, 58-68, doi:10.1016/j.exer.2014.08.011 (2015).
128 Jayadev, R. & Sherwood, D. R. Basement membranes. *Curr Biol* **27**, R207-R211, doi:10.1016/j.cub.2017.02.006 (2017).
129 Pozzi, A., Yurchenco, P. D. & Iozzo, R. V. The nature and biology of basement membranes. *Matrix Biol* **57-58**, 1-11, doi:10.1016/j.matbio.2016.12.009 (2017).
130 Hynes, R. O. The evolution of metazoan extracellular matrix. *J Cell Biol* **196**, 671-679, doi:10.1083/jcb.201109041 (2012).
131 Thomsen, M. S., Routhe, L. J. & Moos, T. The vascular basement membrane in the healthy and pathological brain. *J Cereb Blood Flow Metab* **37**, 3300-3317, doi:10.1177/0271678X17722436 (2017).
132 Leclech, C., Natale, C. F. & Barakat, A. I. The basement membrane as a structured surface - role in vascular health and disease. *J Cell Sci* **133**, doi:10.1242/jcs.239889 (2020).
133 Sarrazin, S., Lamanna, W. C. & Esko, J. D. Heparan sulfate proteoglycans. *Cold Spring Harb Perspect Biol* **3**, doi:10.1101/cshperspect.a004952 (2011).
134 El Masri, R., Cretinon, Y., Gout, E. & Vives, R. R. HS and Inflammation: A Potential Playground for the Sulfs? *Front Immunol* **11**, 570, doi:10.3389/fimmu.2020.00570 (2020).
135 Kumar, A. V., Katakam, S. K., Urbanowitz, A. K. & Gotte, M. Heparan sulphate as a regulator of leukocyte recruitment in inflammation. *Curr Protein Pept Sci* **16**, 77-86, doi:10.2174/1573402111666150213165054 (2015).
136 To, W. S. & Midwood, K. S. Plasma and cellular fibronectin: distinct and independent functions during tissue repair. *Fibrogenesis Tissue Repair* **4**, 21, doi:10.1186/1755-1536-4-21 (2011).
137 Pankov, R. & Yamada, K. M. Fibronectin at a glance. *J Cell Sci* **115**, 3861-3863, doi:10.1242/jcs.00059 (2002).
138 Mahmood, N., Mihalcioiu, C. & Rabbani, S. A. Multifaceted Role of the Urokinase-Type Plasminogen Activator (uPA) and Its Receptor (uPAR): Diagnostic, Prognostic, and Therapeutic Applications. *Front Oncol* **8**, 24, doi:10.3389/fonc.2018.00024 (2018).
139 Jablonska-Trypuc, A., Matejczyk, M. & Rosochacki, S. Matrix metalloproteinases (MMPs), the main extracellular matrix (ECM) enzymes in collagen degradation, as a target for anticancer drugs. *J Enzyme Inhib Med Chem* **31**, 177-183, doi:10.3109/14756366.2016.1161620 (2016).
140 Bonnans, C., Chou, J. & Werb, Z. Remodelling the extracellular matrix in development and disease. *Nat Rev Mol Cell Biol* **15**, 786-801, doi:10.1038/nrm3904 (2014).
141 Kelwick, R., Desanlis, I., Wheeler, G. N. & Edwards, D. R. The ADAMTS (A Disintegrin and Metalloproteinase with Thrombospondin motifs) family. *Genome Biol* **16**, 113, doi:10.1186/s13059-015-0676-3 (2015).
142 Malemud, C. J. Matrix metalloproteinases (MMPs) in health and disease: an overview. *Front Biosci* **11**, 1696-1701, doi:10.2741/1915 (2006).
143 Hayden, M. R., Sowers, J. R. & Tyagi, S. C. The central role of vascular extracellular matrix and basement membrane remodeling in metabolic syndrome and type 2 diabetes: the matrix preloaded. *Cardiovasc Diabetol* **4**, 9, doi:10.1186/1475-2840-4-9 (2005).
144 Tsilibary, E. C. Microvascular basement membranes in diabetes mellitus. *J Pathol* **200**, 537-546, doi:10.1002/path.1439 (2003).
145 Roy, S. & Kim, D. Retinal capillary basement membrane thickening: Role in the pathogenesis of diabetic retinopathy. *Prog Retin Eye Res*, 100903, doi:10.1016/j.preteyeres.2020.100903 (2020).

146 Hill, R. E. & Williams, P. E. Perineurial cell basement membrane thickening and myelinated nerve fibre loss in diabetic and nondiabetic peripheral nerve. *J Neurol Sci* **217**, 157-163, doi:10.1016/j.jns.2003.09.011 (2004).
147 Marshall, C. B. Rethinking glomerular basement membrane thickening in diabetic nephropathy: adaptive or pathogenic? *Am J Physiol Renal Physiol* **311**, F831-F843, doi:10.1152/ajprenal.00313.2016 (2016).
148 Kolset, S. O., Reinholt, F. P. & Jenssen, T. Diabetic nephropathy and extracellular matrix. *J Histochem Cytochem* **60**, 976-986, doi:10.1369/0022155412465073 (2012).
149 Roy, S., Ha, J., Trudeau, K. & Beglova, E. Vascular basement membrane thickening in diabetic retinopathy. *Curr Eye Res* **35**, 1045-1056, doi:10.3109/02713683.2010.514659 (2010).
150 Ashton, N. Vascular changes in diabetes with particular reference to the retinal vessels; preliminary report. *Br J Ophthalmol* **33**, 407-420, doi:10.1136/bjo.33.7.407 (1949).
151 Bogdani, M. *et al.* Extracellular matrix components in the pathogenesis of type 1 diabetes. *Curr Diab Rep* **14**, 552, doi:10.1007/s11892-014-0552-7 (2014).
152 To, M. *et al.* Diabetes-induced morphological, biomechanical, and compositional changes in ocular basement membranes. *Exp Eye Res* **116**, 298-307, doi:10.1016/j.exer.2013.09.011 (2013).
153 Halfter, W. *et al.* Diabetes-related changes in the protein composition and the biomechanical properties of human retinal vascular basement membranes. *PLoS One* **12**, e0189857, doi:10.1371/journal.pone.0189857 (2017).
154 Ashton, N. Vascular basement membrane changes in diabetic retinopathy. Montgomery lecture, 1973. *Br J Ophthalmol* **58**, 344-366, doi:10.1136/bjo.58.4.344 (1974).
155 Roy, S., Sato, T., Paryani, G. & Kao, R. Downregulation of fibronectin overexpression reduces basement membrane thickening and vascular lesions in retinas of galactose-fed rats. *Diabetes* **52**, 1229-1234 (2003).
156 Oshitari, T. *et al.* Effect of combined antisense oligonucleotides against high-glucose- and diabetes-induced overexpression of extracellular matrix components and increased vascular permeability. *Diabetes* **55**, 86-92 (2006).
157 Roy, S. & Lorenzi, M. Early biosynthetic changes in the diabetic-like retinopathy of galactose-fed rats. *Diabetologia* **39**, 735-738 (1996).
158 Roy, S., Maiello, M. & Lorenzi, M. Increased expression of basement membrane collagen in human diabetic retinopathy. *J Clin Invest* **93**, 438-442, doi:10.1172/JCI116979 (1994).
159 Spirin, K. S. *et al.* Basement membrane and growth factor gene expression in normal and diabetic human retinas. *Curr Eye Res* **18**, 490-499 (1999).
160 Ljubimov, A. V. *et al.* Basement membrane abnormalities in human eyes with diabetic retinopathy. *J Histochem Cytochem* **44**, 1469-1479 (1996).
161 Nishikawa, T., Giardino, I., Edelstein, D. & Brownlee, M. Changes in diabetic retinal matrix protein mRNA levels in a common transgenic mouse strain. *Curr Eye Res* **21**, 581-587 (2000).
162 Cherian, S., Roy, S., Pinheiro, A. & Roy, S. Tight glycemic control regulates fibronectin expression and basement membrane thickening in retinal and glomerular capillaries of diabetic rats. *Invest Ophthalmol Vis Sci* **50**, 943-949, doi:10.1167/iovs.08-2377 (2009).
163 Wu, Y., Feng, B., Chen, S. & Chakrabarti, S. ERK5 Regulates glucose-induced increased fibronectin production in the endothelial cells and in the retina in diabetes. *Invest Ophthalmol Vis Sci* **53**, 8405-8413, doi:10.1167/iovs.12-10553 (2012).
164 Cagliero, E., Maiello, M., Boeri, D., Roy, S. & Lorenzi, M. Increased expression of basement membrane components in human endothelial cells cultured in high glucose. *J Clin Invest* **82**, 735-738, doi:10.1172/JCI113655 (1988).

165 Cagliero, E., Roth, T., Roy, S. & Lorenzi, M. Characteristics and mechanisms of high-glucose-induced overexpression of basement membrane components in cultured human endothelial cells. *Diabetes* **40**, 102-110 (1991).
166 Chronopoulos, A. *et al.* High glucose-induced altered basement membrane composition and structure increases trans-endothelial permeability: implications for diabetic retinopathy. *Curr Eye Res* **36**, 747-753, doi:10.3109/02713683.2011.585735 (2011).
167 Palenski, T. L., Sorenson, C. M. & Sheibani, N. Inflammatory cytokine-specific alterations in retinal endothelial cell function. *Microvasc Res* **89**, 57-69, doi:10.1016/j.mvr.2013.06.007 (2013).
168 Chen, S., Mukherjee, S., Chakraborty, C. & Chakrabarti, S. High glucose-induced, endothelin-dependent fibronectin synthesis is mediated via NF-kappa B and AP-1. *Am J Physiol Cell Physiol* **284**, C263-272, doi:10.1152/ajpcell.00192.2002 (2003).
169 Mandarino, L. J., Sundarraj, N., Finlayson, J. & Hassell, H. R. Regulation of fibronectin and laminin synthesis by retinal capillary endothelial cells and pericytes in vitro. *Exp Eye Res* **57**, 609-621, doi:10.1006/exer.1993.1166 (1993).
170 Uechi, G., Sun, Z., Schreiber, E. M., Halfter, W. & Balasubramani, M. Proteomic View of Basement Membranes from Human Retinal Blood Vessels, Inner Limiting Membranes, and Lens Capsules. *J Proteome Res*, doi:10.1021/pr5002065 (2014).
171 Sorokin, L. The impact of the extracellular matrix on inflammation. *Nat Rev Immunol* **10**, 712-723, doi:10.1038/nri2852 (2010).
172 Watson, S. P. Platelet activation by extracellular matrix proteins in haemostasis and thrombosis. *Curr Pharm Des* **15**, 1358-1372 (2009).
173 Lee, T. H., Hsieh, S. T. & Chiang, H. Y. Fibronectin inhibitor pUR4 attenuates tumor necrosis factor alpha-induced endothelial hyperpermeability by modulating beta1 integrin activation. *J Biomed Sci* **26**, 37, doi:10.1186/s12929-019-0529-6 (2019).
174 Sava, P., Cook, I. O., Mahal, R. S. & Gonzalez, A. L. Human microvascular pericyte basement membrane remodeling regulates neutrophil recruitment. *Microcirculation* **22**, 54-67, doi:10.1111/micc.12173 (2015).
175 Song, J. *et al.* Endothelial Basement Membrane Laminin 511 Contributes to Endothelial Junctional Tightness and Thereby Inhibits Leukocyte Transmigration. *Cell Rep* **18**, 1256-1269, doi:10.1016/j.celrep.2016.12.092 (2017).
176 Huynh, J. *et al.* Age-related intimal stiffening enhances endothelial permeability and leukocyte transmigration. *Sci Transl Med* **3**, 112ra122, doi:10.1126/scitranslmed.3002761 (2011).
177 Voisin, M. B., Probstl, D. & Nourshargh, S. Venular basement membranes ubiquitously express matrix protein low-expression regions: characterization in multiple tissues and remodeling during inflammation. *Am J Pathol* **176**, 482-495, doi:10.2353/ajpath.2010.090510 (2010).
178 Yang, X. *et al.* Basement membrane stiffening promotes retinal endothelial activation associated with diabetes. *FASEB J* **30**, 601-611, doi:10.1096/fj.15-277962 (2016).
179 Scott, H. A. *et al.* Matrix stiffness exerts biphasic control over monocyte-endothelial adhesion via Rho-mediated ICAM-1 clustering. *Integr Biol (Camb)* **8**, 869-878, doi:10.1039/c6ib00084c (2016).
180 Hicks, D. & Courtois, Y. The growth and behaviour of rat retinal Muller cells in vitro. 1. An improved method for isolation and culture. *Exp Eye Res* **51**, 119-129, doi:10.1016/0014-4835(90)90063-z (1990).
181 Baldeweg, S. E. *et al.* Insulin resistance, lipid and fatty acid concentrations in 867 healthy Europeans. European Group for the Study of Insulin Resistance (EGIR). *Eur J Clin Invest* **30**, 45-52, doi:10.1046/j.1365-2362.2000.00597.x (2000).

182 Lewis, G. F., Carpentier, A., Adeli, K. & Giacca, A. Disordered fat storage and mobilization in the pathogenesis of insulin resistance and type 2 diabetes. *Endocr Rev* **23**, 201-229, doi:10.1210/edrv.23.2.0461 (2002).
183 Yi, L. *et al.* Simultaneously quantitative measurement of comprehensive profiles of esterified and non-esterified fatty acid in plasma of type 2 diabetic patients. *Chem Phys Lipids* **150**, 204-216, doi:10.1016/j.chemphyslip.2007.08.002 (2007).
184 Clore, J. N., Allred, J., White, D., Li, J. & Stillman, J. The role of plasma fatty acid composition in endogenous glucose production in patients with type 2 diabetes mellitus. *Metabolism* **51**, 1471-1477, doi:10.1053/meta.2002.35202 (2002).
185 Chen, W., Jump, D. B., Grant, M. B., Esselman, W. J. & Busik, J. V. Dyslipidemia, but not hyperglycemia, induces inflammatory adhesion molecules in human retinal vascular endothelial cells. *Invest Ophthalmol Vis Sci* **44**, 5016-5022 (2003).
186 Coll, T. *et al.* Oleate reverses palmitate-induced insulin resistance and inflammation in skeletal muscle cells. *J Biol Chem* **283**, 11107-11116, doi:10.1074/jbc.M708700200 (2008).
187 Dyntar, D. *et al.* Glucose and palmitic acid induce degeneration of myofibrils and modulate apoptosis in rat adult cardiomyocytes. *Diabetes* **50**, 2105-2113, doi:10.2337/diabetes.50.9.2105 (2001).
188 Ramos, C. J., Lin, C., Liu, X. & Antonetti, D. A. The EPAC-Rap1 pathway prevents and reverses cytokine-induced retinal vascular permeability. *J Biol Chem* **293**, 717-730, doi:10.1074/jbc.M117.815381 (2018).
189 van der Wijk, A. E., Vogels, I. M. C., van Noorden, C. J. F., Klaassen, I. & Schlingemann, R. O. TNFalpha-Induced Disruption of the Blood-Retinal Barrier In Vitro Is Regulated by Intracellular 3',5'-Cyclic Adenosine Monophosphate Levels. *Invest Ophthalmol Vis Sci* **58**, 3496-3505, doi:10.1167/iovs.16-21091 (2017).
190 Lo, C. M., Keese, C. R. & Giaever, I. Impedance analysis of MDCK cells measured by electric cell-substrate impedance sensing. *Biophys J* **69**, 2800-2807, doi:10.1016/S0006-3495(95)80153-0 (1995).
191 Robilliard, L. D. *et al.* The Importance of Multifrequency Impedance Sensing of Endothelial Barrier Formation Using ECIS Technology for the Generation of a Strong and Durable Paracellular Barrier. *Biosensors (Basel)* **8**, doi:10.3390/bios8030064 (2018).
192 Byron, A. *et al.* Glomerular cell cross-talk influences composition and assembly of extracellular matrix. *J Am Soc Nephrol* **25**, 953-966, doi:10.1681/ASN.2013070795 (2014).
193 Rashid, S. T. *et al.* Proteomic analysis of extracellular matrix from the hepatic stellate cell line LX-2 identifies CYR61 and Wnt-5a as novel constituents of fibrotic liver. *J Proteome Res* **11**, 4052-4064, doi:10.1021/pr3000927 (2012).
194 Franco-Barraza, J., Beacham, D. A., Amatangelo, M. D. & Cukierman, E. Preparation of Extracellular Matrices Produced by Cultured and Primary Fibroblasts. *Curr Protoc Cell Biol* **71**, 10 19 11-10 19 34, doi:10.1002/cpcb.2 (2016).
195 Califano, J. P. & Reinhart-King, C. A. A Balance of Substrate Mechanics and Matrix Chemistry Regulates Endothelial Cell Network Assembly. *Cell Mol Bioeng* **1**, 122-132, doi:10.1007/s12195-008-0022-x (2008).
196 Naba, A. *et al.* Characterization of the Extracellular Matrix of Normal and Diseased Tissues Using Proteomics. *J Proteome Res* **16**, 3083-3091, doi:10.1021/acs.jproteome.7b00191 (2017).
197 Rothwell, N. J. & Luheshi, G. N. Interleukin 1 in the brain: biology, pathology and therapeutic target. *Trends Neurosci* **23**, 618-625, doi:10.1016/s0166-2236(00)01661-1 (2000).

198 Dinarello, C. A. Blocking interleukin-1beta in acute and chronic autoinflammatory diseases. *J Intern Med* **269**, 16-28, doi:10.1111/j.1365-2796.2010.02313.x (2011).
199 Masters, S. L. *et al.* Activation of the NLRP3 inflammasome by islet amyloid polypeptide provides a mechanism for enhanced IL-1beta in type 2 diabetes. *Nat Immunol* **11**, 897-904, doi:10.1038/ni.1935 (2010).
200 Vandanmagsar, B. *et al.* The NLRP3 inflammasome instigates obesity-induced inflammation and insulin resistance. *Nat Med* **17**, 179-188, doi:10.1038/nm.2279 (2011).
201 Dinarello, C. A. Interleukin-1 in the pathogenesis and treatment of inflammatory diseases. *Blood* **117**, 3720-3732, doi:10.1182/blood-2010-07-273417 (2011).
202 Sama, M. A. *et al.* Interleukin-1beta-dependent signaling between astrocytes and neurons depends critically on astrocytic calcineurin/NFAT activity. *J Biol Chem* **283**, 21953-21964, doi:10.1074/jbc.M800148200 (2008).
203 Yaykasli, K. O. *et al.* ADAMTS9 activation by interleukin 1 beta via NFATc1 in OUMS-27 chondrosarcoma cells and in human chondrocytes. *Mol Cell Biochem* **323**, 69-79, doi:10.1007/s11010-008-9965-4 (2009).
204 Hogan, P. G., Chen, L., Nardone, J. & Rao, A. Transcriptional regulation by calcium, calcineurin, and NFAT. *Genes Dev* **17**, 2205-2232, doi:10.1101/gad.1102703 (2003).
205 Rao, A., Luo, C. & Hogan, P. G. Transcription factors of the NFAT family: regulation and function. *Annu Rev Immunol* **15**, 707-747, doi:10.1146/annurev.immunol.15.1.707 (1997).
206 Lopez-Rodriguez, C. *et al.* Bridging the NFAT and NF-kappaB families: NFAT5 dimerization regulates cytokine gene transcription in response to osmotic stress. *Immunity* **15**, 47-58, doi:10.1016/s1074-7613(01)00165-0 (2001).
207 Pan, M. G., Xiong, Y. & Chen, F. NFAT gene family in inflammation and cancer. *Curr Mol Med* **13**, 543-554, doi:10.2174/1566524011313040007 (2013).
208 Qin, J. J. *et al.* NFAT as cancer target: mission possible? *Biochim Biophys Acta* **1846**, 297-311, doi:10.1016/j.bbcan.2014.07.009 (2014).
209 Lee, J. U., Kim, L. K. & Choi, J. M. Revisiting the Concept of Targeting NFAT to Control T Cell Immunity and Autoimmune Diseases. *Front Immunol* **9**, 2747, doi:10.3389/fimmu.2018.02747 (2018).
210 Kang, S., Li, H., Rao, A. & Hogan, P. G. Inhibition of the calcineurin-NFAT interaction by small organic molecules reflects binding at an allosteric site. *J Biol Chem* **280**, 37698-37706, doi:10.1074/jbc.M502247200 (2005).
211 Roehrl, M. H. *et al.* Selective inhibition of calcineurin-NFAT signaling by blocking protein-protein interaction with small organic molecules. *Proc Natl Acad Sci U S A* **101**, 7554-7559, doi:10.1073/pnas.0401835101 (2004).
212 Savage, S. R., Bretz, C. A. & Penn, J. S. RNA-Seq reveals a role for NFAT-signaling in human retinal microvascular endothelial cells treated with TNFalpha. *PLoS One* **10**, e0116941, doi:10.1371/journal.pone.0116941 (2015).
213 Cobbs, S. L. & Gooch, J. L. NFATc is required for TGFbeta-mediated transcriptional regulation of fibronectin. *Biochem Biophys Res Commun* **362**, 288-294, doi:10.1016/j.bbrc.2007.07.186 (2007).
214 Funk, S. D., Finney, A. C., Yurdagul, A., Jr., Pattillo, C. B. & Orr, A. W. EphA2 stimulates VCAM-1 expression through calcium-dependent NFAT1 activity. *Cell Signal* **49**, 30-38, doi:10.1016/j.cellsig.2018.05.008 (2018).
215 Wang, Y. *et al.* The role of Ca(2+)/NFAT in Dysfunction and Inflammation of Human Coronary Endothelial Cells induced by Sera from patients with Kawasaki disease. *Sci Rep* **10**, 4706, doi:10.1038/s41598-020-61667-y (2020).
216 Karpurapu, M. *et al.* Inhibition of nuclear factor of activated T cells (NFAT) c3 activation attenuates acute lung injury and pulmonary edema in murine models of sepsis. *Oncotarget* **9**, 10606-10620, doi:10.18632/oncotarget.24320 (2018).

217 Garcia-Vaz, E. *et al.* Inhibition of NFAT Signaling Restores Microvascular Endothelial Function in Diabetic Mice. *Diabetes* **69**, 424-435, doi:10.2337/db18-0870 (2020).
218 Zetterqvist, A. V. *et al.* Nuclear factor of activated T cells is activated in the endothelium of retinal microvessels in diabetic mice. *J Diabetes Res* **2015**, 428473, doi:10.1155/2015/428473 (2015).
219 Zetterqvist, A. V. *et al.* Inhibition of nuclear factor of activated T-cells (NFAT) suppresses accelerated atherosclerosis in diabetic mice. *PLoS One* **8**, e65020, doi:10.1371/journal.pone.0065020 (2014).
220 Bendickova, K. *et al.* Calcineurin inhibitors reduce NFAT-dependent expression of antifungal pentraxin-3 by human monocytes. *J Leukoc Biol* **107**, 497-508, doi:10.1002/JLB.4VMA0318-138R (2020).
221 Nagamoto-Combs, K. & Combs, C. K. Microglial phenotype is regulated by activity of the transcription factor, NFAT (nuclear factor of activated T cells). *J Neurosci* **30**, 9641-9646, doi:10.1523/JNEUROSCI.0828-10.2010 (2010).
222 Huang, R., Guo, L., Gao, M., Li, J. & Xiang, S. Research Trends and Regulation of CCL5 in Prostate Cancer. *Onco Targets Ther* **14**, 1417-1427, doi:10.2147/OTT.S279189 (2021).
223 Bringmann, A. *et al.* Muller cells in the healthy and diseased retina. *Prog Retin Eye Res* **25**, 397-424, doi:10.1016/j.preteyeres.2006.05.003 (2006).
224 Xiao, L. *et al.* Mechanisms underlying rate-dependent remodeling of transient outward potassium current in canine ventricular myocytes. *Circ Res* **103**, 733-742, doi:10.1161/CIRCRESAHA.108.171157 (2008).
225 Liu, L., Peng, Z., Huang, H., Xu, Z. & Wei, X. Luteolin and apigenin activate the Oct-4/Sox2 signal via NFATc1 in human periodontal ligament cells. *Cell Biol Int* **40**, 1094-1106, doi:10.1002/cbin.10648 (2016).
226 Liu, L., Peng, Z., Xu, Z., Huang, H. & Wei, X. Mouse embryonic fibroblast (MEF)/BMP4-conditioned medium enhanced multipotency of human dental pulp cells. *J Mol Histol* **49**, 17-26, doi:10.1007/s10735-017-9743-2 (2018).
227 Prasad, A. M. & Inesi, G. Silencing calcineurin A subunit reduces SERCA2 expression in cardiac myocytes. *Am J Physiol Heart Circ Physiol* **300**, H173-180, doi:10.1152/ajpheart.00841.2010 (2011).
228 Bretz, C. A., Savage, S., Capozzi, M. & Penn, J. S. The role of the NFAT signaling pathway in retinal neovascularization. *Invest Ophthalmol Vis Sci* **54**, 7020-7027, doi:10.1167/iovs.13-12183 (2013).
229 Sorrentino, F. S., Allkabes, M., Salsini, G., Bonifazzi, C. & Perri, P. The importance of glial cells in the homeostasis of the retinal microenvironment and their pivotal role in the course of diabetic retinopathy. *Life Sci* **162**, 54-59, doi:10.1016/j.lfs.2016.08.001 (2016).
230 Sompol, P. & Norris, C. M. Ca(2+), Astrocyte Activation and Calcineurin/NFAT Signaling in Age-Related Neurodegenerative Diseases. *Front Aging Neurosci* **10**, 199, doi:10.3389/fnagi.2018.00199 (2018).
231 Manocha, G. D. *et al.* NFATc2 Modulates Microglial Activation in the AbetaPP/PS1 Mouse Model of Alzheimer's Disease. *J Alzheimers Dis* **58**, 775-787, doi:10.3233/JAD-151203 (2017).
232 Shiratori, M., Tozaki-Saitoh, H., Yoshitake, M., Tsuda, M. & Inoue, K. P2X7 receptor activation induces CXCL2 production in microglia through NFAT and PKC/MAPK pathways. *J Neurochem* **114**, 810-819, doi:10.1111/j.1471-4159.2010.06809.x (2010).
233 Ma, B. *et al.* Toll-Like Receptors Promote Mitochondrial Translocation of Nuclear Transcription Factor Nuclear Factor of Activated T-Cells in Prolonged Microglial Activation. *J Neurosci* **35**, 10799-10814, doi:10.1523/JNEUROSCI.2455-14.2015 (2015).
234 Monickaraj, F., Oruganti, S. R., McGuire, P. & Das, A. A potential novel therapeutic target in diabetic retinopathy: a chemokine receptor (CCR2/CCR5) inhibitor reduces

retinal vascular leakage in an animal model. *Graefes Arch Clin Exp Ophthalmol* **259**, 93-100, doi:10.1007/s00417-020-04884-5 (2021).
235 Noda, K., Nakao, S., Ishida, S. & Ishibashi, T. Leukocyte adhesion molecules in diabetic retinopathy. *J Ophthalmol* **2012**, 279037, doi:10.1155/2012/279037 (2012).
236 Ley, K., Laudanna, C., Cybulsky, M. I. & Nourshargh, S. Getting to the site of inflammation: the leukocyte adhesion cascade updated. *Nat Rev Immunol* **7**, 678-689, doi:10.1038/nri2156 (2007).
237 Durand, D. B. *et al.* Characterization of antigen receptor response elements within the interleukin-2 enhancer. *Mol Cell Biol* **8**, 1715-1724, doi:10.1128/mcb.8.4.1715 (1988).
238 Shaw, J. P. *et al.* Identification of a putative regulator of early T cell activation genes. *Science* **241**, 202-205, doi:10.1126/science.3260404 (1988).
239 Fric, J. *et al.* NFAT control of innate immunity. *Blood* **120**, 1380-1389, doi:10.1182/blood-2012-02-404475 (2012).
240 Stahel, M., Becker, M., Graf, N. & Michels, S. SYSTEMIC INTERLEUKIN 1beta INHIBITION IN PROLIFERATIVE DIABETIC RETINOPATHY: A Prospective Open-Label Study Using Canakinumab. *Retina* **36**, 385-391, doi:10.1097/IAE.0000000000000701 (2016).
241 Suehiro, J. *et al.* Genome-wide approaches reveal functional vascular endothelial growth factor (VEGF)-inducible nuclear factor of activated T cells (NFAT) c1 binding to angiogenesis-related genes in the endothelium. *J Biol Chem* **289**, 29044-29059, doi:10.1074/jbc.M114.555235 (2014).
242 Cai, Y. *et al.* Role of NFAT in the Progression of Diabetic Atherosclerosis. *Front Cardiovasc Med* **8**, 635172, doi:10.3389/fcvm.2021.635172 (2021).
243 Rafiee, P. *et al.* Cyclosporin A differentially inhibits multiple steps in VEGF induced angiogenesis in human microvascular endothelial cells through altered intracellular signaling. *Cell Commun Signal* **2**, 3, doi:10.1186/1478-811X-2-3 (2004).
244 Schweighofer, B. *et al.* The VEGF-induced transcriptional response comprises gene clusters at the crossroad of angiogenesis and inflammation. *Thromb Haemost* **102**, 544-554, doi:10.1160/TH08-12-0830 (2009).
245 Johnson, E. N. *et al.* NFATc1 mediates vascular endothelial growth factor-induced proliferation of human pulmonary valve endothelial cells. *J Biol Chem* **278**, 1686-1692, doi:10.1074/jbc.M210250200 (2003).
246 Urso, K. *et al.* NFATc3 regulates the transcription of genes involved in T-cell activation and angiogenesis. *Blood* **118**, 795-803, doi:10.1182/blood-2010-12-322701 (2011).
247 Hammer, S. S. & Busik, J. V. The role of dyslipidemia in diabetic retinopathy. *Vision Res* **139**, 228-236, doi:10.1016/j.visres.2017.04.010 (2017).
248 Abcouwer, S. F. Angiogenic Factors and Cytokines in Diabetic Retinopathy. *J Clin Cell Immunol* **Suppl 1**, doi:10.4172/2155-9899 (2013).
249 Roy, S., Kim, D., Hernandez, C., Simo, R. & Roy, S. Beneficial effects of fenofibric acid on overexpression of extracellular matrix components, COX-2, and impairment of endothelial permeability associated with diabetic retinopathy. *Exp Eye Res* **140**, 124-129, doi:10.1016/j.exer.2015.08.010 (2015).
250 Gardiner, T. A. *et al.* Prevention of retinal capillary basement membrane thickening in diabetic dogs by a non-steroidal anti-inflammatory drug. *Diabetologia* **46**, 1269-1275, doi:10.1007/s00125-003-1147-z (2003).
251 Limb, G. A. *et al.* Differential expression of matrix metalloproteinases 2 and 9 by glial Muller cells: response to soluble and extracellular matrix-bound tumor necrosis factor-alpha. *Am J Pathol* **160**, 1847-1855, doi:10.1016/s0002-9440(10)61131-5 (2002).
252 Stratman, A. N. & Davis, G. E. Endothelial cell-pericyte interactions stimulate basement membrane matrix assembly: influence on vascular tube remodeling, maturation, and stabilization. *Microsc Microanal* **18**, 68-80, doi:10.1017/S1431927611012402 (2012).

253 Davis, G. E. & Senger, D. R. Endothelial extracellular matrix: biosynthesis, remodeling, and functions during vascular morphogenesis and neovessel stabilization. *Circ Res* **97**, 1093-1107, doi:10.1161/01.RES.0000191547.64391.e3 (2005).
254 Wang, S. *et al.* Pericytes regulate vascular basement membrane remodeling and govern neutrophil extravasation during inflammation. *PLoS One* **7**, e45499, doi:10.1371/journal.pone.0045499 (2012).
255 Kose, N. *et al.* Altered expression of basement membrane-related molecules in rat brain pericyte, endothelial, and astrocyte cell lines after transforming growth factor-beta1 treatment. *Drug Metab Pharmacokinet* **22**, 255-266, doi:10.2133/dmpk.22.255 (2007).
256 Hung, C. *et al.* Role of lung pericytes and resident fibroblasts in the pathogenesis of pulmonary fibrosis. *Am J Respir Crit Care Med* **188**, 820-830, doi:10.1164/rccm.201212-2297OC (2013).
257 Armulik, A., Genove, G. & Betsholtz, C. Pericytes: developmental, physiological, and pathological perspectives, problems, and promises. *Dev Cell* **21**, 193-215, doi:10.1016/j.devcel.2011.07.001 (2011).
258 Voisin, M. B. *et al.* Neutrophil elastase plays a non-redundant role in remodeling the venular basement membrane and neutrophil diapedesis post-ischemia/reperfusion injury. *J Pathol* **248**, 88-102, doi:10.1002/path.5234 (2019).
259 Sakhneny, L., Epshtein, A. & Landsman, L. Pericytes contribute to the islet basement membranes to promote beta-cell gene expression. *Sci Rep* **11**, 2378, doi:10.1038/s41598-021-81774-8 (2021).
260 Nourshargh, S. & Alon, R. Leukocyte migration into inflamed tissues. *Immunity* **41**, 694-707, doi:10.1016/j.immuni.2014.10.008 (2014).
261 Roy, S., Cagliero, E. & Lorenzi, M. Fibronectin overexpression in retinal microvessels of patients with diabetes. *Invest Ophthalmol Vis Sci* **37**, 258-266 (1996).
262 Wu, H., Hwang, D. K., Song, X. & Tao, Y. Association between Aqueous Cytokines and Diabetic Retinopathy Stage. *J Ophthalmol* **2017**, 9402198, doi:10.1155/2017/9402198 (2017).
263 Mao, C. & Yan, H. Roles of elevated intravitreal IL-1beta and IL-10 levels in proliferative diabetic retinopathy. *Indian J Ophthalmol* **62**, 699-701, doi:10.4103/0301-4738.136220 (2014).
264 Boss, J. D. *et al.* Assessment of Neurotrophins and Inflammatory Mediators in Vitreous of Patients With Diabetic Retinopathy. *Invest Ophthalmol Vis Sci* **58**, 5594-5603, doi:10.1167/iovs.17-21973 (2017).
265 Oh, I. K., Kim, S. W., Oh, J., Lee, T. S. & Huh, K. Inflammatory and angiogenic factors in the aqueous humor and the relationship to diabetic retinopathy. *Curr Eye Res* **35**, 1116-1127, doi:10.3109/02713683.2010.510257 (2010).
266 Yuuki, T. *et al.* Inflammatory cytokines in vitreous fluid and serum of patients with diabetic vitreoretinopathy. *J Diabetes Complications* **15**, 257-259, doi:10.1016/s1056-8727(01)00155-6 (2001).
267 Hegde, K. R. & Varma, S. D. Electron impact mass spectroscopic studies on mouse retinal fatty acids: effect of diabetes. *Ophthalmic Res* **42**, 9-14, doi:10.1159/000219679 (2009).
268 Lei, X. *et al.* EPO attenuates inflammatory cytokines by Muller cells in diabetic retinopathy. *Front Biosci (Elite Ed)* **3**, 201-211, doi:10.2741/e234 (2011).
269 Portillo, J. C. *et al.* CD40 in Retinal Muller Cells Induces P2X7-Dependent Cytokine Expression in Macrophages/Microglia in Diabetic Mice and Development of Early Experimental Diabetic Retinopathy. *Diabetes* **66**, 483-493, doi:10.2337/db16-0051 (2017).

270 Rymaszewski, Z. *et al.* Human retinal vascular cells differ from umbilical cells in synthetic functions and their response to glucose. *Proc Soc Exp Biol Med* **199**, 183-191 (1992).
271 Grammas, P. & Riden, M. Retinal endothelial cells are more susceptible to oxidative stress and increased permeability than brain-derived endothelial cells. *Microvasc Res* **65**, 18-23 (2003).
272 Browning, A. C. *et al.* Comparative gene expression profiling of human umbilical vein endothelial cells and ocular vascular endothelial cells. *Br J Ophthalmol* **96**, 128-132, doi:10.1136/bjophthalmol-2011-300572 (2012).
273 Rangasamy, S. *et al.* Transcriptomics analysis of pericytes from retinas of diabetic animals reveals novel genes and molecular pathways relevant to blood-retinal barrier alterations in diabetic retinopathy. *Exp Eye Res* **195**, 108043, doi:10.1016/j.exer.2020.108043 (2020).
274 Beltramo, E. *et al.* A study of capillary pericyte viability on extracellular matrix produced by endothelial cells in high glucose. *Diabetologia* **46**, 409-415, doi:10.1007/s00125-003-1043-6 (2003).
275 Beltramo, E., Nizheradze, K., Berrone, E., Tarallo, S. & Porta, M. Thiamine and benfotiamine prevent apoptosis induced by high glucose-conditioned extracellular matrix in human retinal pericytes. *Diabetes Metab Res Rev* **25**, 647-656, doi:10.1002/dmrr.1008 (2009).
276 Rudziak, P., Ellis, C. G. & Kowalewska, P. M. Role and Molecular Mechanisms of Pericytes in Regulation of Leukocyte Diapedesis in Inflamed Tissues. *Mediators Inflamm* **2019**, 4123605, doi:10.1155/2019/4123605 (2019).
277 Stark, K. *et al.* Capillary and arteriolar pericytes attract innate leukocytes exiting through venules and 'instruct' them with pattern-recognition and motility programs. *Nat Immunol* **14**, 41-51, doi:10.1038/ni.2477 (2013).
278 Pieper, C. & Galla, H. J. Ultra structure analysis of cell-cell interactions between pericytes and neutrophils in vitro. *Biochem Biophys Res Commun* **445**, 180-183, doi:10.1016/j.bbrc.2014.01.159 (2014).
279 Wang, S. *et al.* Venular basement membranes contain specific matrix protein low expression regions that act as exit points for emigrating neutrophils. *J Exp Med* **203**, 1519-1532, doi:10.1084/jem.20051210 (2006).
280 Naba, A. *et al.* The extracellular matrix: Tools and insights for the "omics" era. *Matrix Biol* **49**, 10-24, doi:10.1016/j.matbio.2015.06.003 (2016).
281 Tian, C. *et al.* Proteomic analyses of ECM during pancreatic ductal adenocarcinoma progression reveal different contributions by tumor and stromal cells. *Proc Natl Acad Sci U S A* **116**, 19609-19618, doi:10.1073/pnas.1908626116 (2019).
282 McCabe, M. C. *et al.* Alterations in extracellular matrix composition during aging and photoaging of the skin. *Matrix Biol Plus* **8**, 100041, doi:10.1016/j.mbplus.2020.100041 (2020).
283 Wishart, A. L. *et al.* Decellularized extracellular matrix scaffolds identify full-length collagen VI as a driver of breast cancer cell invasion in obesity and metastasis. *Sci Adv* **6**, doi:10.1126/sciadv.abc3175 (2020).
284 Wu, Y. X. *et al.* Dynamically remodeled hepatic extracellular matrix predicts prognosis of early-stage cirrhosis. *Cell Death Dis* **12**, doi:ARTN 163
10.1038/s41419-021-03443-y (2021).
285 Preil, S. A. *et al.* Quantitative Proteome Analysis Reveals Increased Content of Basement Membrane Proteins in Arteries From Patients With Type 2 Diabetes Mellitus and Lower Levels Among Metformin Users. *Circ Cardiovasc Genet* **8**, 727-735, doi:10.1161/CIRCGENETICS.115.001165 (2015).

286 Pokhilko, A. *et al.* Global proteomic analysis of extracellular matrix in mouse and human brain highlights relevance to cerebrovascular disease. *J Cereb Blood Flow Metab* **41**, 2423-2438, doi:10.1177/0271678X211004307 (2021).
287 Byron, A., Humphries, J. D. & Humphries, M. J. Defining the extracellular matrix using proteomics. *Int J Exp Pathol* **94**, 75-92, doi:10.1111/iep.12011 (2013).
288 Randles, M. J., Humphries, M. J. & Lennon, R. Proteomic definitions of basement membrane composition in health and disease. *Matrix Biol* **57-58**, 12-28, doi:10.1016/j.matbio.2016.08.006 (2017).
289 Yun, S. *et al.* Interaction between integrin alpha5 and PDE4D regulates endothelial inflammatory signalling. *Nat Cell Biol* **18**, 1043-1053, doi:10.1038/ncb3405 (2016).
290 Reuten, R. *et al.* Basement membrane stiffness determines metastases formation. *Nat Mater* **20**, 892-903, doi:10.1038/s41563-020-00894-0 (2021).
291 Wu, C. *et al.* Endothelial basement membrane laminin alpha5 selectively inhibits T lymphocyte extravasation into the brain. *Nat Med* **15**, 519-527, doi:10.1038/nm.1957 (2009).
292 Sixt, M. *et al.* Endothelial cell laminin isoforms, laminins 8 and 10, play decisive roles in T cell recruitment across the blood-brain barrier in experimental autoimmune encephalomyelitis. *J Cell Biol* **153**, 933-946, doi:10.1083/jcb.153.5.933 (2001).
293 Menezes, M. J. *et al.* The extracellular matrix protein laminin alpha2 regulates the maturation and function of the blood-brain barrier. *J Neurosci* **34**, 15260-15280, doi:10.1523/JNEUROSCI.3678-13.2014 (2014).
294 Wagner, J. U. G. *et al.* Switch in Laminin beta2 to Laminin beta1 Isoforms During Aging Controls Endothelial Cell Functions-Brief Report. *Arterioscler Thromb Vasc Biol* **38**, 1170-1177, doi:10.1161/ATVBAHA.117.310685 (2018).
295 O'Callaghan, P., Zhang, X. & Li, J. P. Heparan Sulfate Proteoglycans as Relays of Neuroinflammation. *J Histochem Cytochem* **66**, 305-319, doi:10.1369/0022155417742147 (2018).
296 Taha, I. N. & Naba, A. Exploring the extracellular matrix in health and disease using proteomics. *Essays Biochem* **63**, 417-432, doi:10.1042/EBC20190001 (2019).
297 Jailkhani, N. *et al.* Noninvasive imaging of tumor progression, metastasis, and fibrosis using a nanobody targeting the extracellular matrix. *Proc Natl Acad Sci U S A* **116**, 14181-14190, doi:10.1073/pnas.1817442116 (2019).
298 Xie, Y. J. *et al.* Nanobody-based CAR T cells that target the tumor microenvironment inhibit the growth of solid tumors in immunocompetent mice. *Proc Natl Acad Sci U S A* **116**, 7624-7631, doi:10.1073/pnas.1817147116 (2019).
299 Momin, N. *et al.* Anchoring of intratumorally administered cytokines to collagen safely potentiates systemic cancer immunotherapy. *Sci Transl Med* **11**, doi:10.1126/scitranslmed.aaw2614 (2019).
300 Tanabe, K. Calcineurin inhibitors in renal transplantation: what is the best option? *Drugs* **63**, 1535-1548, doi:10.2165/00003495-200363150-00002 (2003).
301 Voisin, M. B., Woodfin, A. & Nourshargh, S. Monocytes and neutrophils exhibit both distinct and common mechanisms in penetrating the vascular basement membrane in vivo. *Arterioscler Thromb Vasc Biol* **29**, 1193-1199, doi:10.1161/ATVBAHA.109.187450 (2009).
302 Liu, H. *et al.* Cysteine-rich protein 61 and connective tissue growth factor induce deadhesion and anoikis of retinal pericytes. *Endocrinology* **149**, 1666-1677, doi:10.1210/en.2007-1415 (2008).
303 Stitt, A. W. *et al.* Substrates modified by advanced glycation end-products cause dysfunction and death in retinal pericytes by reducing survival signals mediated by platelet-derived growth factor. *Diabetologia* **47**, 1735-1746, doi:10.1007/s00125-004-1523-3 (2004).

304 Maller, O. *et al.* Tumour-associated macrophages drive stromal cell-dependent collagen crosslinking and stiffening to promote breast cancer aggression. *Nat Mater* **20**, 548-559, doi:10.1038/s41563-020-00849-5 (2021).
305 Chronopoulos, A., Tang, A., Beglova, E., Trackman, P. C. & Roy, S. High glucose increases lysyl oxidase expression and activity in retinal endothelial cells: mechanism for compromised extracellular matrix barrier function. *Diabetes* **59**, 3159-3166, doi:10.2337/db10-0365 (2010).
306 Kim, D., Mecham, R. P., Nguyen, N. H. & Roy, S. Decreased lysyl oxidase level protects against development of retinal vascular lesions in diabetic retinopathy. *Exp Eye Res* **184**, 221-226, doi:10.1016/j.exer.2019.04.019 (2019).
307 Song, B., Kim, D., Nguyen, N. H. & Roy, S. Inhibition of Diabetes-Induced Lysyl Oxidase Overexpression Prevents Retinal Vascular Lesions Associated With Diabetic Retinopathy. *Invest Ophthalmol Vis Sci* **59**, 5965-5972, doi:10.1167/iovs.18-25543 (2018).
308 Tenti, P. & Vannucci, L. Lysyl oxidases: linking structures and immunity in the tumor microenvironment. *Cancer Immunol Immunother* **69**, 223-235, doi:10.1007/s00262-019-02404-x (2020).
309 Barker, H. E., Cox, T. R. & Erler, J. T. The rationale for targeting the LOX family in cancer. *Nat Rev Cancer* **12**, 540-552, doi:10.1038/nrc3319 (2012).
310 Bignon, M. *et al.* Lysyl oxidase-like protein-2 regulates sprouting angiogenesis and type IV collagen assembly in the endothelial basement membrane. *Blood* **118**, 3979-3989, doi:10.1182/blood-2010-10-313296 (2011).
311 Cosgrove, D. *et al.* Lysyl oxidase like-2 contributes to renal fibrosis in Col4alpha3/Alport mice. *Kidney Int* **94**, 303-314, doi:10.1016/j.kint.2018.02.024 (2018).
312 Bhave, G. *et al.* Peroxidasin forms sulfilimine chemical bonds using hypohalous acids in tissue genesis. *Nat Chem Biol* **8**, 784-790, doi:10.1038/nchembio.1038 (2012).
313 Lee, S. W. *et al.* Peroxidasin is essential for endothelial cell survival and growth signaling by sulfilimine crosslink-dependent matrix assembly. *FASEB J* **34**, 10228-10241, doi:10.1096/fj.201902899R (2020).
314 Mekkawy, A. H., Pourgholami, M. H. & Morris, D. L. Involvement of urokinase-type plasminogen activator system in cancer: an overview. *Med Res Rev* **34**, 918-956, doi:10.1002/med.21308 (2014).
315 Abraham, E. *et al.* Urokinase-type plasminogen activator potentiates lipopolysaccharide-induced neutrophil activation. *J Immunol* **170**, 5644-5651, doi:10.4049/jimmunol.170.11.5644 (2003).
316 Fonovic, M. & Turk, B. Cysteine cathepsins and extracellular matrix degradation. *Biochim Biophys Acta* **1840**, 2560-2570, doi:10.1016/j.bbagen.2014.03.017 (2014).
317 Vizovisek, M., Fonovic, M. & Turk, B. Cysteine cathepsins in extracellular matrix remodeling: Extracellular matrix degradation and beyond. *Matrix Biol* **75-76**, 141-159, doi:10.1016/j.matbio.2018.01.024 (2019).
318 Tocharus, J. *et al.* Developmentally regulated expression of mouse HtrA3 and its role as an inhibitor of TGF-beta signaling. *Dev Growth Differ* **46**, 257-274, doi:10.1111/j.1440-169X.2004.00743.x (2004).
319 Geevarghese, A. & Herman, I. M. Pericyte-endothelial crosstalk: implications and opportunities for advanced cellular therapies. *Transl Res* **163**, 296-306, doi:10.1016/j.trsl.2014.01.011 (2014).
320 Rudy Bilous, R. D. Handbook of Diabetes, 4th Edition. 4th edn, (Wiley-Blackwell, 2010).